The Dissertation Committee for Amit Kumar certifies that this is the approved version of the following dissertation:

Nanoparticles as a carrier for protein and plasmid DNA vaccines in microneedle-mediated transcutaneous immunization

Committee:

Zhengrong Cui, Supervisor

Robert O. Williams, III

Hugh D. Smyth

Christopher A. Jolly

Jason T. McConville

Mingtao Zeng

Nanoparticles as a carrier for protein and plasmid DNA vaccines in microneedle-mediated transcutaneous immunization

by

Amit Kumar, B.Phr.; M.S.

Dissertation

Presented to the Faculty of the Graduate School of

The University of Texas at Austin

in Partial Fulfillment

of the Requirements

for the Degree of

Doctor of Philosophy

The University of Texas at Austin

August 2013

Dedication

This dissertation is dedicated to my parents Navin Kumar and Raka Kumari who have supported me all the way since the beginning of my studies. Also, this dissertation is dedicated to my brother Sumit Kumar who has been a great source of motivation and inspiration.

Acknowledgements

I would like to express my sincere gratitude to my advisor Dr. Zhengrong Cui your ingenuity, creativeness, and high academic standards have paved the way to my scientific understanding. Being in your research group has been a valuable and unforgettable experience. I would also like to thank my dissertation committee members Dr. Robert Williams III, Dr. Hugh Smyth, Dr. Christopher Jolly, Dr. Jason McConville and Dr. Mingtao Zeng for their time and constructive comments. I will never forget the wonderful friendship and constant advice I received from Dr. Saijie Zhu and Mr. Michael Sandoval two of the trust worthiest friend's one can ever hope to have. Heartfelt thanks to Dr. Brian Sloat, Dr. Piyanuch Wonganan, Dr. Letty Rodriguez and Mrs. Xinran Li for their friendship and constant motivation.

I would like to acknowledge Dr. Kaoru Kiguchi and Dr. Jorge M. Blando for their assistance in obtaining and interpreting histological data. I would also like to thank Dr. Irena Fernandez at the DPRI Flow Cytometry Core Facility for her invaluable assistance with the flow cytometry data analysis.

I would like to thank all of the current members of the Cui lab including Dr. Mengmeng Niu, Dr. Yuriko Kiguchi, Mr. Youssef Wahib, Mr. Dayel, and Mr. Sachin Thakkar for their insightful conversations and assistance. I would also like to thank past members of the Cui lab; Dr. Melisande Holzer, Dr. Rebecca De Angel, Dr. Gang Xiao, Dr. Yuehong Xu, Dr. Dharmika Lansakara-P and Dr. Nijaporn Yanasarn.

Nanoparticles as a carrier for protein and plasmid DNA vaccines in microneedle-mediated transcutaneous immunization

Amit Kumar, Ph.D.

The University of Texas at Austin, 2013

Supervisor: Zhengrong Cui

Skin is the largest immune organ and an ideal site to administer vaccines. However, by nature, skin is not permeable to antigens, which are macromolecules. The major hurdle in skin permeation is the outermost stratum corneum layer. Microneedles have proven feasible to create micron-sized channels in the epidermis of the skin, through which protein and plasmid DNA antigens can penetrate into the viable skin epidermis and dermis. However, the immune responses induced by microneedle-mediated transcutaneous immunization with protein or plasmid DNA alone are generally weak, and a vaccine adjuvant is often required to induce strong immune responses. Data from numerous previous studies have shown that nanoparticles as a vaccine carrier can significantly enhance the immunogenicity of antigens, but the feasibility of utilizing nanoparticles as a vaccine carrier to enhance the immune responses induced by microneedle-mediated transcutaneous immunization has rarely been studied. In this

dissertation, using protein antigen (OVA) chemically conjugated onto the surface of solid-lipid nanoparticles and plasmid DNA (pCMV-β, pVax/opt-BoNT/C-Hc50, and pCI-neo-sOVA) physically coated on the surface of cationic polymeric nanoparticles, we showed that the immune responses induced by microneedle-mediated transcutaneous immunization with protein antigens or plasmid DNA vaccines are significantly enhanced by delivering the proteins and plasmid DNA with nanoparticles. Importantly, microneedle-mediated transcutaneous immunization with proteins or plasmid DNA induces not only systemic immune responses, but also mucosal immune responses.

In addition, it is generally believed that microneedles are safe. However, it remained unclear whether the micropores created by microneedles on the skin will also facilitate the permeation of microbes such as bacteria into the skin. In this dissertation, we also designed an unique *ex vivo* model to evaluate the permeation of live bacteria through mouse skin pretreated with microneedles. The results demonstrated that the b risk of potential bacterial infection associated with microneedle treatment is not greater than that associated with a hypodermic needle injection.

Table of Contents

List of Figures

Chapter One

Introduction

1.1 Background

Almost all vaccines, with a few exceptions, are administered by intramuscular (IM) or subcutaneous (SC) injection using hypodermic needles. While needle-based vaccination has led to tremendous advancement in controlling many infectious diseases, this technique comes with several risks such as potential infection at the site of injection, spread of infectious needles and syringes as well as re-use of non-sterile needles and syringes and discomfort to the patient. Thus, alternate means of vaccine delivery have been explored to attain a more effective, safer, and patient-friendly vaccination method [1].

For a long time, skin was considered impermeable for large molecules such as protein antigens, but studies performed by Glenn et al. demonstrated that topical application of protein antigens, such as diphtheria or tetanus toxoids, admixed with cholera toxin (CT) onto a skin area stimulated specific immune responses to the protein antigens in a mouse model [2]. A similar result was obtained when the heat-labile enterotoxin (LT) of *Escherichia coli* [3] or its mutants LTK63 and LTR72 were used as adjuvants [4]. The preliminary results of a clinical trial conducted with human volunteers also demonstrated that topical application of an LT patch onto the skin induced anti-LT immunoglobulin G (IgG) and immunoglobulin A (IgA) responses [5]. After these ground-breaking studies, cutaneous immunization (i.e., immunization by applying

vaccines or antigens topically onto the skin) continuously evolved as a non-invasive technique that benefits from the skin immune system.

Skin is the largest organ of the human body. It acts as a physical barrier between body and the outer environment. Skin is mainly composed of two layers, the epidermis and dermis. Epidermis is made up of stratum corneum and viable epidermis. The stratum corneum is the outer most layer, which is 30–50 μm thick and composed of dead cells called corneocytes embedded in a highly organized lamellar structure formed by intercellular lipids. The barrier property of the skin resides in the stratum corneum layer, which plays a crucial role in shielding the body from the external environment. Just below the stratum corneum is the viable epidermis, which is 200–250 μm thick. The main cell type of the epidermis are keratinocytes; however melanocytes, merkel cells and Langerhans cells (LCs) are also present, although less abundantly. The dermis is 2-3 mm thick. Cells present in the dermis are fibroblasts, mast cells, and dendritic cells (DCs). The dermis layer also has blood vessels, lymph vessels, nerves, and an abundant level of collagen fibers. Below the dermis, there is a layer of the subcutaneous fat tissue [6-8].

Other than the physical barrier function, skin is also a part of the immune system. It is highly accessible and has an unique immunological characteristic. Keratinocytes and LCs of the epidermis layer, fibroblasts, DCs, and mast cells of the dermis layer, and T and B lymphocytes of the skin-draining lymph nodes together form the skin's whole immunization network [6]. Skin has a rich population of DCs, which provide effective immunity against antigens coming through the skin. LCs are the primary DCs in the epidermis which migrate from bone marrow to skin and play a vital role in immune

surveillance and antigen presentation. DCs act as efficient and potent antigen-presenting cells (APCs) for the induction of adaptive immunity [9]. These APCs (i.e., LCs and DCs) capture and process antigens at the site of administration, and migrate to local draining lymph nodes, where they mature and mediate the activation of B and T cells [10]. Conventional vaccination by hypodermic needle-based injection bypasses the APC-rich skin immune system and delivers antigens into the less APC-populated muscle or subcutaneous tissues. Delivery of antigens into skin layers, where a large number of epidermal LCs and dermal DCs are present, can potentially induce a greater immune response [9, 11]. In fact, data from many clinical studies have shown that intradermal administration of influenza vaccine requires a very low dose, relative to intramuscular injection, to produce a similar or even stronger immune response [12, 13]. Another major advantage of cutaneous immunization is its potential safety. Cutaneous immunization minimizes the distribution of antigens and adjuvants inside the body, which may produce slight toxicity if comes directly in contact with the systemic circulation [14].

Recombinant DNA technology has revolutionized vaccine development. The major advantage of recombinant vaccine (protein or plasmid DNA) is that they do not contain the pathogen or its inactivated form; hence they are not capable of causing disease. These vaccines are considered safe and can overcome some of the safety concern associated with live vaccines, such as reversion risks and potential spread to unintended individuals [15, 16]. Also there is no need for the cultivation of pathogenic organism if these vaccines are used. DNA vaccine, based on recombinant DNA technology,

comprises a number of features that make it an attractive alternative over the conventional live attenuated or inactivated vaccines. Manufacturing of DNA vaccine is simple and rapid, and plasmid DNA is very stable during storage. DNA vaccine has the potential to generate strong cellular and humoral immune responses and is well tolerated by patients [17]. Plasmid DNA can be easily manipulated to incorporate multiple antigen genes in the same plasmid [18]. Additionally, plasmid DNA itself has some adjuvant activity because of the presence of unmethylated CpG motifs [19, 20].

Glenn et al. were the first who demonstrated the possibility of cutaneous immunization with protein antigens by using various adjuvants such as cholera toxin (CT), heat-labile enterotoxin (LT) or their mutants [21-23]. In a clinical study, it was shown that Escherichia coli LT patch system can induce a strong immune response in human volunteers [5]. A strong antibody response was also obtained against influenza in human volunteers with the patch system containing immunostimulatory agent LT [24].

DNA vaccine came in existence in the 1990s. In a very first study, Tang et al. demonstrated that immune response can be stimulated by administering a protein-encoding gene into the skin of mice. The authors reported the delivery of plasmid DNA containing human growth hormone gene into the skin using a gene gun in an attempt to express human growth hormone for gene therapy. Through this study, the authors pointed out that plasmid DNA may be used to produce antibodies and may offer an unique method for vaccination [25]. One year later, Ulmer et al. reported that intramuscular injection of naked plasmid DNA can induce immune responses against influenza viral antigens in mice [26]. In the same year, Fynan et al. demonstrated that

other than IM injection, epidermal, mucosal, and intravenous routes can also be used for the administration of DNA vaccine. It was concluded that vaccination with plasmid DNA expressing influenza virus hemagglutinin glycoprotein by gene gun delivery into the epidermis or by administration of plasmid DNA to nasal mucosa are most promising [27]. After these breakthroughs, numerous studies had been performed using various plasmid DNA formulations and delivery methods, and altogether they provided solid evidence that DNA vaccine is potentially viable. In 1999, Shi et al. reported that non-invasive immunization through mouse skin with plasmid DNA induced an immune response against the protein encoded by the plasmid [28]. Watabe et al. later confirmed that the stratum corneum is the major barrier for a successful cutaneous DNA immunization. The authors reported that applying plasmid DNA that encodes an influenza viral antigen onto intact mouse skin could not induce a high level of immune response, even when a very large amount of plasmid DNA was used. However, immunization with the same plasmid after the removal of the stratum corneum by tape-stripping with fast active adhesive glue significantly improved the resultant immune responses, to a level similar to that after IM injection [29], clearly demonstrating the need to overcome the statum corneum barrier for cutaneous DNA immunization to induce strong and effective immune responses.

1.2 Techniques to overcome the stratum corneum barrier

The stratum corneum is the principle barrier for skin penetration. This layer has made it very challenging to deliver high molecular weight hydrophilic molecules such as proteins, peptides, and plasmid DNA into or across the skin [7]. Stratum corneum is

predominantly composed of dead corneocytes surrounded by lipid layers [30]; it offers an extensive barrier to small as well as large hydrophilic compounds. Only certain molecules with a molecular weight under 500 Da can be delivered passively through the stratum corneum [31]. To overcome the stratum corneum barrier and to deliver hydrophilic high molecular weight molecules into the skin, various alternative approaches have been explored, including chemical and physical techniques [32].

1.2.1 Physical techniques

Iontophoresis

Iontophoresis is the transdermal delivery of therapeutic molecules in ionic form. It involves the application of electrical current, typically a few milliamperes, across the skin to deliver hydrophilic and charged molecules. In this technique, an electrical current is applied through two electrodes across the skin surface. This allows the delivery of drug in a controlled fashion because the amount of drug delivered across the skin is directly proportional to the amount of charge passed [33]. Currently, the United States Food and Drug Administration (US FDA) approved iontophoretic systems, such as lidocaine to induce local anesthesia [34], tap-water for the treatment of hyperhidrosis [35], and pilocarpine to induce sweating [36], are available in the market. Plasmid DNA has also been delivered into the skin for immunization using this method; however this method is not very commonly used [37].

Electroporation

Electroporation is another technique that includes the use of transmembrane voltage produced by electric pulses to create reversible pores on the membrane surface. Electroporation temporarily disrupts the lipid bilayer membrane by applying short, high voltage electrical pulses. It has been shown that electroporation can alter the lipid domain of stratum corneum [38, 39], which can help the permeation of small molecules such as fentanyl as well as moderate size molecules such as calcitonin [40]. Electroporation has also been reported to enhance the permeation of lipophilic (timolol), hydrophilic (metoprolol), charged (heparin), and neutral molecules (mannitol) [41-43]. The extent of permeation is dependent upon the magnitude of the applied voltage [44]. Often, electroporation has been combined with intradermal injection of plasmid DNA for vaccination purpose [45, 46].

Sonophoresis/Ultrasound

Ultrasound has been shown to increase drug permeability across skin [47]. A less than 100 KHz frequency has been found to enhance the transdermal permeability more efficiently than higher frequency ultrasounds [48]. Ultrasound of less than 100 KHz frequency causes cavitation, which results in the disruption of the lipid bilayers of the stratum corneum and thus enhances the influx of drugs [49, 50]. Ultrasound can be applied to the skin either before the application of the drug or simultaneously with the application of the drug [51]. This method has been shown to increase skin permeability to various low and high molecular weight molecules such as insulin, heparin and plasmid

DNA [52-54]. In a study performed by Endoh et al., it was demonstrated that intra-amniotic injection of naked DNA with microbubble-enhanced ultrasound generated a very high level of expression of the DNA in fetal mouse skin [53].

Thermal poration

Heat increases skin permeability by creating pores in the stratum corneum. Heat also affects the microcirculation and blood vessel permeability, which are important factors for the administration of drugs in the systemic circulation [33]. Heat technique has been used to deliver conventional drugs and DNA vaccines [55, 56]. Heat also enhances the skin permeability by increasing drug solubility in patch formulation and within the skin [57]. FDA approved Synera® (Nuvo Research Inc., Canada) topical patch (lidocaine and tetracaine) for pain relief is based on this mechanism. The unique heating pod present inside Synera® becomes active once it is removed from the storage pouch. It warms up the area where it is applied, helping enhance the penetration of the anesthetics inside the skin [58].

Skin abrasion

Skin abrasion involves direct removal or disruption of the stratum corneum layer to facilitate the transportation of topically applied compounds [59]. *In vitro* data have shown that this technique can increase the penetration of angiotensin across the skin by 100-fold compared to untreated human skin [60, 61]. A study by Lisziewicz et al. showed

that skin abrasion combined with DNA vaccine, which was formulated as mannosilated particle, induced a strong immune response to HIV virus in monkeys [62].

Needle-free jet injection

Needleless jet injection is a combination of transdermal and parenteral drug delivery methods. The injection devices can be divided into two categories: liquid jet injectors and solid jet injectors. Both injectors deliver a drug through skin by using a driving force and by rapidly disrupting the skin barrier. A well-known needleless injector, PowderJect® (PowderJect Pharmaceuticals, UK), shoots solid particles across stratum corneum using high pressure helium gas. All vaccines formulated in powder or particle forms can be delivered by this method. DNA vaccine coated on gold or tungsten particles has also been delivered into epidermis using PowderJect® [63]. Another needleless injector, Intraject, uses nitrogen gas to drive liquid formulations across the skin [50]. Along with PowderJect®, Intraject has also been used to administer plasmid DNA for genetic immunization [64-70]. For more information about plasmid DNA immunization using jet injection devices, please refer to Sloat et al. [63].

1.2.2 Chemical techniques

Chemical penetration enhancers

A molecule that enhances the permeation of drugs across stratum corneum layer is called chemical penetration enhancer. Chemical penetration method provides certain

advantages over the aforementioned physical methods, including design flexibility with formulation chemistry and easier prospect for a patch application [31]. Chemical enhancers partition into, and interact with, the stratum corneum to induce a temporary, reversible increase in the skin permeability [71]. Chemical enhancers have many classes such as surfactants (e.g., Tween 20), fatty acids (e.g., oleic acid), terpenes (e.g., limonene), and solvents (e.g., ethanol) [72]. However, not all the chemical enhancers have been found to enhance the transdermal permeability significantly, particularly for high molecular weight molecules. Another major limitation of chemical enhancers is that they are often potent irritants to skin [31]; and this safety issue further decreases the number of chemical enhancers that can be included in formulations [39].

In our own previous studies, DNA application site on the skin is routinely hydrated with warm water or low concentration of sodium dodecyl sulfate (SDS) and cleaned with ethanol. Water, SDS and ethanol, can all potentially enhance skin permeation [73-75]. In a study by Heckert et al., it was demonstrated that combination of dimethyl sulfoxide (DMSO) with naked DNA applied topically onto unaltered skin of chicken generated a specific immune response that was stronger than that induced by conventional IM injection [76]. Unfortunately, DMSO is unlikely applicable clinically.

1.2.3 Other novel techniques

Skin appendages such as hair follicles, sebaceous glands, and sweat glands have also been shown to play an important role in increasing skin permeability, particularly for large molecules. Appendages create a channel in the stratum corneum and facilitate the

dermal absorption of topically applied compounds. Another method which has been researched extensively for enhancing skin permeability is the microneedle technology. Microneedles can disrupt the stratum corneum in the micron scale and thus can be used to enhance drug transportation into or across the skin.

1.3 Nanoparticles in immunization: a tool to increase cutaneous permeability and immunogenicity

Many nanoparticulate formulations have been developed as percutaneous carriers to overcome the skin barrier and deliver drugs carried by the nanoparticles inside the skin. Liposomes, niosomes, ethosomes, transfersomes, solid lipid nanoparticles, and polymeric nanoparticles are examples that have been used to enhance the transdermal permeability of drugs. Liposomes, niosomes, ethosomes and transfersomes are all lipid vesicles. Niosomes, ethosomes and transfersomes have been developed to improve some of the features of liposomes and to obtain enhanced skin permeation [77]. The lipid composition of liposomes is similar to that of the epidermis, which enables the liposomes to penetrate the epidermis barrier to a greater extent. In 1980, Mezei et al. reported that skin penetration of triamcinolone acetonide was enhanced by 4- to 5-fold by using a liposomal lotion than an ointment [78].

Cationic liposomes have been extensively used for passive cutaneous delivery of DNA. The positive charges on the liposomes facilitate the complexation of liposomes with DNA due to electrostatic interaction. Cationic liposomes protect DNA from enzymatic degradation and enhance DNA uptake by target cells [79]. Topical delivery of

liposome-DNA complexes (lipoplexes) on the mouse skin was performed for the first time by Li et al. The study demonstrated the successful transfection of hair follicular cells after topical application of liposome-DNA complexes [80, 81]. Later, many more studies were performed using cationic liposomes as a carrier for the topical delivery of plasmid. Other than conventional liposomes, noisomes and transfersomes were also used for topical gene delivery [82]. Ethosomes are negatively charged and thus not suitable for complexation with DNA [83]. Solid lipid nanoparticles were also used as a carrier for cutaneous DNA immunization [84]. Finally, nanoparticles prepared with polymers such as chitosan and poly(lactic-*co*-glycolic acid) (PLGA) have also been used as delivery systems for cutaneous DNA immunization [85].

For many vaccines, an immune adjuvant is required to generate a strong immune response [86-88]. Adjuvants are any substance that accelerates, prolongs or enhances antigen-specific immune responses, but are not immunogenic itself [89]. Particulates having diameters in the nanometer or micrometer ranges have been investigated as potential vaccine carriers and adjuvants by many researchers [87, 90, 91]. Particulate carriers protect the integrity of antigens [92] and facilitate the uptake of antigens by APCs such as DCs and macrophages [93, 94]. Particulate carriers may also allow the controlled release of antigens, which may increase the availability of antigens to immune cells [95, 96]. Finally particulate carriers had also been shown to modulate the type of immune responses induced by antigens, when used alone or in combination with other immunostimulatory compounds [97-99].

There are data showing that delivery of plasmid DNA vaccine using nanoparticulates may improve the potency of the DNA vaccine. For example, in studies performed by Cui et al., a novel nanoparticle-based DNA vaccine delivery system engineered from warm oil-in-water microemulsion precursors was developed [100]. The microemulsions were comprised of emulsifying wax (as the oil phase) and a cationic surfactant, cetyltrimethylammonium bromide (CTAB). Upon cooling these microemulsion precursors, cationic nanoparticles were generated. Plasmid DNA was coated on the surface of these positively charged nanoparticles. Immunization with plasmid DNA-coated nanoparticles subcutaneously by injection with a hypodermic needle, intradermally via a needle-free injection device, or intranasaly all induced enhanced immune responses in mice, compare to immunization with the plasmid DNA alone. In addition, it was shown that cutaneous immunization using plasmid DNA carried by the nanoparticles onto a mouse skin area pretreated with the hair depilation cream Nair® induced a stronger immune response than using the plasmid DNA alone [84, 100-103].

Nanoparticles have also been used as immune adjuvants with protein vaccines. Cui et al. coated cationized galactosidase protein on the surface of anionic nanoparticles and evaluated the immune response in a mouse model after subcutaneous administration. Cationized galactosidase-coated nanoparticles induced stronger immune response in comparison to β-galactosidase with 'Alum' and cationized galactosidase alone. Cationized galactosidase-coated nanoparticles were also found to enhance both Th1 and Th2 cytokine release [104].

1.4 Microneedle-mediated cutaneous immunization

1.4.1 Microneedles: A novel approach for enhancing cutaneous permeation

Microneedles are one of the new technologies studied in transdermal drug delivery. This is a simple, pain-free, and minimally invasive technology that helps the delivery of large molecular weight and hydrophilic compounds across skin. Microneedles consist of a plurality of micro-projections of different shapes, sizes and heights, which are attached to a base support. Application of microneedles onto skin surface creates micron size transport pathways, which allow the permeation of macromolecules inside the skin. According to Kaushik et al. , microneedles perforate stratum corneum, avoiding any contact with nerve fibers and blood vessels present in the dermis layer [105]. Therefore, the major benefit of using microneedles is the pain-free delivery of both small and large molecular weight compounds [105, 106].

The concept of microneedle first came in the 1970's; however technological limitations at that time prevented the product concept from being executed [107]. In 1990s with the beginning of high precision microelectronics industrial tools, microneedle manufacturing also became a reality. The first microneedle array reported in the literature was made from silicon wafer and was developed for gene delivery by Hashmi et al [108]. In that study, the needles were inserted into nematodes to increase molecular uptake and gene transfection. After transfection, the gene of interest was expressed in the progeny of the injected worms [108]. The first paper to report microneedles for transdermal drug

delivery was published by Henry et al. in 1998, who demonstrated that microneedles can be used to increase skin permeability [109]. An array of solid microneedles of 150 μm length was used to create micropores in human epidermis. These micropores increase the skin permeability by three orders of magnitude for a small model compound calcein. The transportation of calcein took place through the leakage pathways created between the needles and the skin. When the needles were removed from the skin, the skin permeability was increased by another order of magnitude [109]. In a follow-up study, McAllister et al. from the same research group studied the permeability of various compounds across cadaver skin using Franz diffusion cell and noted that insulin, bovine serum albumin, and latex nanoparticles (up to 100 nm size) could cross the skin pretreated with microneedles [110]. These early studies demonstrated that skin permeability can be increased using microneedles.

Microneedles are somewhat like traditional needles but are fabricated on the micron scale. The most commonly used fabrication materials are metals, silicon, silicon dioxide, polymers and glass. The first few microneedle devices were fabricated from silicon [108, 109]. Later other materials such as stainless steel [111], dextrin [112, 113], glass [114], ceramic [115], maltose [116], galactose [117] and various polymers [110, 118] have also been used to fabricate microneedles. The most commonly used methods for the manufacturing of microneedles are chemical isotropic etching, injection molding, reactive ion etching, surface/bulk micromachining, polysilicon micromolding, lithography-electroforming-replication, and laser drilling [118-122]. Microneedles are

fabricated in different sizes, shapes, and types. The two basic designs of microneedles are in plane and out plane designs.

1.4.2 Methods of using microneedles to administer vaccine

The use of microneedles in delivering vaccines into the epidermis and dermis compartments of skin is a very attractive approach for cutaneous vaccination. Four different microneedle designs have been developed for the delivery of vaccines inside the skin.

Solid microneedles

The simplest method of cutaneous immunization using microneedles is to create pores on the skin with a solid microneedle array and then apply vaccine onto the perforated skin surface. By piercing the skin, the permeation of vaccine can be increased by many folds. This method has been used to deliver vaccines such as proteins (e.g., bovine serum albumin) and genetic materials (e.g., plasmid DNA) *in vitro* and *in vivo* into the skin [109, 118, 123-127]. For example, Ding et al. demonstrated a major improvement in the immunogenicity of diphtheria toxoid in a mouse model when the antigen was applied onto a skin area pretreated with microneedles [128].

Coated microneedles

Solid microneedles can also be coated with a vaccine. Coating is usually applied by dipping microneedles in a vaccine formulation. Coated microneedles can be inserted

into skin and quickly removed after a few seconds, leaving the vaccine inside the skin. Using this approach, proteins, DNA, and viral particles such as influenza virus particle have been delivered to the skin *in vitro* and *in vivo* [129-136]. Matriano et al. demonstrated that cutaneous immunization with 300-μm long titanium microneedles coated with 1 μg of ovalbumin generated a 100-fold increase in immune responses, compared to intramuscular injection of the same dose [132]. In another study, Widera et al. found that the immune responses induced by cutaneous immunization with microneedles coated with ovalbumin are dose dependent; however, the immune responses were independent of the depth of delivery, the density of microneedles, or the area of application [133].

Hollow microneedles

One hollow microneedle or an array of hollow microneedles can be used to deliver liquid vaccine formulations inside the skin. Hollow microneedles allow a controlled quantity of antigens to be delivered inside the skin with a definite rate. Hollow microneedles have been used to deliver influenza and anthrax vaccines in animal models [137-139]. Van Damme et al. delivered α-RIX influenza vaccine (3.3 μg of hemagglutinin per strain) in human volunteers using 450-μm long hollow microneedles and reported that the immune response induced was similar to that induced by 15 μg hemagglutinin per strain delivered intramuscularly [140].

Dissolvable microneedles

Microneedles can also be prepared from polymers or saccharides with vaccine encapsulated inside. After inserting inside the skin, microneedles and vaccine dissolve within few minutes, and the backing layer is discarded. Sullivan et al. reported that inactivated influenza virus (A/PR/8/34) encapsulated in polyvinylpyrrolidone dissolvable microneedles induced strong humoral and cellular immune responses and also provided a defense again influenza challenge [141].

1.4.3 Microneedle-mediated cutaneous immunization

As discussed earlier, it is a well-known fact that skin offers a great immunologic environment compared to muscle and subcutaneous tissues. However, so far there is no simple, reliable, and safe method available to deliver vaccines into the skin efficiently in a cost effective way to a large population of people. The microneedle device has the potential to address these problems to some extent. The painless microneedles not only can improve patient compliance, but also enable the targeting of antigens to the immune cell-rich skin layers. In the past ten years, many different vaccines and/or antigens, coming mostly under live attenuated microorganisms, proteins and plasmid DNA classes, have been delivered into the skin using microneedles. For example, influenza vaccination using whole inactivated influenza viruses coated on microneedles has been studied extensively. Studies have shown a complete protection against infection after microneedle-mediated cutaneous immunization with influenza virus A/Puerto Rico/8/34 (H1N1), influenza virus A/California/04/09 (H1N1), and influenza virus A/Aichi/2/68 (H3N2) [135, 142, 143]. Along with whole inactivated influenza virus, virus like particles

(VLP) coated on microneedles were also studied. It was shown that cutaneous immunization with avian H5 influenza VLPs coated on stainless steel microneedles induced a stronger immune response in a mouse model, relative to intramuscular injection [144, 145]. Microneedles have also been used for the delivery of recombinant subunit vaccines, such as trimeric influenza hemagglutinin protein. Upon administration, protein antigen coated on microneedles induced an enhanced immunity, relative to the subcutaneous injection of the same protein antigen in mice [146]. In a recent study in our laboratory, we have demonstrated that ovalbumin chemically conjugated onto solid lipid nanoparticles and then administered cutaneously onto a skin area pretreated with microneedles induced a stronger immune response as compared to cutaneous immunization using ovalbumin alone [147]. The dose of the antigen determined whether the microneedle-mediated immunization can induce a stronger immune response than subcutaneous injection of the same antigen conjugated on the solid lipid nanoparticles [147]. Finally, plasmid DNA has also been explored extensively for microneedle-mediated cutaneous immunization, which is discussed below in details.

1.4.4 Microneedle-mediated cutaneous DNA immunization

Cutaneous DNA immunization has been performed using gene gun and electroporation techniques, and was found to improve the immune responses by many folds in human and nonhuman primates [148]. However, gene gun and electroporation techniques are tedious and require a vaccination protocol and equipment [149]. Microneedles as a new technology may deliver DNA vaccine painlessly into the skin and

is potentially suitable for inexpensive mass production. The first study showing the delivery of DNA using microneedles was performed by Hashmi et al. in 1995. In their study, DNA-coated microprobes were injected in the cuticle of nematode *Heterorhabditis bacteriophora* to express a foreign gene, β-galactosidase [108]. After this study, microneedle devices were shown to increase the skin permeability of plasmid DNA *in vitro* [150]. However, there was not any systematic *in vivo* study performed until 2002, when Mikszta et al. reported the first *in vivo* study using microneedles to deliver DNA vaccine topically into the skin. In that study, microenhancer arrays (MEAs, i.e., microneedles) were fabricated using potassium hydroxide etch technique. The array was fabricated on 1 cm^2 microchips and had the projection height ranging from 50-200 μm. Naked plasmid DNA encoding firefly luciferase was administered to mice topically using the MEAs. The arrays were dipped into plasmid DNA solution and scraped multiple times across the skin of mice to create microabrasions. The results demonstrated that the mean luciferase activity in groups treated with 6 or more passes of MEA were 1000- to 2800-fold higher in comparison to topical controls. Untreated skin was used as a control for possible delivery through HFs. The gene expression level in the MEA-treated groups was also found similar or greater than after intramuscular and intradermal injection of plasmids. The results showed that even a single pass of the MEA across the skin enabled gene transfer. The authors also used a plasmid DNA that encodes hepatitis B surface antigen and reported that MEA-based cutaneous immunization induced a stronger immune response with less variability after the second and third immunizations, as compared to immunization by hypodermic needle injection. Both hypodermic needle

injection and MEA-based delivery induced similar antigen-specific cytotoxic T lymphocytes (CTL) responses [151]. The significance of this study is that it demonstrates the feasibility of cutaneous DNA vaccination using microneedles.

In separate studies by Birchall et al. and Coulman et al., it has been demonstrated that microneedles can facilitate the delivery of plasmid DNA into the epidermis layer of the human skin, and the genes encoded by the plasmid can be expressed in the skin. Birchall et al. delivered pCMV-β plasmid into the skin with the help of silicon microneedles and demonstrated a detectable gene expression in the microchannels. In control groups, where DNA was delivered without microneedle treatment, expression was not observed. Coulman et al. also used silicon microneedle arrays to create micropores through the stratum corneum of human skin samples to test the ability of the conduits to facilitate the delivery of pCMV-β plasmid. Their results demonstrated that these micropores facilitated the delivery of plasmid DNA, and gene expression study confirmed that naked plasmid DNA was able to be expressed in excised human skin. However, the presence of a limited conduits that were positive for gene expression indicated that there is a need to optimize the microneedle device morphology, application method, and the DNA formulation in order to obtain a higher gene expression [124, 152].

Alarcon et al. performed an animal study to use microneedles to deliver three different types of influenza vaccines: whole inactivated influenza virus, trivalent split-virion human vaccine, and plasmid DNA encoding the influenza virus hemagglutinin. In their study, rats were chosen as an animal model since rat skin is thicker than the total length of microneedles (i.e.,1 mm). Antigens were administered intradermally using

hollow microneedles and intramuscularly using hypodermic needles. Results showed that intradermal delivery using hollow microneedles generated an antibody response similar to intramuscular injection; however dose sparing effect was achieved when microneedles were used [137].

Various other enhancement techniques have also been used in combination with microneedles in order to further improve the delivery of drugs and vaccines. These techniques include iontophoresis [125, 153], radio frequencies and electroporation [131, 154]. Hooper et al. combined electroporation and microneedle technique to deliver small pox DNA vaccine in order to induce humoral immune response in nonhuman primates [131]. The current FDA approved small pox vaccine is composed of live vaccinia virus and is administered through skin using a bifurcated needle. This technology was developed almost 2 centuries ago and has several limitations such as localized skin infection and non-serious/serious adverse effects [155]. Thus a DNA vaccine appears to be a safer option. In this study, a plasmid DNA vaccine encoding four vaccinia virus genes was efficiently delivered by skin electroporation using plasmid DNA-coated microneedle arrays in a mouse model. This study used a novel device that performed electroportion using a microneedle array. After insertion into the skin the DNA dissolved from the microneedles and electroporation helped them to transfect the surrounding cells. The DNA vaccine induced strong antibody responses against all four immunogens. Moreover, vaccinated mice were completely protected against a lethal intranasal challenge with vaccinia virus [131]. Another study that combined microneedles with electroporation technique was performed by Daugimont et al. The purpose of their study

was to test the effect of the combination on plasmid DNA transfection in the skin. Gold-coated Radel hollow microneedles were used for intradermal injection as well as electrodes for electroporation. However, this setup demonstrated a severe limitation in DNA electrotransfer. Only a limited amount of DNA was delivered because of the small volume of microreservoirs attached to hollow microneedles and the high viscosity of DNA solution. Also, the needles produced less favorable electric field distribution than the plate electrode [156]. In a study performed by Pearton et al., microneedle delivery system was combined with sustained release plasmid DNA hydrogel formulation. Hydrogel formulation acted as a reservoir for plasmid DNA. Freshly excised human skin was used to characterize DNA diffusion and β-galactosidase gene expression. After creating micro-channels using microneedles, channels were filled with DNA hydrogel, which worked as a sustained release depot. The results showed that the DNA hydrogel gradually released DNA, which expressed the β-galactosidase reporter gene in the viable epidermis [127].

Studies were also performed to assess the cytotoxic T lymphocyte response after microneedle-mediated cutaneous DNA immunization. In a study by Gill et al., cutaneous immunization was performed using microneedles (length 700 μm and width 160 μm) coated with a plasmid encoding hepatitis C virus nonstructural 3/4A protein. The immune response induced in the microneedle-treated group was compared to intramuscular DNA delivery or cutaneous DNA delivery using gene gun. Vaccination with plasmid-coated microneedles effectively primed specific CTLs responses. Microneedles were found similarly efficient in priming CTLs as gene gun and

hypodermic needles [136]. In a study performed by Zhou et al., microneedle-based DNA delivery was demonstrated to enhance both humoral and cellular immune responses. The study compared the immune response generated by intramuscular and microneedle-mediated cutaneous immunization with a plasmid DNA encoding HBsAg in C57BL/6 mice. A significantly higher antibody response was induced by microneedle-mediated cutaneous immunization as compared to intramuscular injection. High levels of IL-12 and gamma interferon were also released from the splenocytes of mice that received the microneedle-mediated cutaneous immunization. Finally, HBsAg-specific CTL activity was also higher in mice immunized using microneedles than in mice immunized by intramuscular injection [157]. Chen et al. performed a study with a mouse model to test DNA vaccine for HSV-2 (herpes simplex virus) infection using a nanopatch containing microneedles [158]. HSV-2 infection is one of the most predominant sexually transmitted infections and a major cause of genital ulcer in the world [159]. Additionally, HSV-2 can also cause a very rare disease called neonatal herpes [160]. A nanopatch that has microprojections was coated with HSV-2-gD2 DNA vaccine and applied to the inner earlobe of the ears of mice. Immunomicroscopy results confirmed that the vaccine was delivered in the APC-rich epidermal layer. Cutaneous immunization with the nanopatch induced a strong antibody response and an equal protection rate against HSV-2 virus challenge when compared to mice dosed by intramuscular injection of the DNA vaccine [158]. Kask et al. also performed a similar study and used nanopatch to administer plasmid DNA vaccine against HSV-2 infection. Nanopatch microprojections coated with DNA vaccine were administered in a mouse model (ventral ear), and the results were

compared with standard intramuscular DNA vaccination. The vaccine administered by the nanopatch was found highly immunogenic and supported the survival of most mice. The topical nanopatch vaccination method was found more effective than the traditional intramuscular injection [161].

DeMuth et al. and Saurer et al. demonstrated that plasmid DNA (encoding firefly luciferase) combined with polyelectrolyte multilayers films (PEM) coated on the surface of microneedles can be used to deliver the DNA vaccine into the skin. PEM has demonstrated the potential for vaccine encapsulation into thin films. PEM also stabilizes environmentally-sensitive encapsulated materials and controls the release of the materials. The films erode after the insertion of the microneedles into the skin and release the DNA [162, 163].

Many studies have been performed to administer influenza DNA vaccine using microneedles. So far the most dominating way for influenza vaccination is administering trivalent inactivated or live-attenuated virus vaccine [164]. However, the recent influenza vaccine pandemic in 2009 pointed out that the manufacturing and administering influenza vaccine requires at least 6-7 months of time after identification of the virus, and thus there is a need to explore a new expedited method of influenza vaccine manufacturing and administration [165]. To address this concern, Kim et al. proposed to deliver an influenza DNA vaccine with the help of a microneedle patch. They compared the immunity induced by administering influenza DNA vaccine through the skin using microneedles and that induced by intramuscular injection in the same dose in a mouse model. Microneedles were coated with the avian H5 influenza DNA vaccine and

administered to the skin. Vaccination using microneedles generated a very high level of antibody response and hemagglutination inhibition titers, as compared to the conventional intramuscular injection. It also significantly improved the protection against infection with avian influenza virus [166]. A similar influenza DNA vaccination study using microneedles was also reported by Song et al. In their study, the authors delivered the influenza hemagglutinin DNA vaccine coated on microneedles in the skin and compared the immune response induced with that induced by intramuscular injection of plasmid DNA. A lower dose of DNA (3 μg) via the microneedle-mediated cutaneous route induced a stronger humoral immune response and a better protective immunity after challenge than intramuscular injection of a lower (3 μg) or even a higher dose of the DNA (10 μg). Microneedle-mediated cutaneous immunization with a higher dose of the DNA further improved the immune responses and post-challenge protection. It was concluded that microneedle-mediated cutaneous DNA immunization can induce stronger humoral and cellular immune responses than intramuscular immunization with the same plasmid DNA [167].

In a study by Pearton et al., the significance of optimizing key parameters for an effective microneedle-mediated plasmid DNA delivery was emphasized. Key parameters investigated in the study included loading of DNA on microneedles, stability and functionality of the coated DNA, skin penetration capability of coated microneedles, and gene expression in human skin. Microneedles were fabricated from stainless steel, and plasmid DNA was coated. Optimization of coating method increases the loading capacity and decreases the skin insertion force significantly. Physical stability of the coated DNA

was further improved through the addition of saccharide excipients. The DNA-coated microneedles facilitated the expression of reporter gene in viable human skin [168]. An earlier study performed by Chen et al. also pointed out the importance of the coating method in microneedle-mediated vaccine delivery. The study introduced a gas jet drying approach, which dispersed a small amount of coating solution to wet densely packed microprojections on a patch in order to obtain a desired uniform coating. It also helps to remove the extra coating solution lodged between the needles on the base surface. The coating remains intact during skin administration and releases the vaccine within 3 minutes. This coating approach was demonstrated to be feasible for coating a wide variety of vaccines including DNA vaccine [169].

1.4.5 Microneedle-mediated cutaneous immunization using DNA coated on nanoparticles

Data from numerous previous studies have shown that coating of plasmid DNA on cationic nanoparticles can significantly enhance the resultant immune responses in comparison to using naked DNA alone, including when the DNA coated nanoparticles were administered cutaneously [84, 170, 171]. In a study performed in our lab, we compared the immune responses induced by plasmid DNA, alone or coated on cationic nanoparticles, after topical application onto a skin area pretreated with microneedles.

Cationic PLGA (poly(lactic-*co*-glycolic acid)) nanoparticles were prepared using a nanoprecipitation-solvent evaporation method [172]. Plasmid DNA (pCMV-β) was mixed with cationic nanoparticles to coat the nanoparticles by electrostatic interaction.

The net charge of the resultant DNA-nanoparticle complexes was dependent upon the ratio of the plasmid DNA to cationic nanoparticles in the mixture. We prepared net positively charged and net negatively charged plasmid DNA-nanoparticle complexes and evaluated their *in vitro* permeation through skin and the *in vivo* immune responses induced by them after topical application onto a skin area pretreated with microneedles. Our results showed that pCMV-β, alone or coated on the PLGA nanoparticles, were not able to permeate through intact skin; however permeation was detected through mouse skin that was pretreated with microneedles [85]. The permeation of the naked pCMV-β plasmid was more extensive than the pCMV-β coated on the cationic PLGA nanoparticles, and the permeation of pCMV-β on the net negatively charged pCMV-β-coated PLGA nanoparticles through the skin pretreated with microneedles was more extensive than the permeation of pCMV-β on the net positively charged pCMV-β-coated PLGA nanoparticles [85].

In a study in mice, microneedle-mediated cutaneous immunization with pCMV-β plasmid DNA carried by the cationic nanoparticles induced a stronger immune response than with the plasmid DNA alone [85], clearly demonstrating that microneedle-mediated cutaneous immunization with plasmid DNA coated on cationic nanoparticles can enhance the immune response induced by the plasmid DNA. Furthermore, the net positively charged pCMV-β-coated PLGA nanoparticles were found more effective than the net negatively charged pCMV-β-coated PLGA nanoparticles. In addition, the immune responses induced by cutaneous immunization with net positively charged pCMV-β-coated PLGA nanoparticles were found similar or stronger than by intramuscular

immunization with the same pCMV-β plasmid, alone or coated on the PLGA nanoparticles. Importantly, specific IgA response was also detected in the sera, lung washes, and fecal samples in mice cutaneously immunized with the net positively charged plasmid DNA coated PLGA nanoparticles (Kumar and Cui, unpublished data), demonstrating that microneedle-mediated cutaneous immunization with plasmid DNA coated on cationic PLGA nanoparticles is capable of inducing mucosal immune responses as well. Finally, we have shown that microneedle-mediated cutaneous immunization with plasmid DNA coated on the cationic PLGA nanoparticles can also induce strong specific cellular immune responses (Kumar and Cui, unpublished data) [85]. For more information about nanoparticles as delivery systems for DNA vaccines, please refer to Cui et al. [173].

1.4.6 Microneedle-mediated cutaneous immunization with protein antigen

Protein-based vaccine had also been administered using microneedles. In one of the earliest study, Matriano et al. used Macroflux microprojection array patch as a novel delivery system for the intracutaneous administration of protein antigen. The Macroflux skin patch comprises titanium microprojections with an adhesive backing layer. A model protein antigen, ovalbumin (OVA), was coated on microprojection array, which was dissolved from the microneedles after insertion into the skin of guinea pig. OVA is a very frequently used model protein for evaluating the suitability of microneedles in transdermal immunization. The results demonstrated that the microprojections were able to penetrate at an average depth of 100 μm and deliver 1 to 80 μg of OVA into the skin.

Immune response data showed that microneedle-mediated immunization with a lower dose of antigen (1 or 5 µg) produced a 50-fold greater immune response, compared to the same dose of antigen given by the standard subcutaneous or intramuscular immunization [132].

In another study using rabbits as an animal model, various routes were used to deliver recombinant protective antigen (rPA) of *Bacillus anthracis*, and their effects were compared. The results demonstrated that intradermal administration using hollow microneedles, intramuscular injection and intranasal administration, all routes showed a complete protection against lethal anthrax spore challenge. Topical immunization with rPA on a microneedle-pretreated skin area showed only 33% protection, however the immune response induced was greater than that induced in animals where microneedles were not used [139]. In a follow up study, it was found that in order to generate same level of antibody response, intradermal delivery of rPA using hollow microneedles needed a lower dose of antigen than intramuscular injection. Delivery of 10 µg rPA using a hollow microneedle showed 100 % protection in rabbits after anthrax spore challenge, whereas IM injection of the same dose of rPA only achieved 71% protection [138].

Widera et al. showed that the immune responses induced by microneedle-mediated cutaneous immunization using protein antigens are dose dependent. Intracutaneous immunization using ovalbumin coated on microneedles was investigated to determine the influence of depth of vaccine delivery, dose of vaccine delivered, density of microneedles used, and area of application on the resulting immune responses. The results showed that the immune response was independent of depth of delivery,

density of microneedles or area of application. However, the dose of antigen affected the resultant immune responses. A significant difference was found in the immune responses induced when low, medium and high antigen doses were used [133].

Ding et al. performed microneedle-mediated immunization using diphtheria toxoid and influenza subunit vaccine. Cholera toxin (CT) was administered as vaccine adjuvant. The results showed that microneedle pretreatment had no effect on the immune response induced when the influenza subunit vaccine was administered alone. However, a strong immune response was generated when CT was used as adjuvant, irrespective of microneedle pretreatment. In contrast, microneedle pretreatment was found effective to attain a strong anti-DT IgG immune response with toxin-neutralizing activity. Use of CT as adjuvant further improved the anti-DT immune response to a level almost equivalent to that when mice were subcutaneously injected with DT-alum. The authors concluded that microneedle pre-treatment is important in cutaneous immunization with protein antigens, and it can lead to an immune response comparable to that induced by subcutaneous injection of protein antigens [128].

In another study performed by Ding et al. in the same year, DT antigen was cutaneously administered on microneendle pretreated mouse skin in combination with various adjuvants such as lipopolysaccharide, Quil A, CpG or CT. CT was found to be most effective in boosting the immunogenicity of DT [174].

Study has also been performed to deliver influenza protein vaccine using microneedles. In a very recent study performed by Kommareddy et al., influenza antigen monobulks were coated on microstructures. Immune responses generated by trivalent

vaccine coated microstructured patches were compared with the immune response generated by conventional IM vaccinations in a guinea pig model. Their results showed that immunization using the vaccine coated microneedles induced antibody titers similar to that induced by the traditional trivalent vaccine administered intramuscularly [175]. Zhu et al had also demonstrated a similar result earlier in 2009 [135].

1.4.7 Microneedle-mediated cutaneous immunization using protein antigen carried by nanoparticles

Nanoparticles have also been used as antigen carrier and adjuvant for microneedle-mediated cutaneous immunization with proteins. In studies performed by Bal et al., N-trimethyl chitosan (TMC) nanoparticles were used to deliver diphtheria toxoid (DT) and OVA antigens cutaneously using mironeedles. DT-TMC nanoparticles, DT-TMC solution and DT alone were administered through microneedle-treated skin in a mouse model. Results showed that cutaneous immunization with DT-TMC mixture solution induced a higher IgG response compared to DT-TMC nanoparticles or DT alone. Transport of TMC-NP through microneedle conduits was found less than to TMC-solution [176]. A year later in another study using OVA as antigen, mice were immunized cutaneously with OVA carried by N-trimethyl chitosan (TMC) nanoparticles using microneedles. OVA conjugated with TMC, OVA mixed with TMC and OVA alone were also administered cutaneously through microneedle pre-treated skin area. Percentage OVA+ DCs in the lymph node and serum antibody concentration was determined. The results showed that TMC–OVA conjugates induced the highest antibody

level (IgG) in the serum and also generated more OVA+ DCs in the lymph nodes in comparison to the OVA carrying nanoparticles, most probably because TMC–OVA conjugates could have penetrated the skin more readily in comparison to nanoparticles [165].

Slutter et al. also used OVA as antigen for cutaneous immunization. OVA was combined with cationic liposome and CpG adjuvant, to test the immune responses and the transportation of the antigens to lymph nodes after they were administered through four different routes. In this study mice were immunized intranodally, intradermally, cutaneously (using microneedles) and intranasally with liposomal OVA/CpG or OVA/CpG solution. Results showed that irrespective of the route of administration, the IgG2a level was found higher (Th1 response) when liposomal OVA/CpG was administered in comparison to OVA/CpG solution. However, serum IgG titers did not reveal any benefit of using the liposomes [177]. Ding et al. also performed the cutaneous immunization using microneedles with DT prepared in cationic liposomes. They concluded that microporation of skin and use of cholera toxin as an adjuvant is both important to obtain a significant antibody titer. However, they couldn't found any role of the liposomal vesicle in antigen formulation in enhancing the immune response over using free antigen alone [178].

In another study, Hirschberg et al. combined two vesicles formulations, L595 vesicles (composed of sucrose-laurate ester and octaoxyethylene-laurate ester, size 75 nm) and sPC vesicles (composed of soybean–phosphatidylcholine and Span-80, size 170 nm), with hepatitis B surface antigen (HBsAg) and performed cutaneous immunization

with them using microneedles. The results showed that the microneedle treatment was an important step for the antigens containing vesicles to produce an antibody response. The combined vesicle formulation didn't induce any IgG response against HBsAg after delivering through intact skin. However, only when CT adjuvanted antigen carrying vesicles were administered through microneedle treated skin, IgG antibody was detected [179].

Guo et al. used dissolving polyvinylpyrrolidone (PVP) microneedles containing liposomal particles for cutaneous delivery of antigen and adjuvant. OVA was used as a model protein antigen, CpG oligos were used as adjuvant, and cationic liposomes were used as a delivery vehicle. Mice were immunized using antigen loaded microneedles, and the results demonstrated that anti-OVA IgG level was higher in the group immunized with OVA-CpG OND encapsulated in liposomes in comparison to the other groups such as OVA, OVA-CpG OND, OVA encapsulated in liposome, and IM injection with OVA. Also cutaneous immunization with OVA-CpG OND encapsulated in liposomes changed the immune response type from Th2 to a balanced Th1/Th2 [180].

1.5 Conclusions

Close to 15 years after the successful demonstration of cutaneous immunization by Glenn et al., many more studies pointed out the potential of the needle-free cutaneous immunization. Painless vaccine patches help to enhance patient compliance. They can be self-administered, which reduces the need for medical facility and staff. Vaccine patches can also reduce the spread of infectious needles and syringes as well as re-use of non-

sterile needles and syringes. Above all, skin itself provides a very favorable immunological environment for cutaneous immunization. However, there are still issues that need to be addressed to make cutaneous immunization commercially successful. Most of the cutaneous immunization studies have been performed with small animals. Many of them have a different skin thickness and permeability in comparison to human skin. There are also other important structural and immunological differences [181, 182]. Thus any data obtained from an animal study may not be directly applied to humans. Additionally, many different approaches have been developed by various research groups to enhance cutaneous permeability of vaccines, which includes physical and chemical techniques and various nanoparticle-based formulations. However, many of these approaches cause moderate to significant disruption of the skin barrier. Therefore, it is a challenge to develop a safe, effective and truly non-invasive cutaneous immunization technique to increase the permeability of vaccine formulation.

Microneedle-mediated cutaneous delivery has been extensively explored to enhance the cutaneous permeability of antigen vaccines. For microneedle-mediated cutaneous immunization, parameters such as microneedle diameter, length, tip geometry and density need to be optimized because all of these parameters can influence skin perforation and antigen delivery [183]. The difference in the thickness of animal skin (such as mice skin) and human skin is another concern. For successful and reproducible skin penetration by microneedles, optimization of the microneedle applicator device is also needed [183]. Therefore in order to bring microneedles to the market for transdermal delivery of a particular vaccine, it is very important to properly choose the type of microneedle (e.g.,

hollow, solid, biodegradable) and their geometry, material, density, length, diameter, as well as application device.

1.6 Objectives

From chapter 1, it is clear than nanoparticles as an antigen carrier have vaccine adjuvant activity. In addition, the delivery of antigens (proteins and plasmid DNA) and nanoparticles into the skin using microneedles has also been confirmed. Based on these, we generated the following hypothesis:

The immune responses induced by microneedle-mediated transcutaneous immunization with protein-based vaccine or plasmid DNA vaccine can be significantly enhanced by carrying the vaccine with nanoparticle.

The aims of this project were:

i. **To evaluate the permeation and antibody response of protein antigen (ovalbumin) conjugated on nanoparticles after it is applied onto a skin area pretreated with microneedles.** The permeation of live bacteria through a mouse skin area pretreated with microneedles was also evaluated (Chapter II).

ii. **To evaluate the antibody responses induced by plasmid DNA coated on cationic PLGA nanoparticles after it is applied onto a skin area pretreated with microneedles.** In this study, we also evaluated the effect of the net surface charge of the DNA-nanoparticle complexes on (i) *in vitro* and *in vivo* permeation of the plasmid DNA through mouse skin and (ii) the *in*

vivo immune responses induced by transcutaneous immunization with the plasmid DNA (Chapter III).

iii. **To evaluate the botulinum neurotoxin (BoNT)-neutralizing antibody responses induced by a plasmid DNA that encodes the heavy chain fragment of BoNT serotype C and is coated on cationic PLGA nanoparticles after topically applying onto a skin area pretreated with microneedles.** In this study, we also evaluated the effect of antigen, antigen dose and mouse strain on the resultant immune responses (Chapter IV).

Chapter Two

Assessment of the permeation of antigen protein conjugated nanoparticles and live bacteria through microneedle-treated mouse skin

International Journal of Nanomedicine, June 2011, 2011 (6), 1253-1264.

2.1 Introduction

Microneedles have been researched extensively to improve intradermal or transdermal drug delivery [106, 184-187]. The feasibility of microneedle-mediated delivery of nanoparticles into or through the skin was also confirmed [110, 188]. Initially, McAllister *et al*. (2003) reported the permeation of latex nanoparticles of up to 100 nm through human cadaver epidermis after the skin was treated with solid microneedles (150 μm long, base diameter of 80 μm) [110]. Coulman *et al*. (2009) showed the permeation of polystyrene nanoparticles (138 ± 25 nm) through the micropores created in human skin by microneedles of 280 μm long with a base diameter of 200 μm [188]. In contrast, Zhang *et al*. (2010) did not observe any permeation of poly(lactic-co-glycolic) acid (PLGA) nanoparticles (166, 206, or 288 nm) through human skin pre-treated with microneedles of 200 μm long [189], but they did show the penetration of the nanoparticles into the epidermis and dermis of the skin [189].

New generation vaccines based on recombinant DNA technology generally need a vaccine adjuvant to be strongly immunogenic, and data from numerous studies have shown that many polymeric or solid lipid nanoparticles as a vaccine antigen carrier have potent adjuvant activity [190]. One of the very attractive applications of the combination of microneedle and nanoparticle technologies is in vaccine delivery [32]. In fact, there

have been significant and successful efforts to utilize solid microneedles coated with nanoparticle-based vaccine formulations, mainly virus-like particles, to carry out transcutaneous immunization in animals and clinical trials [32, 133, 138, 141, 142, 144, 145, 176, 191-198]. However, the feasibility of transcutaneous immunization by applying antigens carried by nanoparticles onto a skin area pre-treated with microneedles was not very thoroughly evaluated. Although the application of a vaccine formulation onto the skin prior to or after the skin area is treated with microneedles is associated with the slight inconvenience of being a two-step process, it does have advantages. For example, the dose of vaccines that can be applied is not as limited as when the vaccine is to be coated on solid microneedles, and coating of a vaccine on microneedles in a mass production scale is still a topic of active research [199]. Recently, Bal *et al*. (2010) showed that application of diphtheria toxoid (DT) formulated into nanoparticles (211 ± 4 nm) prepared with N-trimethyl chitosan (TMC) onto a mouse skin area pre-treated with solid microneedles (300 μm long) induced anti-DT antibody immune responses. However, the responses were not stronger than when the DT was used alone [176]. Interestingly, it was reported that the simple physical mixture of the DT with the TMC nanoparticles was more immunogenic than DT alone [176]. Therefore, there continues to be a need to test whether transcutaneous immunization onto a skin area pre-treated with microneedles with an antigen carried by nanoparticles is more effective than with the antigen alone.

Previously, Sloat *et al*. (2010) reported the engineering of solid lipid nanoparticles of 200 nm from lecithin/glyceryl monostearate (GMS)-in-water emulsions [200, 201]. It

was shown that subcutaneous injection of protein antigens conjugated onto the nanoparticles induced strong, functional antibody and cellular immune responses [200, 202]. In the present study, using ovalbumin (OVA) as a model antigen chemically conjugated onto the nanoparticles (OVA-nanoparticles, mean diameter of 230 nm) and three different microneedle rollers with different size of microneedles, the antibody responses induced by the OVA-nanoparticles or OVA alone, when applied onto a mouse skin area pre-treated with the microneedle rollers, were evaluated and compared. Prior to *in vivo* animal immunization study, the permeation of the OVA-nanoparticles through mouse skin treated with microneedle rollers was evaluated *in vitro*. Microneedle rollers are commercially available and used for cosmetic (self-application) and clinical treatment of skin. it was shown that compared to the insertion of microneedles on a flat patch, the sequential insertion of microneedles on a microneedle roller required less insertion force [184].

Finally, a very important issue related to microneedle-based drug delivery was rarely studied: the potential risk of bacterial or viral infections via the micropores created by microneedles. Bacteria and viruses are physically nanoparticles or microparticles. Therefore, any micropores that allow the permeation of nanoparticles should also allow the permeation of bacteria or viruses. It is generally assumed that the risk of infection associated with microneedle treatment is low, and many microneedle-related safety studies in clinical trials were focused on the degree of irritation and pain caused by the microneedles [140, 203-205]. The first study on the ability of microbes to traverse microneedle-induced micropores was reported by Donnelly *et al*. (2009), in which the

permeation of microbes through porcine skin pre-treated with a microneedle array (280 µm long, base diameter of 250 µm) was confirmed *in vitro* [206]. In the present study, an *ex vivo* model was designed to evaluate the permeation of live bacteria through a mouse skin area pre-treated with microneedles of different needle sizes. For this study, a non-pathogenic *Escherichia coli* DH5α strain was used.

2.2 Materials and Methods

2.2.1 Materials

Dermaroller® microneedle rollers were purchased from Cynergy, LLC (Carson City, NV). Digital pictures of the microneedle roller are shown in Figs. 2.1A-B. There are 192 needles in 8 rows on each roller. Three different microneedle rollers were used. The dimensions of the microneedles on different rollers are shown in Fig. 2.1C. Based on the size of the microneedles, the microneedle rollers were named as rollers with large (1000 μm long, base diameter 80 μm), medium (500 μm long, base diameter 50 μm), and small (200 μm long, base diameter 20 μm) microneedles. OVA, fluorescein-5(6)-isothiocyanate (FITC), 2-iminothiolane (Traut's reagent), 3,3',5,5'-tetramethylbenzidine (TMB) solution, sodium bicarbonate, sodium carbonate, Tween 20, and phosphate-buffered saline (PBS) were from Sigma-Aldrich (St. Louis, MO). Lecithin (soy, refined) was from Alfa Aesar (Ward Hill, MA). Glyceryl monostearate (GMS) was from Gattefosse Corp. (Paramus, NJ). The 1,2-dipalmitoyl-*sn*-glycero-3- phosphoethanolamine-N-[4-(p-maleimidophyl)butyramide] (DPPE-maleimide) and 1,2-dioleoyl-sn-glycero-3-phosphoethanolamine-N-carboxyfluorescein (DOPE-fluorescein) were from Avanti Polar Lipids (Alabaster, AL). Goat anti-mouse IgG was from Southern Biotechnology Associates, Inc. (Birmingham, AL).

2.2.2 Preparation of nanoparticles

Nanoparticles were prepared as previously described [200, 201]. Briefly, soy lecithin (3.5 mg) and GMS (0.5 mg) were placed into a 7-ml glass vial. One milliliter of de-ionized and filtrated (0.22 μm) water was added into the vial, followed by heating on a hot plate to 70-75°C with stirring and brief intermittent periods of sonication (Ultrasonic Cleaner Model 150T, VWR International, West Chester, PA). Once a homogeneous milky slurry was formed, Tween 20 was added in a step-wise manner to a final concentration of 1% (v/v) to form emulsions, which were then allowed to stay at room temperature while stirring to form nanoparticles. The endotoxin level in the nanoparticle preparation was estimated to be 0.18-0.57 EU/ml using a ToxinSensor™ Chromogenic LAL Endotoxin Assay Kit from GenScript (Piscataway, NJ) [202]. The size and zeta potential of the nanoparticles were determined using a Malvern Zetasizer® Nano ZS (Westborough, MA).

To prepare maleimide-nanoparticles, DPPE-maleimide, which has a reactive maleimide group, was included in the lipid mixture (5%, w/w) [200, 202]. To fluorescently label the nanoparticles, DOPE-fluorescein (5%, m/m of total lipids) was included in the lecithin and GMS mixture during the nanoparticle preparation [200, 202].

2.2.3 Conjugation of OVA onto the nanoparticles

The conjugation of OVA onto the nanoparticles was completed as previously described [200-202]. Prior to conjugation, OVA was thiolated using Traut's Reagent. OVA was diluted into carbonate buffer (0.1 M, pH 9.6), followed by the addition of Traut's reagent (20 × molar excess) and a 60 min incubation at room temperature.

Thiolated OVA was desalted using a PD10 column (GE Healthcare, Piscataway, NJ). To react the thiolated OVA with nanoparticles, 1 ml of freshly prepared maleimide-nanoparticles were mixed with the thiolated OVA (10 mg) in PBS (0.1 M, pH 7.4) and stirred under nitrogen gas for 12-14 h at room temperature. Un-conjugated OVA was removed by repeated ultracentrifugation (600,000 × *g*) and washing (with PBS) for 3 times. The amount of OVA conjugated onto the nanoparticles was estimated as previously described using fluorescein-labeled OVA [200, 202]. OVA was labeled with fluorescein following the manufacturer's instruction (Promega) before being conjugated onto the nanoparticles.

2.2.4 *In vitro* permeation of OVA or OVA-NPs through a skin area treated with microneedle rollers

In vitro permeation assay using Franz diffusion cells was completed as previously described [110]. The lower dorsal skin of C57BL/6 mice was used in all permeation studies. Hair was trimmed using an electric clipper 24 h before the collection of the skin, which was stored at -20^{o}C for a maximum period of one month and used whenever needed. After the fat layer was carefully removed, the skin was placed onto the flat surface of a balance, and the microneedle rollers were rolled in 4 perpendicular lines over the skin surface, 5 times each for a total of 20 times, with an applying pressure of 350-400 g, which was constantly measured using the balance while rolling the microneedle roller [207]. The skin was then mounted onto the Franz diffusion cells from PermeGear, Inc. (Hellertown, PA) dorsal side facing upward. The receiver compartment contained 5

mL of PBS (pH 7.4, 10 mM) and was maintained at 37^{o}C with a Haake SC 100 Water Circulator from ThermoScientific (Wellington, NH). The diffusion area of the skin was 0.64 cm^{2}. The donor compartment was loaded with fluorescein-labeled OVA or fluorescein-OVA-nanoparticles in PBS (500 µL, pH 7.4, 10 mM) and covered with parafilm to prevent evaporation. The amount of OVA protein loaded into the donor compartment was 0.6 mg. After 0, 1, 2, 4, 8, and 24 h, samples (200 µL) were withdrawn from the receiver compartment and immediately replenished with fresh PBS. The fluorescence intensity in the sample was measured using a BioTek Synergy™ HT Multi-Mode Microplate Reader (Winooski, VT).

2.2.5 Methylene blue staining for visualization of micropores

Hair on the dorsal skin of C57BL/6 mice was trimmed before the mice were euthanized to remove the skin. The skin sample was treated with a Nair® lotion (Church and Dwight Co., Princeton, NJ), rinsed with water, paper-dried, and placed onto the flat surface of a balance. Microneedle rollers were rolled once over the skin surface with an applying pressure of 350-400 g. The skin was then stained with 20 µL of methylene blue solution for no more than 5 min followed by the removal of excessive stain using normal saline swabs and later with alcohol swabs. Stained skin was visualized using a Stereoscopic Zoom Nikon SMZ1500 microscope (Melville, NY). As a control, skin was also punctured with a 21 G hypodermic needle (BD, Franklin Lakes, NJ).

2.2.6 Immunization studies

All animal studies were carried out following the National Institutes of Health guidelines for animal care and use. Animal protocol was approved by the Institutional Animal Care and Use Committee at The University of Texas at Austin. Female C57BL/6 mice (18-20 g) were used for the immunization studies. Twenty-four hours prior to the application of the vaccine formulations, hair in the dorsal side of mice was carefully trimmed. The skin was cleaned with an alcohol swab, and a 2 cm^2 area was marked on the skin surface. Mice were anesthetized and placed onto the flat surface of a balance to monitor the applied pressure during the application of microneedle rollers. Microneedle rollers were disinfected with 70% of ethanol and then rolled in two perpendicular lines over the lower dorsal marked skin surface, 10 times each, again for a total of 20 times [187], with an applying pressure of 350-400 g. OVA in PBS or OVA-conjugated nanoparticles in PBS were carefully dripped onto the treated area, which were then covered with a piece of self-adhesive Tegaderm® patch (3 M, St. Paul, MN), which was carefully removed 24 h later. Immunization was repeated 10 days apart for two more times. As a positive control, a group of mice were subcutaneously injected 3 times with OVA-conjugated nanoparticles in PBS. Two weeks (or as where mentioned) after the last immunization, mice were bled for antibody assay. The dose of OVA was 10.5 or 70 μg per mouse.

2.2.7 Enzyme-linked immunosorbent assay (ELISA)

ELISA was completed as previously described [200, 201]. Briefly, EIA/RIA flat bottom, medium binding, polystyrene, 96-well plates (Corning Costar, Corning, NY)

were coated with 100 ng of OVA in 100 µL of carbonate buffer (10 mM, pH 9.6) overnight at 4^{o}C. Plates were washed with PBS/Tween 20 (10 mM, pH 7.4, 0.05% Tween 20, Sigma–Aldrich) and blocked with 5% (v/v) horse serum in PBS/Tween 20 for 1 h at 37^{o}C. Samples were diluted 10-fold serially in 5% (v/v) horse serum in PBS/Tween 20, added to the plates following the removal of the blocking solution, and incubated for an additional 2 h at 37^{o}C. The serum samples were removed, and the plates were washed five times with PBS/Tween 20. Horse radish peroxidase (HRP)-labeled goat anti-mouse immunoglobulin (IgG, Southern Biotechnology Associates Inc., Birmingham, AL, 5000-fold dilution in 1.25% (v/v) horse serum in PBS/Tween 20) was added into the plates, followed by another hour of incubation at 37^{o}C. Plates were again washed five times with PBS/Tween 20. The presence of bound antibody was detected following a 30 min incubation at room temperature in the presence of TMB solution, followed by the addition of 0.2 M sulfuric acid as the stop solution. The absorbance was read at 450 nm using a BioTek Synergy^{TM} HT Multi-Mode Microplate Reader.

2.2.8 Transepidermal water loss (TEWL)

Mice were anesthetized. Hair in the lower dorsal skin was trimmed. Twenty four hour later, the trimmed area was disinfected with 70% ethanol and then treated with the microneedle rollers as mentioned above. Negative control mice received hair-trimming only. Before and immediately after the needle treatment (0 h), TEWL was measured using a VapoMeter from Delfin Technologies, Inc. (Stamford, CT) following the manufacturer's instruction. At least three readings were taken at every time points. If

there were any uncharacteristic spikes during this period, a more representative reading was used. TEWL readings were also recorded 2, 3, 4, and 24 h later. For mice treated with the roller with large microneedles, the TEWL readings were also recorded 48 h after the treatment. The experiment was repeated with at least 4 mice per group.

2.2.9 *In vitro* permeation of bacteria through the skin area treated with microneedle roller

Hair trimmed mice were treated with the microneedle rollers on the lower dorsal skin (10 times each in two perpendicular direction, total of 20 times) and then immediately euthanized. The skin in the treated area was collected and used to evaluate the permeation of live bacteria on the same day. As controls, intact skin (hair trimmed) or skin punctured with a 21 G needle once were also used. In addition, for the microneedle roller with large microneedles, mice were treated with the roller and euthanized immediately or 1, 3, 6, or 24 h later to collect the skin in the treated area. The collected skin was mounted onto the Franz diffusion cells to evaluate the microbial permeation. Mouse skin in the treated area and the working surface in a laminar flow cabinet were disinfected with 70% ethanol before the treatment. All dissecting tools were autoclaved before use.

E. coli DH5α bacteria were used to evaluate the permeation of live bacteria through the treated skin. Bacteria were grown in Luria-Bertani (LB) medium (Sigma-Aldrich), harvested, and re-suspended into the same volume of sterile PBS (pH 7.4, 10 mM). The OD600 value of the suspension was determined to be 1.27 ± 0.11. The

bacterial suspension was diluted in sterile PBS (pH 7.4, 10 mM) for 1000-fold and then placed (500 µL) into the donor compartment of the diffusion cells. Four hours later, the sample in the receiver compartment was withdrawn, diluted 1-, 10- and 100-fold in sterile PBS, and then spread (50 µL) onto LB agar plates, which were incubated at 37^{o}C overnight to count the number of colonies formed. The number of bacteria diffused through the skin was reported as colony forming unit (CFU), and it was assumed that each colony was developed from a single bacterial cell. The diffusion cells and the parafilm used to cover the cells were thoroughly disinfected with 70% of ethanol three times before use, and all other items were autoclaved before use.

2.2.10 Statistical analysis

Statistical analyses were completed using ANOVA followed by Fisher's protected least significant difference procedure. A p-value of ≤ 0.05 (two-tail) was considered statistically significant.

2.3 Results and discussion

2.3.1 Microneedle roller treatment allows skin permeation of OVA-conjugated nanoparticles

The OVA-nanoparticles were 230 ± 22 nm, with a polydispersity index of 0.2. Their zeta potential was -31 ± 1 mV. The amount of OVA conjugated onto the nanoparticles was determined to be 96.6 ± 11.0 μg OVA per mg of nanoparticles [202]. Mouse lower dorsal skin samples were harvested, treated with microneedle rollers, and used to evaluate the permeation of the OVA-nanoparticles. Shown in Fig. 2.2 are the microscopic pictures of the skin stained with methylene blue solution immediately following treatment with different microneedle rollers. As a control, the picture of the skin punctured by a 21 G hypodermic needle was also shown (Fig. 2.2A). The single pore created by the hypodermic needle was about 1 mm in diameter, which is expected because the nominal outer diameter of a 21 G needle is 819.2 μm. The pores created by the microneedles were much smaller, and it seemed that the diameter of the micropores created with a roller with larger microneedles tended to be larger than that created with a roller with smaller microneedles (Figs. 2.2), in agreement with what was previously reported by Zhou et al. [187], who used ZTGS^{TM} microneedle rollers. Due to the extensive diffusion of the blue dye, an accurate measurement of the diameters of those micropores was not attempted.

As shown in Figs. 2.3A and B, neither OVA protein in solution nor OVA conjugated on nanoparticles can permeate through the intact skin, demonstrating the

physical integrity of the skin samples. In contrast, both OVA and OVA-nanoparticles were able to permeate through the skins pre-treated with microneedle rollers (Figs. 2.3A, B). Moreover, pre-treatment with a roller with larger microneedles allowed more extensive permeation than treatment with a roller with smaller microneedles. For example, within 24 h, only a minimum amount of OVA-nanoparticles permeated through the skin pre-treated with the roller with small microneedles (200 μm long, base diameter of 20 μm), whereas 13.6 ± 2.4% of the OVA-nanoparticles permeated through the skin treated with the roller with large microneedles (1000 μm long, base diameter of 80 μm) (Fig. 2.3A). As expected, pre-treatment with the microneedle rollers allowed more extensive permeation of the OVA in solution than the OVA conjugated onto nanoparticles (Figs. 2.3A and B), considering that the OVA-nanoparticles are much larger than the OVA molecules. For example, within 24 h, 28.3 ± 6.5% of the OVA in solution diffused through the pores created by the roller with large microneedles, which is significantly higher than the 13.6 ± 2.4% for the OVA-nanoparticles. To confirm that it was the OVA-nanoparticles, not the OVA protein hydrolyzed from the OVA-nanoparticles, that diffused through the pores created by the microneedle rollers, the permeation of the nanoparticles alone (labeled with fluorescein, fluorescein-nanoparticles) was also monitored. As shown in Fig. 2.3C, the rate of the diffusion of the fluorescein-nanoparticles was similar to the diffusion of the fluorescein-labeled OVA-nanoparticles. Finally, the diffusion of the DOPE-fluorescein from the fluorescein-nanoparticles, placed into a dialysis tube (molecular weight cut, 50,000), was evaluated as well, and it was found that within 24 h, the release of the DOPE-fluorescein from the

nanoparticles was not detectable, regardless whether the release medium was PBS or PBS with 0.5% of sodium dodecyl sulfate (SDS) (data not shown), which indicated that the observed permeation of the fluorescein-nanoparticles in Fig. 2.3C was not caused by the diffusion of the DOPE-fluorescein molecules from the fluorescein-nanoparticles and then through the skin.

Taken together, data in Fig. 2.3 demonstrated that the OVA-nanoparticles of 230 ± 22 nm permeated through the micropores created by microneedle , even by roller with the smallest microneedles (200 μm long, base diameter of 20 μm), and that as expected, the extent of permeation was dependent on the size of the microneedles used. This observation is in agreement with what was reported by Coulman *et al*. (2009), who showed the permeation of 138 ± 22 nm polystyrene nanoparticles through human skin pre-treated with microneedles (280 μm long, base diameter of 200 μm) [188], but is in disagreement with the reports by Zhang *et al*. (2010) and Bal *et al*. (2010) using PLGA nanoparticles (166, 206, or 288 nm) and DT-TMC nanoparticles (211 ± 4 nm), respectively [176, 189]. In Bal et al.'s study, the length of the microneedles used was 300 μm [176]. The size of the nanoparticles used in the present study was similar to that used by Bal et al. It is interesting to find that the OVA-nanoparticles permeated through the skin area pre-treated with the smallest microneedles (200 μm long, base diameter of 20 μm). It is speculated that besides the particle size, other factors such as the materials used to prepare the nanoparticles, the surface charge of the nanoparticles, the strain and source of the animals used to harvest the skin, to name a few, all contributed to the different observations in different studies.

Finally In the present study, for easy detection, the diffusion of the fluorescein labeled nanoparticles through the skin and into the receiver compartment was measured, and data in Fig. 2.3 clearly showed the OVA-nanoparticles diffused into the receiver compartment. We are aware that for transcutaneous immunization, one expects to target the antigen inside the skin, particularly the epidermis, not necessarily to deliver the antigen through the skin because the skin epidermis has abundant antigen-presenting cells [208].

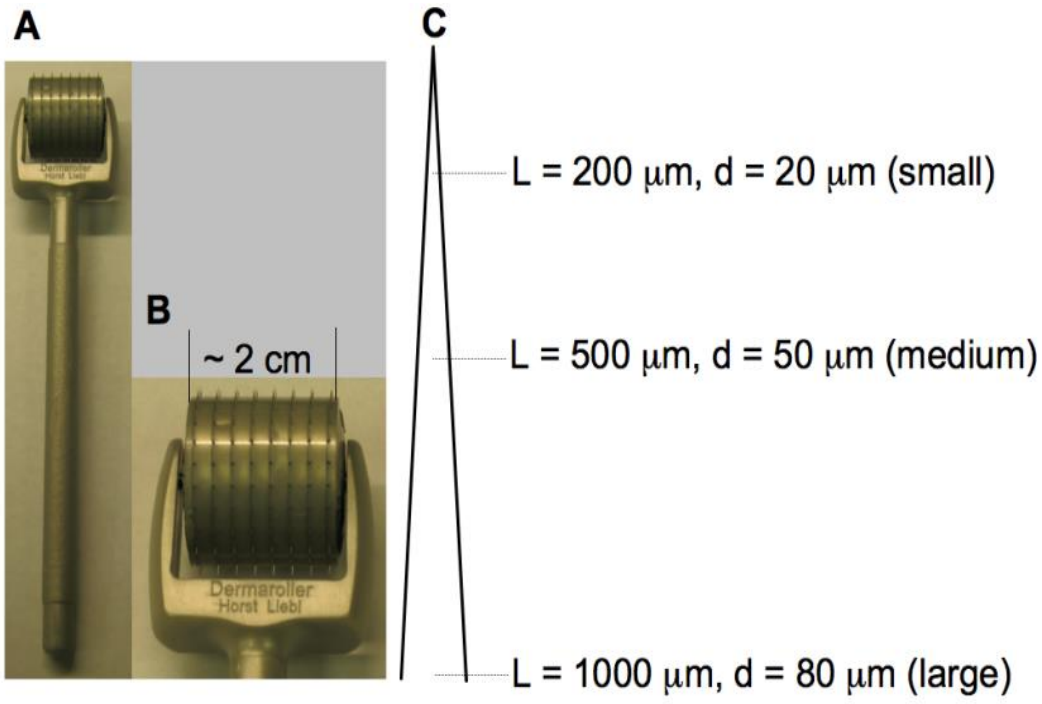

Figure 2.1 Digital photos of a Dermaroller® microneedle roller.

(A-B) Digital photos of a Dermaroller® microneedle roller (1000 μm long, base diameter of 80 μm). (C) A diagram of the microneedles on three different Dermaroller® microneedle rollers used (not to scale). L indicates the length of the microneedles; d is the base diameter of the microneedles.

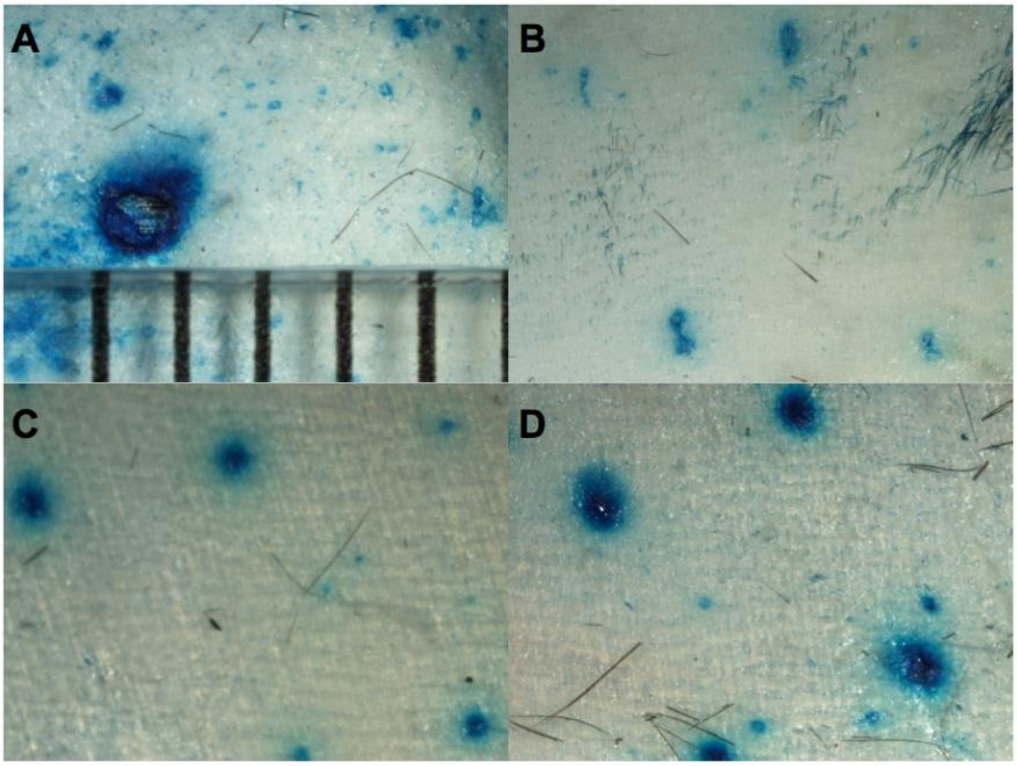

Figure 2.2 Magnified microscopic view of mouse skin after treatment with microneedles.

Magnified microscopic view of mouse skin after treatment with a 21 G hypodermic needle (A) or microneedle rollers with different size microneedles (small (B), medium (C), and large (D)). The skin was stained with methylene blue solution. The distance between the bars in A is 1 mm. All photos were taken under the same magnification.

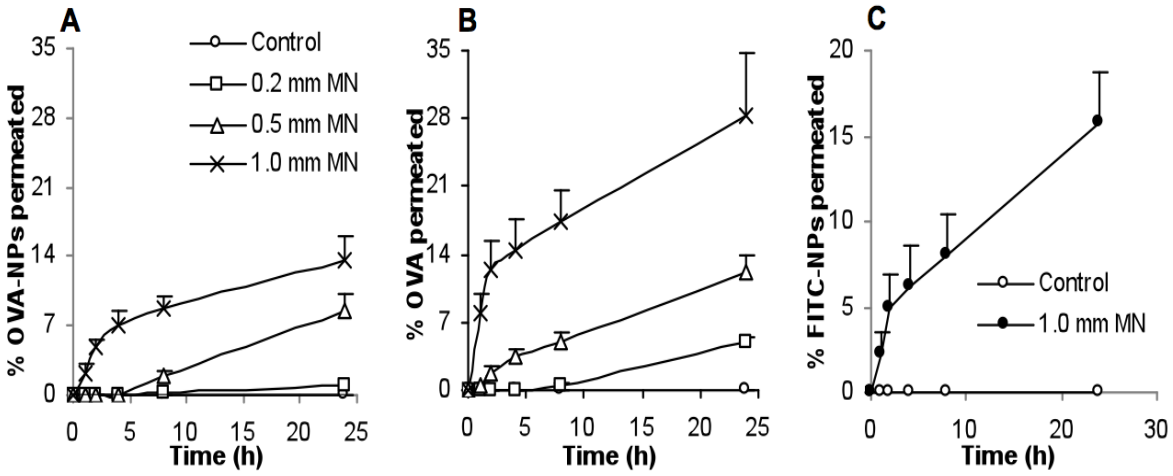

Figure 2.3 Permeation of OVA-NPs through microneedle treated skin.

Permeation of fluorescein-OVA-NPs (**A**), fluorescein-OVA (**B**), or fluorescein-NPs (OVA-free) (**C**) through mouse skin treated with different microneedles (small-200, medium-500, and large-1000 µm). MN represents microneedle. Data shown are mean ± S.E.M. (n = 5-7).

2.3.2 OVA-nanoparticles applied onto a mouse skin area pre-treated with microneedles induced a stronger OVA-specific antibody response than OVA alone

As shown in Fig. 2.4A, both OVA in solution or OVA-nanoparticles failed to induce an anti-OVA IgG response when dosed onto intact mouse skin (i.e., hair trimmed). However, pre-treatment with the microneedle roller with large microneedles (1000 μm long, base diameter of 80 μm) allowed both OVA alone and OVA-nanoparticles to induce an anti-OVA IgG response (Fig. 2.4A). Importantly, the anti-OVA IgG level in mice that received the OVA-nanoparticles was significantly higher than that in mice that received the OVA alone (Fig. 2.4A), demonstrating that when dosed onto a mouse skin area pre-treated with microneedles, formulating a protein antigen into nanoparticles can enhance its immunogenicity .

Bal *et al*. (2010) showed that microneedle-mediated delivery of DT incorporated into their TMC nanoparticles did not induce a strong antibody response than the DT alone [176]. Therefore, it does not appear that formulating any protein antigen in any nanoparticles will be beneficial. Many factors, including the physical, chemical, and immunological properties of the nanoparticles, antigen itself, and the dimension of the microneedles, may be responsible for the disagreement observed. Interestingly Bal *et al*. (2010) actually reported that when DT was physically mixed with the TMC nanoparticles and applied onto mouse skin pre-treated with microneedles, it induced a stronger anti-DT immune response than DT alone [176], promoted the authors to predict that conjugation of antigen with polymeric nanoparticles, instead of incorporation of antigens inside nanoparticles, could be a better option to further potentiate the immune responses by

microneedle-mediated vaccination [176]. Apparently, our data in Fig. 2.4A are supportive of their prediction. Therefore, more research on formulating the antigen of interest into the proper nanoparticles is warranted for a successful microneedle-mediated immunization with antigens carried by nanoparticles.

Shown in Fig. 2.4B are the anti-OVA IgG induced by the OVA-nanoparticles applied onto a mouse skin area pre-treated with different microneedle rollers. As expected, pre-treatment with the roller with large microneedles afforded the induction of a significantly stronger anti-OVA IgG response than with the rollers with small and medium microneedles (Fig. 2.4B). However, pre-treatment with the roller with small microneedle and the roller with medium microneedle did not lead to different levels of anti-OVA IgG responses (Fig. 2.4B). The *in vitro* diffusion data in Fig. 2.3A showed that the roller with medium microneedles (500 μm long, base diameter of 50 μm) allowed significantly more permeation of the OVA-nanoparticles than the roller with small microneedles (200 μm long, base diameter of 20 μm). It is possible that the amounts of OVA-nanoparticles that can permeate through the micropores created by those two different size microneedles were not different enough to be detected by measuring the resultant anti-OVA antibody levels. Therefore, it is likely that for any specific nanoparticle formulation, the optimal dimension of the microneedles to be used needs to identified individually.

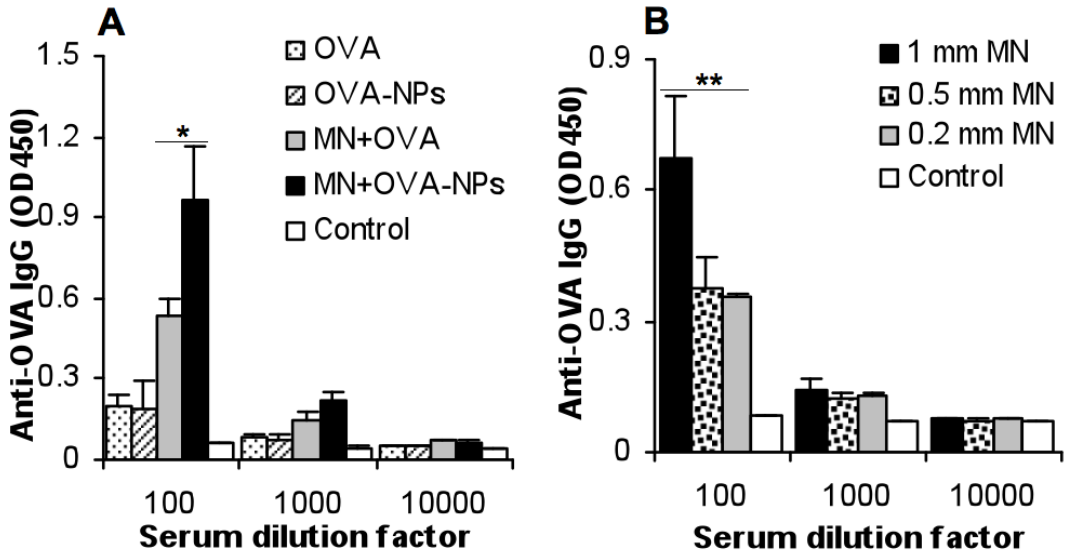

Figure 2.4 Immunization with OVA-nanoparticles.

(A) Serum anti-OVA IgG induced by OVA or OVA-NPs applied onto a skin area treated or un-treated with a microneedle roller (1000 µm long; base diameter of 80 µm). (B) Anti-OVA IgG induced by OVA-NPs applied onto a skin area treated with different microneedles. Data reported are mean ± S.E.M. from 5 mice per group. The dose of the OVA was 70 µg per mouse. Data reported in B are one week after the last immunization. MN indicates microneedle roller treatment. *, $p = 0.03$, MN+OVA vs. MN+OVA-NPs; **, $p = 0.0001$, ANOVA of the three different microneedles.

2.3.3 The dose of the OVA determines whether the OVA-nanoparticles were more immunogenic when applied onto a skin area pre-treated with microneedles or when injected subcutaneously using a hypodermic needle

In order to compare the antibody responses induced by the OVA-nanoparticles applied onto a skin area pre-treated with microneedles with the same OVA-nanoparticles applied by subcutaneous injection, mice were dosed with OVA-nanoparticles containing 10.5 μg of OVA initially. As shown in Fig. 2.5A, the anti-OVA IgG levels induced by the OVA-nanoparticles by subcutaneous injection or by transcutaneous immunization following the microneedle treatment were not significantly different ($p = 0.38$, 100 fold dilution). Moreover, it appeared that antibody response induced by the OVA-nanoparticles dosed onto a skin area pre-treated with microneedles was dose-dependent. For example, OVA-nanoparticles at a dose of 70 μg per mouse applied onto a skin area pre-treated with the microneedles induced a stronger anti-OVA IgG response than at a dose of 10.5 μg (Fig. 2.5A). However, when the OVA dose was increased from 10.5 μg per mouse to 70 μg per mouse, transcutaneous immunization following microneedle treatment induced a weaker anti-OVA IgG response than subcutaneous injection (Fig. 2.5B), indicating that the dose of the antigen determines whether transcutaneous immunization following microneedle treatment with antigens carried by nanoparticles is more immunogenic than subcutaneous injection. The dose of 70 μg OVA per mouse was initially selected because data from a previous study showed that subcutaneous immunization with 70 μg of OVA in OVA-conjugated nanoparticles induced a strong antibody response. The dose of 10.5 μg OVA (i.e., 15% of 70 μg) per mouse was used

later because the *in vitro* data in Fig. 2.3A showed that within 24 h, only about 15% of the OVA-nanoparticles permeated through a mouse skin area pre-treated with the roller with large microneedles. Of course it is likely that *in vivo,* less than 15% of the OVA-nanoparticles have permeated through the skin treated with the same microneedle roller due to factors such as accelerated closure of the micropores and the less than ideal permeation condition. Moreover, it is known that microneedle puncture is less efficient *in vivo* than *in vitro* because of the more flexible skin tissue, unflat skin surface, the cushioning effect of fat and muscle layers *in vivo* [209]. Nonetheless, transcutaneous immunization with a nanoparticle-based vaccine formulation onto a skin area pre-treated with microneedles has the potential to elicit a stronger immune response than by subcutaneous injection with a hypodermic needle.

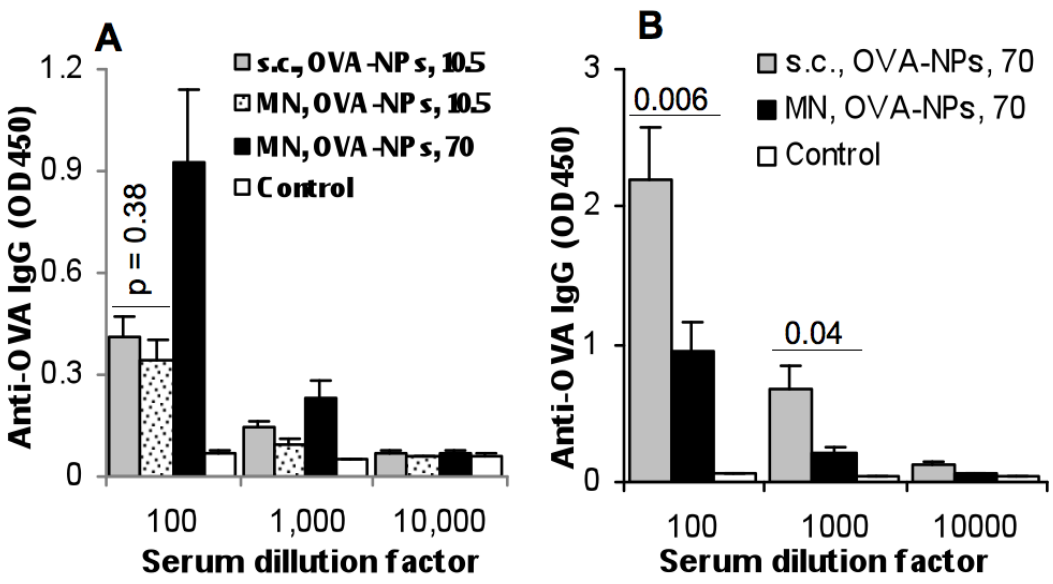

Figure 2.5 Effect of antigen dose on immune response.

The effect of the dose of the OVA as an antigen on the antibody responses induced by the OVA-NPs. Shown are anti-OVA IgG when the dose of the OVA in the OVA-NPs was 10.5 μg per mouse (**A**) or 70 μg per mouse (**B**). The microneedle roller used was the one with large microneedles. Data shown are mean ± S.E.M. from 5 mice per group.

2.3.4 Microneedle roller treatment reversibly increased the transepidermal water loss from the treated skin area

Microneedle treatment enhanced the permeation of protein-carrying nanoparticles into the treated skin area, but it was expected to alter the integrity of the skin as well. To evaluate the extent to which treatment with microneedle rollers had damaged the integrity of the skin, TEWL values were measured. As shown in Fig. 2.6, immediately after treatment with the microneedle rollers, the TEWL values in the treated skin area increased significantly, and the roller with larger microneedles led to a larger increase in TEWL value. The TEWL values then gradually decreased and reached a level similar to that of the intact skin within 24 h when the rollers with small and medium microneedles were used (Fig. 2.6), in agreement with what was previously reported [187]. However, it took a longer period of time, 48 h, for the TEWL value on the skin area pre-treated with the roller with large microneedles (1000 μm long, base diameter of 80 μm) to reach the intact level (Fig. 2.6).

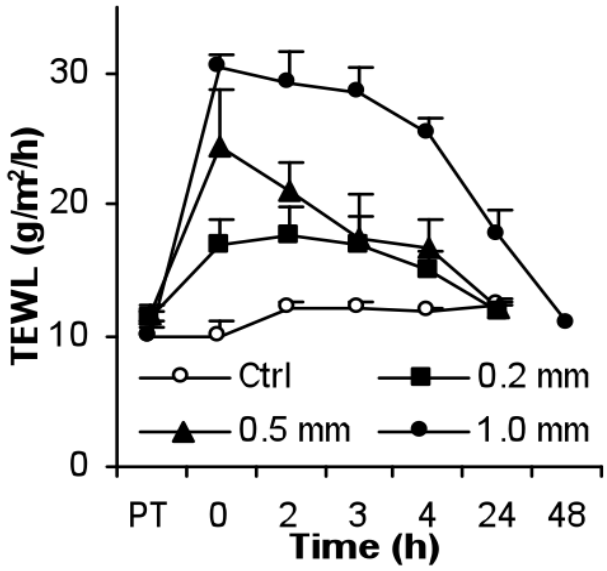

Figure 2.6 Transepidermal water loss of skin after treatment with microneedles.

TEWL values of the skin at different time points after treatment with different microneedles. PT = prior to treatment with microneedles. Ctrl = untreated. Data shown are mean ± S.E.M. (n = 4).

2.3.5 The micropores created by microneedles permit the permeation of live bacteria through the skin

The kinetics of the TEWL values in Fig. 2.6 confirmed that treatment with microneedles caused physical damages, although reversible, to the skin, which was previously known [187]. However, the relevancy of the reversible physical damage was not well understood. Specifically, it is unknown to what extent the micropores created by the microneedles may enhance the penetration of microbes through the treated skin area, considering that microbes such as bacteria and viruses are physically nanoparticles or microparticles present in the environment and on the skin surface. This information is clinically relevant as it will allow the prediction of the potential risks or lack of risks of microbial infections associated with treatment with microneedles. Recognizing this issue, Donnelly (2009) studied the *in vitro* permeation of radiolabeled microbes through porcine skin pre-treated with microneedles [206]. In their study, harvested porcine skin was saturated with bacteria and then treated with microneedles to evaluate the extent to which the microneedles can carry pre-existing microbes through the skin [206]. In the present study, an *ex vivo* system was devised to evaluate the extent to which pre-existing micropores created by the microneedles will allow the permeation of live bacteria through the skin. Anesthetized mice were treated with the microneedle rollers and immediately euthanized to harvest the treated skin samples, which were then used to evaluate the permeation of live non-pathogenic *E. coli* DH5α. *E. coli* is a rod-shaped bacterium of about 200-500 nm in diameter and 2 μm long, which is physically a nano-rod particle [210]. As shown in Fig. 2.7A, live *E. coli* DH5α bacterial cells can permeate

through the micropores created by the microneedle rollers on the skin, and pre-treatment with a roller with larger microneedles allowed the permeation of more bacteria. It was determined that using the present method, the microneedle rollers created about 250 pores per cm^2 on the treated skin area. The area in the Franz diffusion cells was 0.64 cm^2, which means that number of bacterial CFU shown in Fig. 2.7A represented the total number of bacteria permeated through roughly 160 micropores created by the microneedle rollers within 4 h. Data in Fig. 2.7B showed that the micropores created by the microneedles also closed rather quickly. Within 3-6 h after the microneedle treatment, the pores became impermeable for the *E. coli* bacteria, in agreement with what was previously reported that after microneedle treatment, skin recovers its barrier function within 3-4 h [211].

Data in Fig. 2.7A indicated that the number of *E. coli* bacterial cells permeated through the single pore created by a 21 G hypodermic needle within 4 h was equal to the number of *E. coli* permeated through the micropores (about 160) created by the roller with large microneedles (1000 μm long, base diameter of 80 μm) within the same period of time. In other words, one single pore created by the 21 G hypodermic needle was equivalent to about 160 micropores created by the roller with large microneedles. Clinically a 21 G needle is normally used to withdraw blood, and smaller needles are generally used for vaccination. It is expected that the risk of bacterial infections associated with microneedle treatment is more likely less than the risk associated with a hypodermic needle injection. Nonetheless, the finding in the present study does ascertain the need for sterilization of any formulation that is to be applied onto a skin area pre-

treated with microneedles and the need to keep the application area clean prior to and after the microneedle treatment. Of course, the microneedles *per se* should be pathogen-free as well.

All aforementioned experiments were carried out using C57BL/6 mice or their skin. It is known that human skin is significantly thicker than mouse skin. Therefore, any findings made in a mouse model will ultimately need to be validated in humans. Before transition to humans, porcine skin is a good model to more accurately predict what is expected in humans because porcine skin is very similar to human skin [212].

Finally, microneedles have been exploited in various ways to deliver vaccine : i) solid microneedles coated with vaccines, ii) dissolvable microneedles with vaccine incorporated in the needles, iii) hollow microneedle-based injection, and iv) the application of a vaccine formulation onto the skin prior to or after the skin area was treated with microneedles. At this moment, transcutaneous immunization on a skin area pre-treated with microneedles has the slight limitation of being a two-step procedure. However, it is not impossible that this limitation can be overcome by future creative engineering. Moreover, all four ways mentioned above have their own unique advantages and disadvantages [199]. Solid microneedles of sufficient strength are commercially available, and it is economical to mass produce them. However, coating of a particular vaccine onto solid microneedles must involve the reformulation to optimize the viscosity and protein concentration to avoid aggregation [199]. The long-term stability of dry coated microneedle vaccine is likely better than liquid injectables, but the stability of a particular vaccine is dependent on refined formulation and appropriate packaging [133].

In addition to these all, immunization through coated solid microneedle is also a multistep process. Immunization needs administration of needles, waiting time of 1-2 minutes to get the coating dissolved and finally application of a patch over the treated area. The manufacturing of dissolvable microneedles with sufficient strength is still a challenge, and laboratory scale production of dissolvable microneedles usually involves the melting of polymers at a high temperature that is detrimental to protein stability [213]. Hollow microneedles for injection suffer from the concerns of potential clogging, back pressure from densely packed skin layers and aggregation and syringeability for highly concentrated formulations [199]. In addition, the stability of the proteins and leakage issues during storage of prefilled hollow microneedles are still a practical concern [199]. Therefore, the perceived inconvenience associated with the two-step procedure of transcutaneous immunization prior to or after microneedle treatment should not preclude more research efforts. Moreover, knowledge learned using the solid microneedles is always transferable to other microneedle systems.

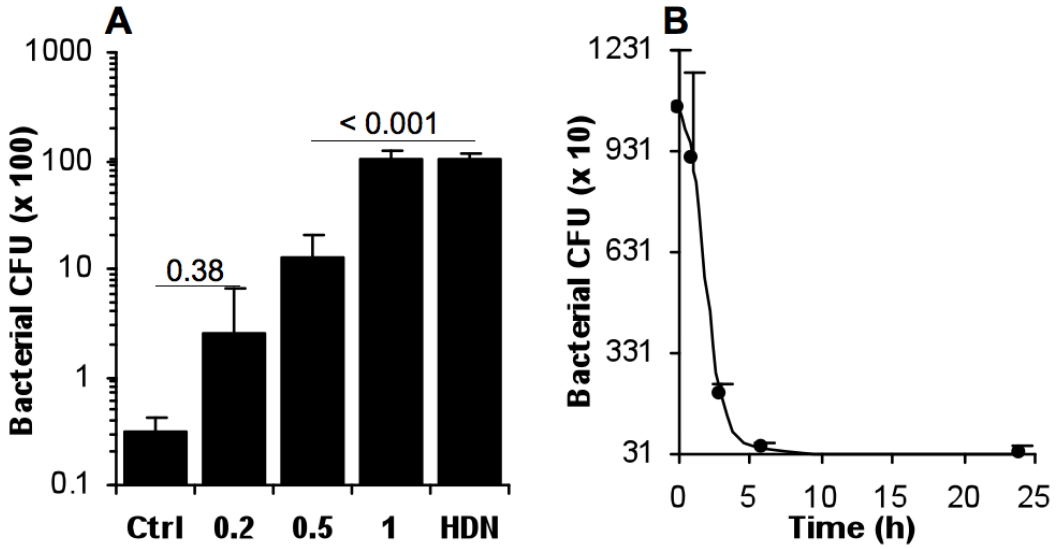

Figure 2.7 Permeation of *E. coli* DH5α through microneedle treated skin.

(A) Number of bacteria, indicated by bacterial CFU, permeated through the micropores created by different microneedles on an area of 0.64 cm^2. As controls, intact skin or skin with a single pore created by a 21 G hypodermic needle (HDN) were used. (B) Number of bacteria (CFU) permeated through micropores created by the roller with large microneedles at different time after the microneedle treatment. All numbers were after 4 h of permeation. Data shown are mean ± S.D. (n = 3).

2.4 Conclusion

Pre-treatment with microneedles allowed skin permeation of nanoparticles with antigen protein conjugated on them. Transcutaneous immunization onto a skin area pre-treated with microneedles with the protein antigen carried by nanoparticles induced a stronger antigen-specific antibody response than with the protein antigen alone. The dose of the antigen used to immunize mice determined whether the microneedle-mediated immunization can induce a stronger immune response than when same nanoparticle-based vaccine formulation was dosed by subcutaneous injection. The damage to the physical integrity of the skin caused by the microneedles, though reversible, may permit the permeation of live bacterial cells through the skin, but the risk of bacterial infections associated with microneedles is not expected to be higher than that associated with injection with a hypodermic needle. With the increasing interest in nanoparticles as a drug delivery system, more research on skin permeation of nanoparticles prior to or after microneedle treatment is warranted.

Chapter Three

Microneedle-mediated transcutaneous immunization with plasmid DNA coated on cationic PLGA nanoparticles

Journal of Controlled Release, Oct 2012, 163 (2), 230-239.

3.1 Introduction

Microneedle-mediated transcutaneous immunization has evolved as a promising immunization modality to induce strong immune responses using a very low dose of antigen/vaccine [132]. Immunization with plasmid DNA is one of the most promising applications of gene therapy [214]. Normally, DNA immunization is carried out by intramuscular injection of naked plasmid DNA [26]. However, Mikszta et al. (2002) reported that microneedle-mediated transcutaneous immunization with naked plasmid DNA can potentially induce a stronger immune response than hypodermic needle-based intramuscular injection of the same plasmid DNA [151]. The present study was designed to test whether microneedle-mediated transcutaneous immunization with plasmid DNA coated on the surface of cationic nanoparticles will induce a stronger immune response than with plasmid DNA alone. Data from numerous previous studies have shown that coating of plasmid DNA onto cationic nanoparticles can significantly enhance the resultant immune responses, including when plasmid DNA-coated nanoparticles were applied topically onto the skin [84, 170, 171]. However, it remains unknown whether microneedle-mediated transcutaneous immunization with DNA carried by cationic nanoparticles is more effective than with the naked DNA alone. Microneedle-mediated transcutaneous DNA immunization has mainly been performed using plasmid DNA

coated on solid microneedles [131, 136, 158], which allowed the physical delivery of the DNA directly into the skin. Another method of microneedle-mediated transcutaneous immunization is to apply vaccines or antigens onto a skin area before or after treatment with solid microneedles. This method of transcutaneous immunization allows the administration of a large amount of antigens topically. Mass production of solid microneedles is commercially feasible, and solid microneedle rollers are currently being used in humans already. Moreover, data from several recent studies showed that nanoparticles can permeate through the micropores created by microneedles [110, 188], and transcutaneous immunization with protein antigens carried by nanoparticles onto a skin area pretreated with microneedles is feasible [147, 176, 215]. Therefore, in the present study, we carried out transcutaneous immunization by applying plasmid DNA coated on cationic nanoparticles onto a skin area pretreated with microneedles.

The plasmid DNA was carried by cationic nanoparticles prepared with poly (lactic-*co*-glycolic acid) (PLGA) and 1,2-dioleoyl-3-trimethylammonium-propane (DOTAP), both are biocompatible. DNA is negatively charged under neutral pH. When mixed with cationic nanoparticles, it binds to the nanoparticles by electrostatic interaction. The net charge of the resultant plasmid DNA-cationic nanoparticle complexes is influenced by the ratio of the plasmid DNA to cationic nanoparticles in the mixture. We prepared net positively charged and net negatively charged plasmid DNA-nanoparticle complexes, which allowed us to evaluate the effect of the surface charge of the DNA-nanoparticle complexes on (i) their *in vitro* permeation through a skin area

pretreated with microneedles and (ii) the immune responses induced by plasmid DNA coated on the nanoparticles *in vivo*, which has rarely been studied before.

3.2 Materials and methods

3.2.1 Materials

Dermaroller® microneedle roller was from Cynergy, LLC (Carson City, NV). There are 192 needles (1000 μm in length, 80 μm in base diameter) on the roller. The β-galactosidase gene-encoding pCMV-β was from American Type Culture Collection (ATCC, Manassas, VA) [216], and the anthrax protective antigen (PA63)-encoding pGPA plasmid was kindly provided by Dr. Dennis Klinman [217]. Large scale plasmid preparation was performed by GenScript (Piscataway, NJ). PLGA (Resomer RG 504H), acetone, pluronic F68, 3,3',5,5'-tetramethylbenzidine (TMB) solution, sodium bicarbonate, sodium carbonate, Tween 20, phosphate-buffered saline (PBS) and fetal bovine serum (FBS) were from Sigma-Aldrich (St. Louis, MO). Horse serum, penicillin, streptomycin and picogreen were from Invitrogen (Carlsbad, CA). DOTAP and 1,2-dioleoyl-sn-glycero-3-phosphoethanolamine-N-carboxyfluorescein (DOPE-fluorescein) were from Avanti Polar Lipids, Inc. (Alabaster, AL). Mouse IL-4 and IFN-γ ELISA sets were from BD Biosciences (San Diego, CA). Goat anti-mouse IgG, IgM, IgA, IgE, IgG1 and IgG2a were from Southern Biotechnology Associates, Inc. (Birmingham, AL).

3.2.2 Preparation of cationic PLGA nanoparticles

The cationic PLGA nanoparticles were prepared by the nanoprecipitation-solvent evaporation method [172]. PLGA polymer (3-20 mg) and DOTAP (0-40 mg) were accurately weighed and dissolved in acetone (2 ml). The organic phase was added drop

wise into 10 ml of 1% pluronic F68 (as a hydrophilic stabilizer) with moderate stirring (800 rpm) for 3 h at room temperature until acetone is completely evaporated to form nanoparticles. Unentrapped DOTAP was removed by ultracentrifugation (23,000 rpm, 4°C, 45 min). The resultant nanoparticles were resuspended in 200 µl water. DOTAP-free nanoparticles were prepared similarly, except that DOTAP was not included in the acetone. To fluorescently label the nanoparticles, DOPE-fluorescein (5%, v/v) was included in the PLGA and DOTAP mixture during the nanoparticle preparation. The size and zeta potential of the nanoparticles were determined using a Malvern Zetasizer® Nano ZS (Westborough, MA). The morphology and size of the cationic nanoparticles were examined as previously described using an FEI Tecnai Transmission Electron Microscope (TEM) [218].

3.2.3 Determination of the final concentration of DOTAP in cationic nanoparticles

The DOTAP concentration was determined according to a previously described colorimetric method [219]. Briefly, 1% methyl orange (0.25 ml) was reacted with DOTAP in the presence of chloroform (6.5 ml) and a buffer solution (1.25 ml, 0.5 M citric acid and 0.2 M disodium hydrogen orthophosphate) to produce a yellow color complex. The intensity of the yellow color is proportional to the concentration of the methyl orange-DOTAP complexes measured spectrophotometrically at 415 nm.

3.2.4 Coating of plasmid DNA on the surface of the cationic nanoparticles

Plasmid DNA (pCMV-β or pGPA) was coated on the surface of the cationic nanoparticles by gently mixing equal volumes of cationic nanoparticles in a suspension with plasmid DNA in a solution to obtain a final DNA concentration of 200 µg/ml. To identify the appropriate ratios for the preparation of the net positively and net negatively charged DNA-coated PLGA nanoparticles, an increasing amount of nanoparticles (0.001-0.12 mg) were mixed with a fixed amount of DNA (1 µg), and the mixture was incubated for at least 30 min at room temperature for the adsorption of the DNA onto the surface of the nanoparticles [170].

3.2.5 Stability of the plasmid DNA coated on the nanoparticles

To estimate the degree to which the plasmid DNA coated on the nanoparticles was protected from DNase I digestion, net positively and net negatively charged pCMV-β-nanoparticle complexes containing 10 µg of pCMV-β were treated with 1 unit of DNase I (Fermentas, Glenn Burnie, MD) at 37°C in 400 µl reaction buffer (10 mM Tris–HCl, pH 7.5, 2.5 mM $MgCl_2$) for 30 min. The samples obtained were separated on a 1% agarose gel with ethidium bromide for 1 h at 100 V. Images were acquired using a high performance UV trans-illuminators (UVP LLC, Upland, CA). DNA alone, treated or untreated with DNase I, was used as a control.

3.2.6 *In vitro* permeation of DNA-coated nanoparticles through mouse skin pretreated with microneedles

In vitro permeation study was performed using jacketed Franz diffusion cells with a 0.64-cm^2 diffusion area [110]. The lower dorsal skin of BALB/c mice was used for all permeation studies. Hair was trimmed 24 h before the collection of the skin. Skins were stored at -20^oC for a maximum period of one month. The fat layer of skin was carefully removed. The skin was then placed onto the flat surface of a balance, and the microneedle roller was rolled in 4 perpendicular lines over the skin surface, 5 times each for a total of 20 times, with an applying pressure of 350-400 g [147, 207]. The pressure was constantly monitored using the balance. Treated skin area was then clamped in between the donor and the receiver compartments of the Franz diffusion cell (PermeGear, Inc., Hellertown, PA), dorsal side facing the donor compartment. The donor compartment was filled with pCMV-β alone or pCMV-β-coated net positively or net negatively charged nanoparticles in water (250 µl). The amount of pCMV-β plasmid placed into the donor compartment was 50 µg. The receiver compartment was filled with 5 ml of PBS (pH 7.4, 10 mM), which was constantly stirred with a magnetic stirrer, and the temperature was maintained at 37^oC with the help of a Haake SC 100 Water Circulator from ThermoScientific (Wellington, NH). This maintained the skin surface temperature at 32°C [116]. At various time points, samples (150 µl) were withdrawn from the receiver compartment and immediately replenished with the same volume of fresh PBS. The amount of plasmid diffused into the receiver compartment was determined using picogreen dye and a BioTek Synergy^{TM} HT Multi-Mode Microplate Reader (Winooski, VT). As a control, the permeation of DNA through intact skin was also evaluated.

3.2.7 *In vitro* release of plasmid from the nanoparticles

Net positively charged and net negatively charged DNA-coated nanoparticles with 10 μg of pCMV-β were incubated in 1 ml water at 37°C. At time points 2, 4, 10 and 24 h, the particles were centrifuged to collect the supernatant. One milliliter fresh water was added immediately back to the vials to resuspend the pellets. The amount of DNA in the supernatant was determined using picogreen.

3.2.8 *In vitro* transfection of DC2.4 cells

DC2.4 cells were from ATCC and maintained in RPMI1640 medium with 10% FBS, 10 U/ml of penicillin, and 100 μg/ml of streptomycin. On day 1, cells (20,000 per well) were plated in a 24-well plate and incubated overnight at 37^{o}C, 5% CO_2. On day 2, cells were incubated with the DNA formulations containing 0.3 μg/well of pCMV-β in a total volume of 400 μl culture medium. Four hours later, the medium was replaced with fresh medium, and the cells were incubated overnight. Cells were washed with PBS and harvested. Cell pellets were resuspended in a lysis buffer (20 mM Tris, 100 mM NaCl, 1 mM EDTA, 0.5% Triton X-100) and then freeze-and-thawed 3 times. Insoluble materials were removed by centrifugation (14,000 rpm, 4°C, 5 min), and supernatant was collected. β-Galactosidase activity was measured in the supernatant using a β-gal assay kit following the manufacturer's instruction (Invitrogen). The total protein content in the supernatant was determined using Bradford reagent (Sigma-Aldrich) [84].

3.2.9 *In vitro* cellular uptake study

DC2.4 cells (2.5 x 10^4/well) were seeded in a 24-well plate and incubated at 37°C, 5% CO_2 overnight. The pCMV-β plasmid, labeled using a *Label* IT® fluorescein nucleic acid labeling kit (Mirus, Madison, WI), was complexed with cationic nanoparticles to form net positively and net negatively charged nanoparticles. Cells were incubated with the nanoparticles for 4 h at 37°C, 5% CO_2, washed 3 times with warm PBS, and re-suspended in 200 µl cell lysis buffer. The amount of pCMV-β added was 2 µg/well. The cell lysates were transferred to a clear bottom black side 96-well plate (Corning, NY), and the fluorescence intensities of the samples were measured at 485/528 nm using BioTek Synergy® Multi-Mode Microplate Reader. Data are reported as % cell uptake, which was calculated using a standard curve generated from known concentrations of fluorescein-labeled DNA [220].

3.2.10 Fluorescence microscopy

DC2.4 cells (1.5 x 10^5) were seeded on poly-D-lysine-coated glass cover slips and incubated in 6-well plates at 37°C, 5% CO_2 for 24 h. After the cells were adhered to the cover slips, they were treated with fluorescein-labeled pCMV-β alone or fluorescein-labeled pCMV-β-coated nanoparticles and incubated for 4 h at 37°C, 5% CO_2. For the net positively charged nanoparticles, cells were incubated for only 1 h. After the incubation, cells were washed three times with PBS and fixed with paraformaldehyde (3% in PBS) for 20 min at room temperature. The cover slips were again washed with warm PBS for 3 times and mounted onto clean glass slides using Vectashield H-1200 with 4´,6-diamidino-2-phenylindole (DAPI) (Vector laboratories, Burlingame, CA). Slides were

observed under an Olympus BX60 microscope (Olympus America, Inc., Center Valley, PA).

3.2.11 Immunization studies

All animal studies were carried out following the National Institutes of Health guidelines for animal care and use. The animal protocol was approved by the Institutional Animal Care and Use Committee at The University of Texas at Austin. Female BALB/C (8-10 weeks), female hairless SKH1-Elite mice (14-16 weeks) or female C57BL/6 mice (8-10 weeks) were from Charles River (Wilmington, MA). Mice (n = 5/group) were immunized 3 times with either plasmid DNA or DNA-coated nanoparticles topically on an area treated with the microneedle roller. Briefly, 24 h prior to the initiation of the immunization, hair, if any, in the dorsal side of mice was carefully trimmed. Mice were anesthetized, the targeted skin area was wiped with an alcohol swab, and a 2-cm^2 area was marked on the lower dorsal skin surface. Mice were placed onto the flat surface of a balance, and the microneedle roller was rolled in two perpendicular lines over the marked skin surface, 10 times each, for a total of 20 times [147, 187], with an applying pressure of 350-400 g, which was measured using the balance. Plasmids alone or plasmid-coated nanoparticles in water were carefully dripped onto the microneedle-treated area, which were then covered with a piece of self-adhesive Tegaderm® patch (3 M, St. Paul, MN) [221]. The Tegaderm patch was carefully removed 24 h later. Immunization was repeated 10 or 14 days apart for two more times. As a positive control, a group of mice were intramuscularly (gastrocnemius muscles) injected 3 times with plasmid alone or plasmid-

coated net positively charged nanoparticles. Three weeks (or as where mentioned) after the last immunization, mice were bled to collect serum samples. Antibody response in blood serum was determined using enzyme-linked immunosorbent assay (ELISA) as previously described [200].

3.2.12 *In vitro* cytokine release and splenocyte proliferation assays

Splenocyte preparation, cytokine release, and splenocyte proliferation assays were performed as previously described [84, 100]. Splenocytes (3×10^6 per well) were stimulated with 0 or 10 µg/ml of β-galactosidase for 48 h at 37°C, 5% CO_2 before measuring cytokines (IL-4 and IFN-γ) in the supernatant using ELISA kits. Splenocytes (3×10^6 per well) were stimulated with 0 or 10 µg/ml of β-galactosidase for 120 h at 37°C, 5% CO_2 before measuring cell numbers using an MTT assay [222].

3.2.13 Expression of MHC I/II and CD80/86 molecules on BMDCs

Bone marrow dendritic cells (BMDCs) were generated from bone marrow precursors obtained from femur bones of C57BL/6 mice [223]. Fully grown BMDCs were seeded into 6-well plate (10,000 cells/well) and incubated overnight at 37°C, 5% CO_2. Cationic nanoparticles (200 µg per well), net positively charged nanoparticles (5 µg pCMV- β/well), net negatively charged nanoparticles (5 µg plasmid/well), or DNA alone (5 µg well) were added in the well, and the cells were incubated for 15 h at 37°C, 5% CO_2. As controls, cells were also treated with PBS or lipopolysaccharides from *E. coli* (LPS, 200 ng/well, Sigma-Aldrich). Cells were washed with a staining buffer (1% FBS

and 0.1% NaN_3 in PBS, BD Pharmingen), stained with anti-CD80, anti-CD86, anti-I-A[b] MHC II, or anti-H-2Kb MHC I Ab for 20 min at 4^{o}C, washed again with staining buffer, and analyzed with a Guava EasyCyte 8HT microcapillary flow cytometer (Millipore Corporation, Hayward, CA).

3.2.14 *In vivo* uptake and expression of pCMV-β plasmid, alone or coated on nanoparticles

Mice (n = 3/group) were treated with microneedle as mentioned previously, and pCMV-β alone or pCMV-β-coated nanoparticles (20 μg/mouse), was carefully applied onto the microneedle-treated area. Twenty-four hours later, the treated skin area was washed with water for 5 min and then carefully dissected. One half of the skin was used for the extraction of total RNA, while the another half was used to extract total DNA. Total cellular RNA was isolated from skin tissues using TRIzol reagent (Invitrogen). Isolated RNA was reversed transcribed with random hexamers using the SuperScript first-strand synthesis system (Invitrogen). Real-time PCR of β-galactosidase gene was carried out using the Power SYBR Green PCR Master Mix kit (Applied Biosystems, Foster City, CA) with the following primers: 5′-TTG ATC CGT TGT TCT TGT CA-3′ (forward) and 5′-GGC CAG GAA ATA CAA GAC AA-3′ (reverse). All samples were normalized to β-actin (5′-TTG ATC CGT TGT TCT TGT CA-3′ (forward) and 5′-GGC CAG GAA ATA CAA GAC AA-3′ (reverse)). Data were analyzed using the Applied Biosystems ViiA^{TM} 7 Software (Applied Biosystems). Genomic DNA was extracted from skin tissues using DNAzol reagent (Qiagen, Valencia, CA). Real-time PCR was carried

out as mentioned above. Each 20-µl reaction contained 500 ng of genomic DNA, 100 nM of each primer, and 10 µl of 2x SYBR Premix (Applied Biosystems).

3.2.15 Statistical analysis

Statistical analyses were performed using analysis of variance followed by Fisher's protected least significant difference procedure. A P value of ≤ 0.05 (two-tailed) was considered statistically significant.

3.3 Results and discussion

3.3.1 Preparation and characterization of cationic PLGA nanoparticles

Plasmid DNA-coated nanoparticles were prepared by coating pre-prepared cationic PLGA nanoparticles with plasmid DNA. PLGA nanoparticles were prepared by the nanoprecipitation-solvent evaporation method. As shown in Fig. 3.1A, the size of PLGA nanoparticles was dependent on the concentration of PLGA used. Decreasing the concentration of PLGA resulted in smaller nanoparticles, in agreement with findings by Chorny et al. [224] and Nafee et al. [225]. With 1.5 mg/ml of PLGA, nanoparticles of 46 ± 1 nm were obtained (Fig. 3.1A).

Nanoparticles prepared with less than 1.5 mg/ml PLGA were not reproducible. Therefore, 1.5 mg/ml of PLGA was used to prepare cationic nanoparticles by including various amount of the cationic DOTAP lipid. As shown in Fig. 3.1B, the concentration of DOTAP significantly affected the size and zeta potential of the resultant nanoparticles; increasing the concentration of DOTAP increased the size and zeta potential of the resultant nanoparticles. The size and zeta potential of the nanoparticles stopped increasing when about 1 mg/ml of DOTAP was used (i.e., between 0.62 mg/ml to 1.25 mg/ml) (Fig. 3.1B). In the end, the PLGA nanoparticles prepared with 20 mg/ml of DOTAP were selected to coat plasmid DNA, because in our pilot studies, nanoparticles prepared using less than 20 mg/ml DOTAP were not able to bind sufficient amount of plasmid DNA onto their surface, which is required for *in vivo* studies [226]. The final amount of DOTAP remaining in the PLGA nanoparticles was determined to be 1.5 %.

Thus, the theoretical PLGA/DOTAP ratio in the nanoparticles was 5:1 (w/w). Fig. 3.1C is a typical TEM picture of the cationic PLGA nanoparticles, which were spherical and uniform in size, with a diameter of less than 100 nm. The size of the cationic nanoparticles did not significantly change after one month of storage at room temperature or at 4°C (data not shown). The polydispersity index of nanoparticles did not change as well (data not shown).

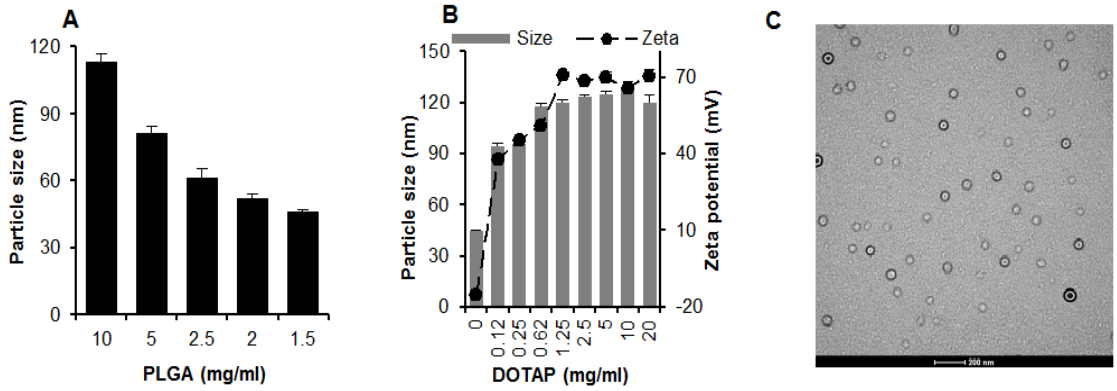

Figure 3.1 Preparation and characterization of cationic nanoparticles.

(A) The effect of the concentration of PLGA on the size of PLGA nanoparticles. (B) The effect of the concentration of DOTAP on the size and zeta potential of the cationic nanoparticles. (C) A typical TEM of cationic nanoparticles (bar = 200 nm). Data reported in A + B are mean ± S.E.M. (n = 3).

3.3.2 Preparation and characterization of plasmid DNA-coated PLGA nanoparticles

A study was performed to identify the effect of the ratio of the cationic nanoparticles to plasmid DNA on the size and zeta potential of the resultant DNA-nanoparticle complexes. To accomplish this, an increasing amount of cationic nanoparticles (0.001-0.12 mg) were mixed with a fixed amount of pCMV-β (1 μg), and the size and zeta potential of the resultant complexes were determined. The sizes of the resultant DNA-nanoparticle complexes were around 115 nm for all ratios tested, except that for the 10:1 ratio (i.e., 0.01 mg NPs), a relatively larger size was observed (Fig. 3.2A). In fact, at the 10:1 ratio, the zeta potential of the DNA-nanoparticle complexes was close to zero, suggesting that the larger particle size was likely a result of particle aggregation [170]. The DNA-nanoparticle complexes prepared at 2:1 and 40:1 ratios were used to prepare net negatively charged ((-) NP) and net positively charged ((+) NP) plasmid DNA-coated nanoparticles, respectively, for further studies. At room temperature, both net positively and net negatively charged DNA-coated nanoparticles were stable in an aqueous suspension (data not shown). In order to evaluate whether the DNA coated on the surface of the nanoparticles was protected from enzymatic degradation, the DNA-coated nanoparticles were incubated with DNase I for 30 min. As shown in Fig. 3.2B, free DNA was completely digested after incubation with DNase I, while the DNA that was coated on the surface of the nanoparticles was protected, to a certain extent, from DNase digestion. The level of protection was higher for the net positively charged pCMV-β-coated nanoparticles (lane 1) than for the net negatively charged nanoparticles (lane 2).

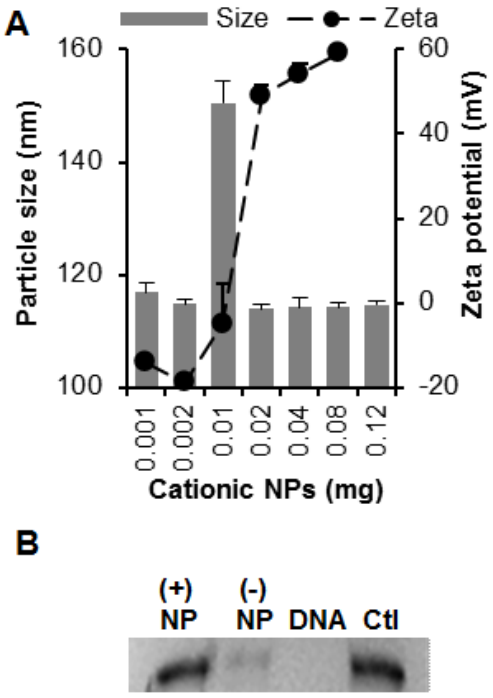

Figure 3.2 Preparation and characterization of plasmid DNA-coated nanoparticles. (A) The size and zeta potential of pCMV-β-cationic nanoparticle complexes at various nanoparticles to plasmid ratios. An increasing amount of cationic nanoparticles (0.001-0.12 mg) were mixed with a fixed amount of DNA (1 µg) in equal volumes and allowed to incubate at room temperature for at least 30 min before measuring size and zeta potential. All data reported are mean ± S.E.M. (n = 3). (B) Agarose gel electrophoresis assessing the stability of pCMV-β coated on the cationic nanoparticles. (+) NP, pCMV-β-coated net positively charged nanoparticles; (-) NP, pCMV-β-coated net negatively charged nanoparticles; DNA, pCMV-β alone; Ctl, pCMV-β not treated with DNase I.

3.3.3 Cationic PLGA nanoparticles facilitated the cellular uptake of plasmid DNA coated on their surface

To evaluate the extent to which the cationic PLGA nanoparticles can deliver plasmid DNA coated on their surface into antigen-presenting cells (APC), the uptake of fluorescein-labeled pCMV-β, alone or coated on the cationic PLGA nanoparticles, by dendritic cells (DC2.4) was measured. As expected, the uptake of free pCMV-β by DC2.4 cells was minimal (Fig. 3.3A). However, coating of pCMV-β on the nanoparticles significantly increased its uptake by DC2.4 cells, especially for the net positively charged pCMV-β-coated nanoparticles (Fig. 3.3A).

Fluorescence microscopic data also confirmed the enhancement of the uptake of the pCMV-β by coating it on the cationic PLGA nanoparticles. As shown in Fig. 3.3B, the green fluorescence signal was significantly stronger in DC2.4 cells that were incubated with the net positively charged pCMV-β-coated PLGA nanoparticles for only 1 h than in DC2.4 cells that were incubated with the net negatively charged pCMV-β-coated PLGA nanoparticles for even 4 h. For a comparison, a green fluorescence signal was not detected in DC2.4 cells incubated with the free fluorescein-labeled pCMV-β alone (Fig. 3.3B).

Finally, the ability of the cationic PLGA nanoparticles to deliver plasmid DNA coated on their surface into cells was further evaluated by measuring the expression of β-galactosidase gene in DC2.4 cells. As expected, β-galactosidase activity was not detected in cells incubated with pCMV-β alone, but was significantly higher in cells that were incubated with pCMV-β coated on PLGA nanoparticles (Fig. 3.3C). The β-galactosidase

activity in cells transfected with the net negatively charged pCMV-β-coated PLGA nanoparticles was comparable to that in cells transfected with the net positively charged pCMV-β-coated PLGA nanoparticles (Fig. 3.3C), despite that the uptake of the DNA in the net positively charged pCMV-β-coated PLGA nanoparticles was significantly higher than that in the net negatively charged pCMV-β-coated PLGA nanoparticles (Fig. 3.3A). This is likely because the incubation time with the nanoparticles in cell uptake experiment was only up to 4 h, whereas the transfection study was performed for a longer time period (24 h). In addition, in the transfection study, we measured the β-galactosidase activity, not the amount of β-galactosidase. It is possible that above certain level, the amount of β-galactosidase protein in a sample and its activity measured are not directly proportional.

Taken together, it is clear that the cationic PLGA nanoparticles increased the cellular uptake of plasmid DNA coated on their surface *in vitro*, and the net positively charged DNA-coated PLGA nanoparticles were more effective than the net negatively charged DNA-coated nanoparticles in increasing the cellular uptake of the plasmid DNA, likely because of the strong electrostatic interactions between the net positively charged nanoparticles and the negatively charged cell surface [227].

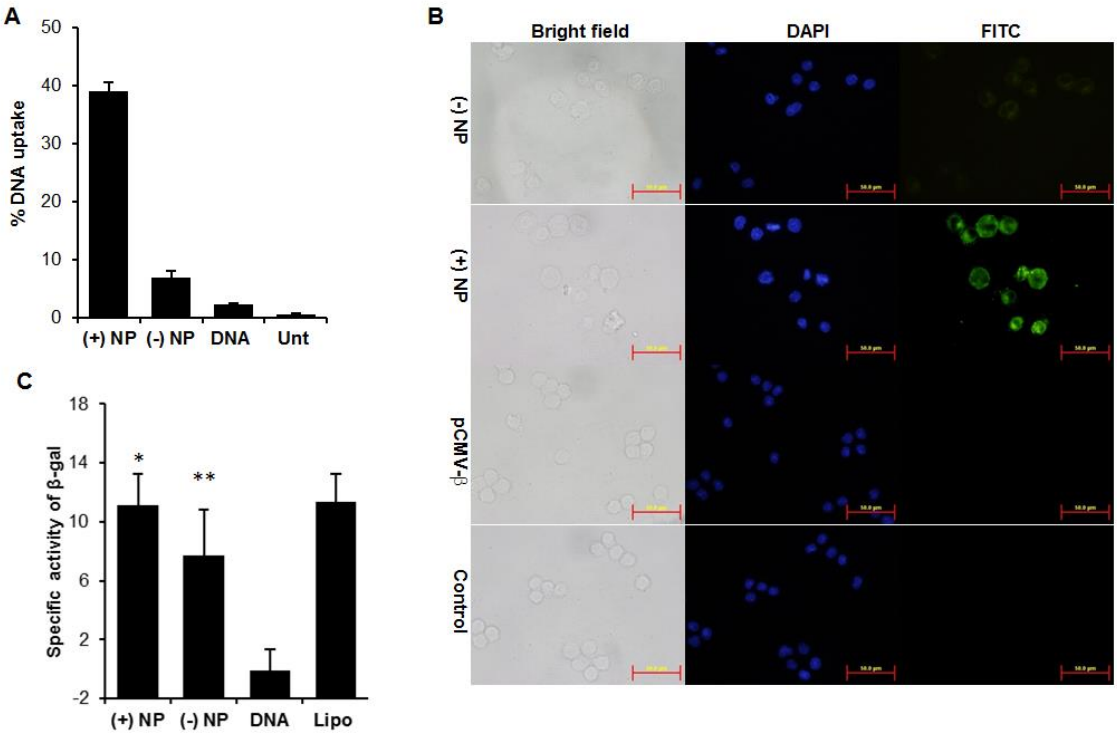

Figure 3.3 *In vitro* uptake and transfection of plasmid DNA coated nanoparticles.

In vitro uptake of plasmid DNA coated on nanoparticles by DC2.4 cells. (A) DC 2.4 cells were incubated with fluorescein-labeled pCMV-β-coated nanoparticles or fluorescein-labeled pCMV-β alone for 4 h, and the extent of nanoparticle uptake was determined by measuring the fluorescence intensity. (B) Fluorescent microscopic images of DC 2.4 cells after up to 4 h of incubation with pCMV-β-coated nanoparticles or pCMV-β alone. For the net positively charged pCMV-β-coated nanoparticles, cells were incubated for only 1 h. Cell nucleus was stained with DAPI (blue). pCMV-β was labeled with FITC (green). (C) *In vitro* transfection of DC 2.4 cells with pCMV-β-coated nanoparticles, pCMV-β alone, or pCMV-β complexed with Lipofectamine. (*, $p = 0.94$, (+) NP vs. Lipo; **, p =

0.34, (-) NP vs. Lipo). Data shown are mean ± S.E.M. (n = 4 in A, 8 in C). Lipo, pCMV-β complexed with lipofectamine; Unt, Untreated.

3.3.4 Pretreatment of mouse skin with microneedles allowed the permeation of plasmid DNA coated on the surface of cationic PLGA nanoparticles through the skin *in vitro*

To evaluate the extent to which plasmid DNA coated on the surface of the cationic PLGA nanoparticles can permeate into mouse skin pretreated with microneedles, the diffusion of pCMV-β, alone or coated on the cationic PLGA nanoparticles, through a mouse skin area pretreated with microneedles was measured. As shown in Fig. 3.4A, pCMV-β, alone or coated on the nanoparticles, was not able to permeate through intact skin (i.e., skin that was not pretreated with microneedles), but it can permeate through the skin that was pretreated with microneedles. The permeation of the naked pCMV-β plasmid was more extensive than the pCMV-β coated on the cationic PLGA nanoparticles (Fig. 3.4A). Moreover, the permeation of pCMV-β on the net negatively charged pCMV-β-coated PLGA nanoparticles through the skin pretreated with microneedles was more extensive than the permeation of pCMV-β on the net positively charged pCMV-β-coated PLGA nanoparticles (Fig. 3.4A). For example, 19.6 ± 3.5% of pCMV-β that was on the net negatively charged pCMV-β-coated PLGA nanoparticles permeated through the microneedle-treated mouse skin within 8 h, as compared to only 12.1 ± 2.8% for the pCMV-β on the net positively charged pCMV-β-coated PLGA nanoparticles during the same period (Fig. 3.4A).

To confirm that it was the DNA-coated nanoparticles that permeated through micropores, not the DNA alone released from the DNA coated nanoparticles, the permeation of the fluorescein-labeled net positively charged nanoparticles (i.e.,

nanoparticle were labeled with fluorescein) was also monitored. As shown in Fig. 3.4B, almost 6.5 ± 1.1% of net positively charged nanoparticles permeated through the microneedle-treated mouse skin within 8 h, which indicates that it was the DNA-coated nanoparticles that were permeating through the skin, not just the DNA alone released from the nanoparticles. The permeation of net positively charged nanoparticles determined by this method was found less, as compared to the permeation of net positively charged nanoparticles determined by measuring plasmid DNA using picogreen (Fig. 3.4A), likely because some of the DNA may have been released from the nanoparticles in the donor compartment and permeated to the receiver compartment themselves through the micropores.

Fig. 3.4C shows the cumulative release of pCMV-β from the pCMV-β-coated net positively and net negatively charged nanoparticles. It is clear that the release of the pCMV-β from net negatively charged nanoparticle was faster than from the net positively charged nanoparticle (Fig. 3.4C). Therefore, it is likely that the relatively more extensive permeation of pCMV-β in the net negatively charged nanoparticles through the skin that was pretreated with microneedles was partially due to the direct diffusion of pCMV-β that was released from the PLGA nanoparticles in the donor compartment of the Franz diffusion apparatus.

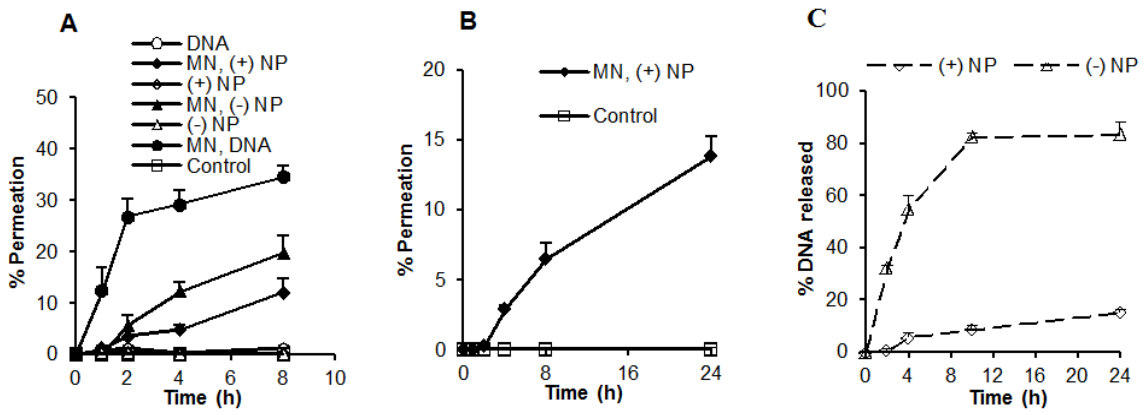

Figure 3.4 Permeation of plasmid DNA-coated nanoparticles through microneedle treated skin.

Permeation of plasmid DNA alone or coated on nanoparticles (A), and permeation of net positively charged DNA-coated nanoparticles (B) through a mouse skin area treated or untreated with microneedles. (C) Release of DNA from net positively charged and net negatively charged DNA coated nanoparticles after incubation *in vitro* at 37°C. Plasmid used was pCMV-β. MN = microneedle. All data reported are mean ± S.E.M. (n = 3).

3.3.5 Microneedle-mediated transcutaneous immunization using the plasmid DNA-coated cationic PLGA nanoparticles induced strong immune responses

In a pilot study, female BALB/C mice were transcutaneously immunized with an anthrax protective antigen (PA63) gene-encoding plasmid, pGPA (10 μg/mouse/dose), three times, 10 days apart. Six weeks after the last immunization, anti-PA IgG response was detected only in mice that were pretreated with microneedles before the transcutaneous immunization (data not shown), and the pGPA-coated net positively charged PLGA nanoparticles induced the strongest anti-PA IgG response (see Fig. 3.5A for anti-PA IgG titer). Therefore, further transcutaneous immunization studies were carried out only on a mouse skin area that was pretreated with microneedles. In the second immunization study, the β-galactosidase-encoding pCMV-β plasmid, alone or coated on the cationic PLGA nanoparticles, was used to immunize the immunocompetent hairless SKH-1 Elite mice [228]. The SKH-1 mice were used because the hair (and hair follicle) density in them is significantly lower than that in the hairy BALB/c or C57BL/6 mice and close to that of humans [56]. Mice were dosed every two weeks for three times with 20 μg of pCMV-β per mouse per dose. Shown in Fig. 3.5B are the anti-β-gal IgG levels in mouse serum samples 21 days after the last immunization. Transcutaneous immunization with pCMV-β alone induced an anti-β-gal IgG response, but it was significantly weaker than when the pCMV-β was coated on the PLGA nanoparticles (Fig. 3.5B), supporting our hypothesis that microneedle-mediated transcutaneous immunization with plasmid DNA coated on cationic nanoparticles can induce a stronger immune response than with plasmid DNA alone. Moreover, the net positively charged

pCMV-β-coated PLGA nanoparticles induced a stronger anti-β-gal IgG response than the net negatively charged pCMV-β-coated PLGA nanoparticles (Fig. 3.5B). Importantly, the anti- β-gal IgG level in mice that were transcutaneously immunized with the net positively charged pCMV-β-coated PLGA nanoparticles was higher than in mice that were intramuscularly injected with the same amount of pCMV-β alone ($p = 0.009$). Therefore, we further characterized only the immune responses induced by transcutaneous immunization with the net positively charged pCMV-β-coated PLGA nanoparticles.

Shown in Figs. 3.5C-E are the anti-β-gal IgG1, IgG2a, and IgA responses in the serum samples of SKH1 Elite mice 42 days after the last immunization with the net positively charged pCMV-β-coated PLGA nanoparticles. Both strong IgG1 and IgG2a were induced. As expected, the antibody response induced by intramuscularly injected pCMV-β alone was slightly IgG2a biased [229]. Anti-IgA was detected in the transcutaneously immunized mice, but not in mice intramuscularly injected with the pCMV-β (Fig. 3.5E), indicating that transcutaneous immunization with the net positively charged pCMV-β-coated PLGA nanoparticles also induced a specific mucosal response. The skin is an integrated part of the mucosal immune system. It was previously reported that transcutaneous immunization can induce mucosal immunity [2, 76]. Anti-β-gal IgE was not detected in any of the immunized mice (data not shown), indicating the lack of allergic responses.

Data in Figs. 3.5F-G showed that the splenocytes isolated from mice that were transcutaneously immunized with the net positively charged pCMV-β-coated PLGA

nanoparticles, after re-stimulation with β-galactosidase, secreted high levels of both IL-4 and IFN-γ which in combination with the IgG1/IgG2a subtypes in Figs. 3.5C-D, show that the immune responses induced by transcutaneous immunization with the net positively charged pCMV-β-coated PLGA nanoparticles were $CD4^+$ T helper (Th) type Th1 and Th2 balanced. Furthermore, data in Fig. 3.5H showed that the splenocytes isolated from mice that were transcutaneously immunized with the net positively charged pCMV-β-coated PLGA nanoparticles also proliferated significantly after *in vitro* re-stimulation with β-galactosidase.

Data in Fig. 3.5 showed that transcutaneous immunization with the net positively charged pCMV-β-coated PLGA nanoparticles induced a stronger immune response than intramuscular immunization with the same dose of the pCMV-β plasmid alone. In order to understand whether the pCMV-β-coated on the PLGA nanoparticles are as immunogenic when dosed by transcutaneous immunization as when dosed by intramuscular injection, a third immunization study was carried out by dosing C57BL/6 mice with the net positively charged pCMV-β-coated PLGA nanoparticles by the transcutaneous route (after pretreatment with microneedles) or by intramuscular injection (every two weeks for 3 times, 20 μg of pCMV-β per mouse per dose). When measured 21 days after the last immunization, the serum total anti-β-galactosidase IgG levels induced by both routes were not significantly different (Fig. 3.6A), although there were a couple of weaker responders in the transcutaneously immunized mice (Fig. 3.6A). This is significant considering that only a small fraction of the pCMV-β coated on the PLGA nanoparticles had entered the skin after transcutaneous immunization, whereas all the

pCMV-β coated on the PLGA nanoparticles were injected into mice by the intramuscular route. We expect that transcutaneous immunization using a lower dose of pCMV-β coated cationic nanoparticles (e.g., 1 or 5 μg/mouse/dose) will induce a stronger immune response than intramuscular injection of the same DNA coated cationic nanoparticles due to dose sparing effect [132]. In addition, data shown below are supportive of the immunological advantages of transcutaneous immunization using the DNA-coated nanoparticles over intramuscular injection.

Shown in Fig. 3.6B is the anti-β-gal IgA response in the serum samples 49 days after the last immunization with the net positively charged pCMV-β-coated PLGA nanoparticles. Anti-β-gal IgA was detected only in the transcutaneously immunized mice, but not in the intramuscularly injected mice (Fig. 3.6B), again indicating the ability of transcutaneous immunization to induce specific mucosal responses. Figs. 3.6C-D showed that high levels of IL-4 and IFN-γ were secreted by the splenocytes isolated from the mice immunized with net positively charged pCMV-β-coated PLGA nanoparticles transcutaneously or intramuscularly. However, IL-4 secretion in transcutaneously immunized mice was significantly higher than in the intramuscularly immunized mice (Fig. 3.6C), which is also advantageous considering that there is need to increase the humoral immune responses induced by intramuscularly injected plasmid DNA, especially in large animals and humans [230]. Finally, the splenocytes isolated from transcutaneously immunized mice and intramuscularly immunized mice both proliferated at comparable levels, after *in vitro* re-stimulation with β-galactosidase (Fig. 3.6E). Taken together, transcutaneous and intramuscular immunizations with net positively charged

pCMV-β-coated nanoparticles induced comparable levels of total IgG and proliferative responses, but transcutaneous immunization induced mucosal response as well, which is significant, considering mucosal immunity is needed to prevent infection through the mucosa.

It was noted that the values of IgG, IgA, IFN-γ and proliferation index are all relatively lower in Fig. 3.6 than in Fig. 3.5; this is likely because in Fig. 3.6, the mice used were C57BL/6, whereas in Fig. 3.5, the immuno-competent hairless SKH-1 mice were used. As expected, the anti-β-gal IgA levels in mouse serum samples were low (Fig. 3.5E and 3.6B). This is likely because IgA is mainly in the mucous secretion, and only small amount is in the blood. In fact, in an ongoing experiment, we immunized C57BL/6 mice with net positively charged plasmid DNA-coated nanoparticles transcutaneously on a skin area pretreated with microneedles (every two weeks for 3 times, 4 μg of an OVA-encoding plasmid, pCI-neo-sOVA, per mouse), anti-OVA IgA with a titer of 80-160 was detectable in the mouse fecal sample extracts, but not in the serum samples (data not shown).

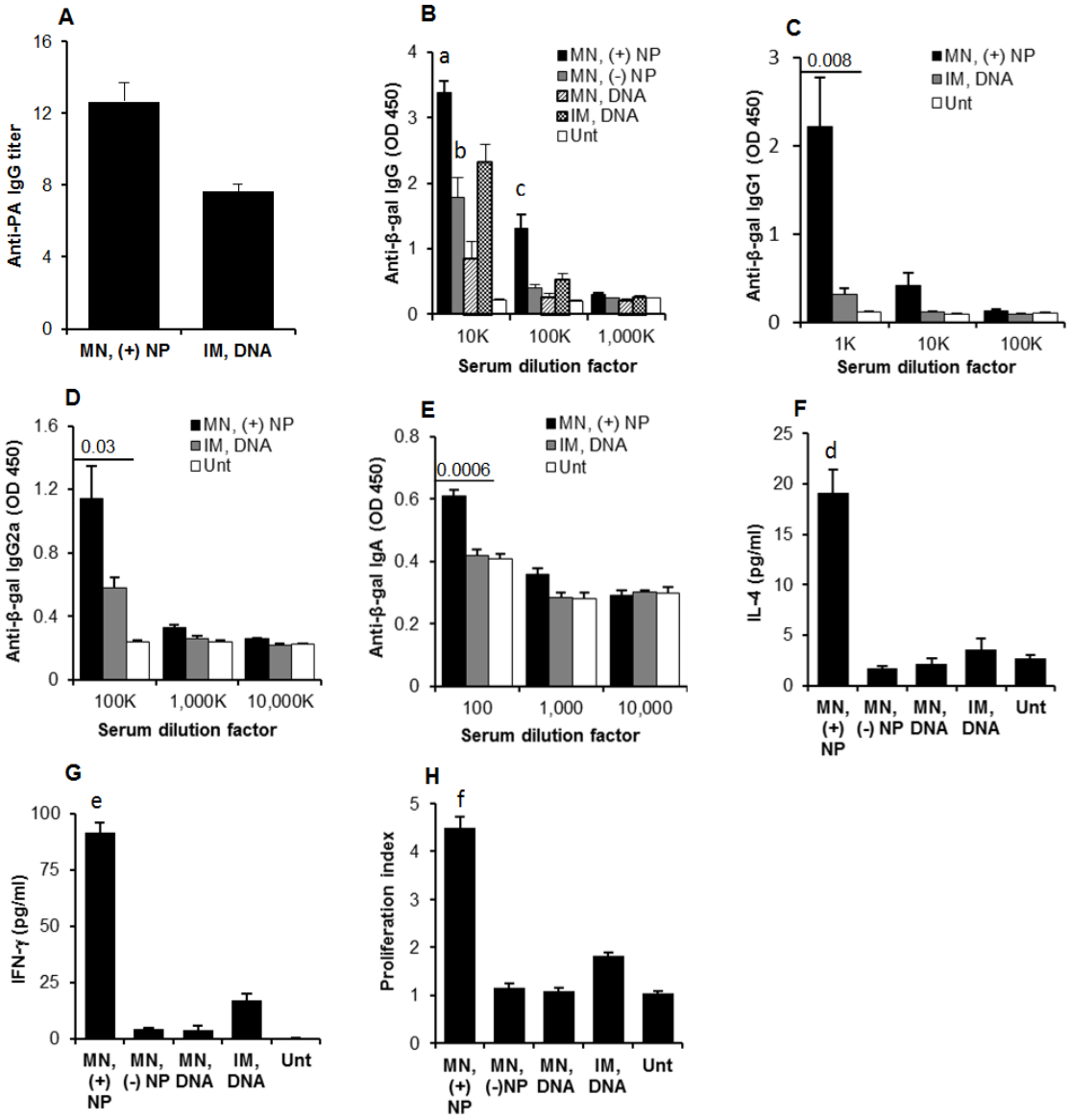

Figure 3.5 Immunization with pGPA or pCMV-β-coated cationic PLGA nanoparticles.

(A) Anti-PA IgG titers in the sera of mice transcutaneously immunized with net positively charged pGPA-coated nanoparticles or intramuscularly injected with pGPA

alone. BALB/c mice were dosed on day 0, 10, and 20 with 10 μg pGPA plasmid. Data reported are 42 days after last immunization. (B) Serum anti-β-gal IgG induced by pCMV-β, alone or coated nanoparticles, applied onto a skin area treated with microneedles (a, p = 0.009, (+) NP vs. IM, 10K dilution; b, p = 0.196, (-) NP vs. IM, 10K dilution; c, p = 0.008, (+) NP vs. IM, 100K dilution). (C-E) Anti-β-gal IgG1 (C), anti-β-gal IgG2a (D), and anti-β-gal IgA (E) induced by pCMV-β-coated net positively charged nanoparticles applied onto a skin area pre-treated with microneedles. (F-G) *In vitro* release of IL4 (F) and IFN-γ (G) from splenocytes after in vitro restimulation with β-galactosidase for 48 h. (d, p = 0.004, (+) NP vs. IM; e, p = 0.0001, (+) NP vs. IM). (H) *In vitro* proliferation of splenocytes after restimulation with β-galactosidase for 120 h (f, p = 0.0007, (+) NP vs. IM). In B-H, SKH1 Elite mice were dosed on day 0, 14, and 28 with 20 μg pCMV- β plasmid per mouse. Data in B are 21 days after the last immunization, Data in C-H are 42 days after the last immunization. All data are reported as mean ± S.E.M (n = 5). (MN, microneedle; IM, intramuscular; Unt, untreated).

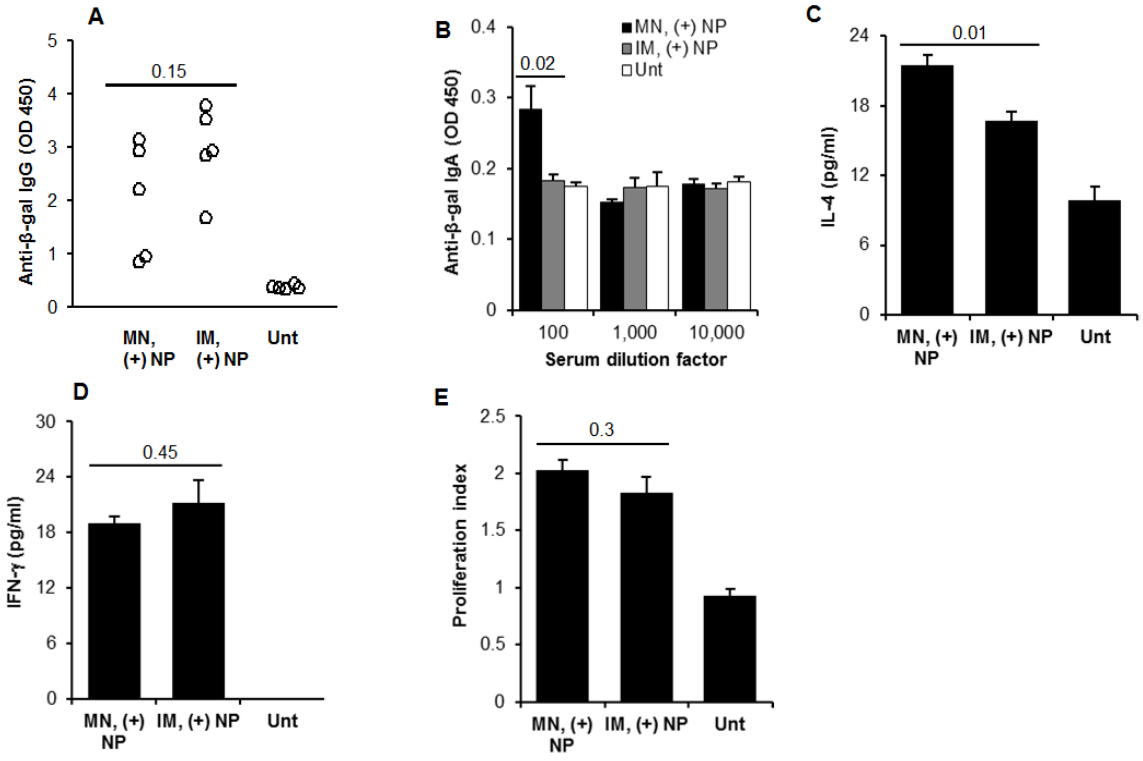

Figure 3.6 Immunization with pCMV-β-coated net positively charged nanoparticles. (A-B) Serum anti-β-gal IgG (from individual mice after 10,000-fold dilution) (A) and anti-β-gal IgA (B) induced by pCMV-β-coated net positively charged nanoparticles applied onto a skin area pre-treated with microneedles or injected intramuscularly. (C-D) *In vitro* release of IL-4 and IFN-γ from splenocytes restimulated with β-galactosidase for 48 h. (E) *In vitro* proliferation of splenocytes restimulated with β-galactosidase for 120 h. C57BL/6 mice were dosed on day 0, 14, and 28 with 20 µg pCMV-β plasmid per mouse. Data in A are 21 days after the last immunization, while data in B-E are 49 days after the

last immunization. All data reported are mean ± S.E.M. from 5 mice per group. (MN, microneedle; IM, intramuscular; Unt, untreated).

3.3.6 Net positively charged DNA-coated nanoparticles more effectively up-regulated the expression of CD86 on BMDCs

To evaluate the effect of nanoparticles on the expression of major histocompatibility complex (MHC) and co-stimulatory molecules on dendritic cells, the expression of MHC I, MHC II, CD80 and CD86 on mouse BMDCs was measured after in vitro stimulation with cationic nanoparticles, net positively charged DNA-coated nanoparticles and net negatively charged DNA-coated nanoparticles. Plasmid DNA alone and LPS were used as controls. As shown in Fig. 3.7, all formulations effectively up-regulated the expression of CD86 molecules. However, it appears that the net positively charged pCMV-β-coated nanoparticles were more effective than the other, suggesting that net positively charged DNA-coated nanoparticles can more efficiently stimulate the maturation of DCs. There was no difference in the expression of CD 80, MHC I and MHC II among all the treatments (data not shown).

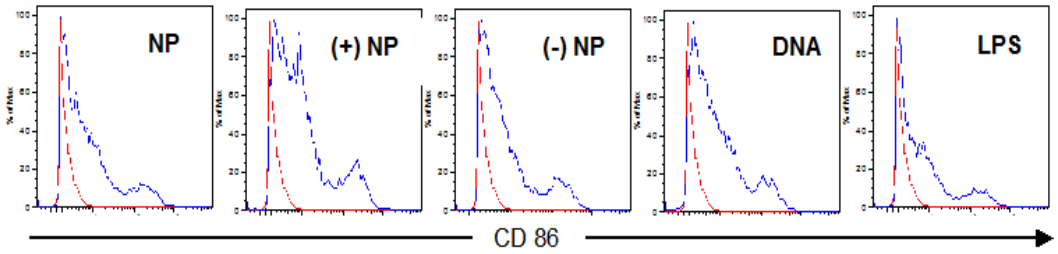

Figure 3.7 Flow cytometric graphs showing the expression of CD86 on mouse BMDCs.

Flow cytometric graphs showing the expression of CD86 on mouse BMDCs after 15 h incubation with cationic PLGA nanoparticles (NP), pCMV-β-coated net positively charged nanoparticles ((+) NP), pCMV-β-coated net negatively charged nanoparticles ((-) NP), pCMV-β alone (DNA), or LPS. Experiment was repeated three times with similar results. Peaks in the left are cells incubated with fresh medium.

3.3.7 Net positively charged DNA-coated nanoparticles significantly enhanced the expression of the antigen encoded by the plasmid applied topically onto a skin area pretreated with microneedles

As shown in Fig. 3.8A, a significant amount of pCMV-β plasmid was recovered in the skin area pretreated with microneedles after the administration of net positively charged pCMV-β-coated nanoparticles, net negatively charged pCMV-β-coated nanoparticles or pCMV-β alone, but there was no difference among them. However, the net positively charged pCMV-β-coated nanoparticles led to a significantly higher level of β-galactosidase mRNA expression in the skin samples, as compared to the net negatively charged pCMV-β-coated nanoparticle or pCMV-β alone (Fig. 3.8B).

Taken the data in Fig. 3.7 and Fig. 3.8 together, it seems that the ability of the net positively charged DNA-coated nanoparticles to induce a strong immune response after transcutaneous immunization is related to their ability to increase the expression of the antigen gene encoded by the plasmid coated on them and to more effectively stimulate dendritic cell maturation.

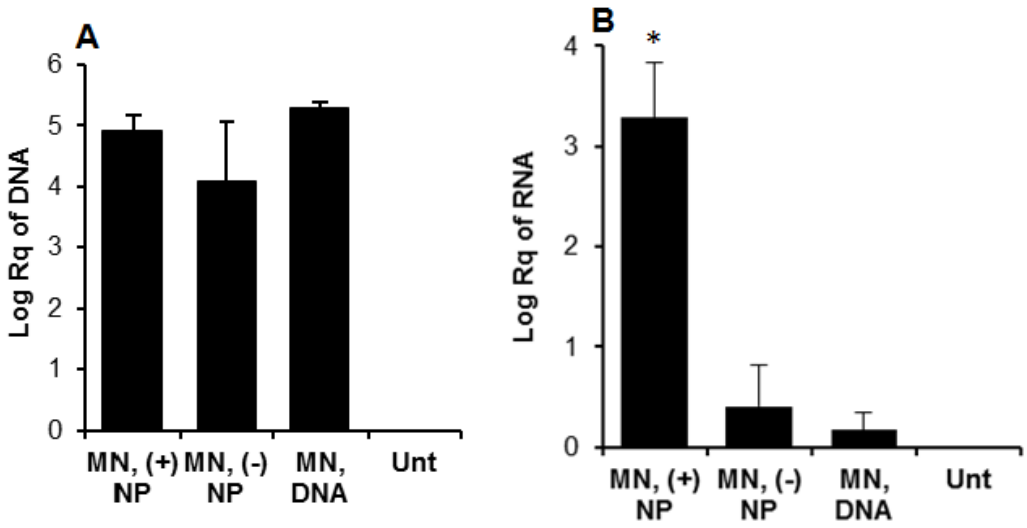

Figure 3.8 *In vivo* uptake and expression of pCMV-β plasmid.

In vivo uptake of pCMV-β plasmid (A) and expression of β-galactosidase gene (mRNA level) (B) 24 h after pCMV-β, alone or coated on nanoparticles, was applied on a mouse skin area pretreated with microneedles. A 100 µl (20 µg pCMV-β) of each formulation was applied on C57BL/6 mice (8-10 weeks) at 0 h. pCMV-β recovered from the skin samples and the β-galactosidase mRNA level in the skin samples were determined 24 h later using qRT PCR. MN, microneedles. Data reported are mean ± S.E.M. (n = 3). (*, p = 0.005, MN, (+) NP vs. MN, (-) NP; MN, (+) NP vs. MN, DNA).

3.4 Conclusion

A biodegradable PLGA-DOTAP nanoparticle-based plasmid DNA delivery system for microneedle-mediated transcutaneous immunization was successfully developed. To our best knowledge, this represents the first report that showed that microneedle-mediated transcutaneous immunization with plasmid DNA carried by the nanoparticles induced a stronger immune response than with the plasmid DNA alone. Moreover, we also found that the net surface charge of the DNA-coated nanoparticles affected their *in vitro* skin permeation and ability to induce immune responses *in vivo*. Transcutaneous immunization with plasmid DNA-coated net positively charged nanoparticles induced a stronger immune response than with plasmid DNA-coated net negatively charged nanoparticles. Furthermore, transcutaneous immunization was able to induce specific mucosal immunity as well. The ability of the net positively charged plasmid DNA-coated nanoparticles to induce a strong immune response after transcutaneous immunization is likely related to their ability to increase the expression of the antigen gene encoded by the plasmid and to stimulate dendritic cell maturation.

Chapter Four

Induction of botulinum neurotoxin (BoNT)-neutralizing antibody responses by microneedle-mediated transcutaneous immunization with a BoNT/C-Hc50 encoding plasmid coated on cationic PLGA nanoparticles

4.1 Introduction

Botulism is a lethal neuroparalytic disease caused by botulinum neurotoxins (BoNTs). BoNTs are produced by one of the seven structurally similar *Clostridium botulinum* serotypes, designated A to G [231]. Serotypes A, B, E and F cause human botulism, whereas serotypes C and D are responsible for animal botulism [232]. BoNTs are one of the most poisonous substances known in nature and have the potential to be used in bioterrorism or as a biological weapon [233]. Previously, an investigational pentavalent botulinum toxoid (PBT) vaccine was available for use against botulism. However, the Center for Disease Control and Prevention (CDC) has found that older PBT vaccines (> 30 years) generally have declined immunogenicity, decreased potency, and increased occurrence of adverse effects at injection site [234]. High manufacturing cost, long duration to produce a sufficient amount of the product, and safety issues in producing the toxins are some of the reasons preventing the PBT vaccine from being replaced frequently [234]. As of November 2011, the PBT vaccine has been discontinued by the CDC [235].

Plasmid DNA based vaccines have recently generated great interest, and it is easy to manufacture and store [236]. In fact, a plasmid DNA vaccine that encodes the heavy chain domain of serotype A BoNT (BoNT/A) had been evaluated in an animal model before, but the DNA vaccine showed a lower immunogenicity in comparison to vaccine candidates prepared with BoNT/A toxoid or protein fragment [237]. Traditionally, DNA vaccine has been administered intramuscularly [26]. However, data from many studies have shown that transcutaneous DNA immunization, especially with the help of microneedles, can induce strong immune responses [151]. Microneedles create micron-sized channels within the epidermis of the skin [105, 147, 238, 239], through which plasmid DNA may permeate into the skin in a pain-free manner. Originally, Mikszta *et al*. reported that microneedle-mediated transcutaneous immunization with 'naked' plasmid DNA can potentially induce a stronger immune response than hypodermic needle-based intramuscular injection of the same plasmid DNA [151]. In a previous study, we showed that microneedle-mediated transcutaneous immunization with plasmid DNA (i.e., pCMV-β-gal, with β-gal as a model antigen) coated on cationic poly (lactic-co-glycolic acid) (PLGA) nanoparticles induced stronger immune responses than with the 'naked' DNA alone [85], likely because of net positively charged plasmid DNA-coated PLGA nanoparticles effectively increased the expression of the antigen gene encoded by the plasmid at the DNA application area in the skin [85].

In the present study, we evaluated the feasibility of inducing BoNT-neutralizing antibody responses in a mouse model by microneedle-mediated transcutaneous immunization with a plasmid DNA that encodes the Hc50 fragment of serotype C BoNT.

The BoNT/C-Hc50-encoding plasmid was coated on the cationic PLGA nanoparticles and topically applied onto a mouse skin area pretreated with microneedles. In addition, we also evaluated the effect of antigen, antigen dose and mouse strain used in the study on the resultant immune responses.

4.2 Materials and methods

4.2.1 Materials

Dermaroller® microneedle roller was from Cynergy, LLC (Carson City, NV). There are 192 needles (1000 μm in length, 80 μm in base diameter) on the roller. To construct the BoNT/C-Hc50-encoding plasmid, pVax/opt-BoNT/C-Hc50, the nucleotides encoding the 50 kDa C-terminal fragment of the heavy chain of serotype C1 BoNT (i.e., Hc50) was optimized with human codon preference by the DNAworks program [240]. The codon-optimized BoNT/C-Hc50 (encoding the amino acid 849-1291 in BoNT/C, GenBank Acc# D90210) was then synthesized by a PCR-based method and cloned into the pVax1 vector (Life Technologies, Carlsbad, CA). The DNA sequence of the synthesized gene was confirmed by DNA sequencing analysis. The pCI-neo-sOVA plasmid (6772 bp), which encodes soluble chicken egg ovalbumin (OVA), was from Addgene (plasmid # 25098, Cambridge, MA). All plasmids were purified using a QIAGEN Midiprep kit according to the manufacturer's instruction (Valencia, CA). Large scale plasmid preparation was performed by GenScript (Piscataway, NJ). PLGA (Resomer RG 504H), acetone, Pluronic F68, 3,3',5,5'-tetramethylbenzidine (TMB) solution, sodium bicarbonate, sodium carbonate, Tween 20, phosphate-buffered saline (PBS) and fetal bovine serum (FBS) were from Sigma-Aldrich (St. Louis, MO). Horse serum, penicillin and streptomycin were from Life Technologies (Carlsbad, CA). The 1,2-dioleoyl-3-trimethylammonium-propane (DOTAP) was from Avanti Polar Lipids,

Inc. (Alabaster, AL). Goat anti-mouse IgG, IgA, IgG1 and IgG2a antibodies were from Southern Biotechnology Associates, Inc. (Birmingham, AL).

4.2.2 Preparation of cationic PLGA nanoparticles

The cationic PLGA nanoparticles were prepared by the nanoprecipitation-solvent evaporation method as previously described [85, 172]. Briefly, PLGA (3 mg) and DOTAP (40 mg) were accurately weighed and dissolved in acetone (2 ml). The organic phase was added drop-wise into 10 ml of 1% Pluronic F68 (as a hydrophilic stabilizer) with moderate stirring (800 rpm) for 3 h at room temperature until acetone is completely evaporated to form nanoparticles. The nanoparticles were centrifuged (50,100 x rcf, 4°C, 45 min) and then re-suspended in 200 µl water.

4.2.3 Coating of plasmid DNA on the surface of the nanoparticles

Plasmid DNA (pVax/opt-BoNT/C-Hc50 or pCI-neo-sOVA) was coated on the surface of the cationic nanoparticles by gently mixing equal volumes of cationic nanoparticles in a suspension with the plasmid DNA in a solution to obtain a final DNA concentration of 200 µg/ml. To identify the appropriate ratio of nanoparticles vs. plasmid DNA to prepare the net positively charged DNA-coated PLGA nanoparticles, an increasing amount of nanoparticles (0.001-0.12 mg) were mixed with a fixed amount of DNA (1 µg), and the mixture was incubated for at least 30 min at room temperature for the DNA to adsorb onto the surface of the nanoparticles. The sizes and zeta potentials of

the resultant DNA-coated nanoparticles were measured using a Malvern Zetasizer® Nano ZS (Westborough, MA)

4.2.4 Immunization studies

All animal studies were carried out following the National Institutes of Health guidelines for care and use of laboratory animals. The animal protocols were approved by the Institutional Animal Care and Use Committee (IACUC) at The University of Texas at Austin and the IACUC at Texas Tech University Health Science Center. Female hairless SKH1-Elite mice (6-8 weeks) or female C57BL/6 mice (8-10 weeks) were from Charles River Laboratories (Wilmington, MA). Mice (n = 5-6/group) were immunized 3 times topically on an area treated with the microneedle roller as previously described [85, 147]. Briefly, 24 h prior to the initiation of the immunization, hair, if any, in the dorsal side of mice was carefully trimmed. Mice were anesthetized, the target skin area was wiped with an alcohol swab, and a 2-cm^2 area was marked on the lower dorsal skin surface. Mice were placed onto the flat surface of a balance, and the microneedle roller was rolled in two perpendicular lines over the marked skin surface, 10 times each, for a total of 20 times, with an applying pressure of 350-400 g, which was measured using the balance. Plasmid-coated nanoparticles in water were carefully dripped onto the microneedle-treated area, which was then covered with a piece of self-adhesive Tegaderm® patch (3 M, St. Paul, MN). The Tegaderm® patch was carefully removed 24 h later. Immunization was repeated 14 days apart for two more times. As a positive control, a group of mice were intramuscularly injected in the gastrocnemius muscles 3 times with plasmid DNA-

coated cationic nanoparticles. Four weeks (or as where mentioned) after the last immunization, serum, fecal, and bronchoalveolar lavage (BAL) fluid samples were collected after the mice were euthanized. Specific antibody levels in the samples were determined using enzyme-linked immunosorbent assay (ELISA) as previously described [200, 201]. IgG and IgG1 serum antibody concentrations were measured using an ELISA Quantization kit (Bethel Lab. Inc., Montgomery, TX) as described previously [241].

4.2.5 Enzyme-linked immunospot (ELISpot) assay

Splenocytes from the immunized mice were assessed by ELISpot assay for the secretion of IFN-γ. Spleens were extracted from the immunized mice to prepare single splenocyte preparation [84, 100, 222]. $CD4^+$ cells were sorted from the splenocytes using magnetic activated cell sorter (MACS, Miltenyi Biotec Inc. CA) according to the manufacturer's instruction. The magnetic microbeads were conjugated with anti-CD4 mAb (GK 1.5) (Miltenyi) [242]. Frequencies of IFN-γ spot-forming cells (SFC) were determined by ELISPot assay following the manufacture's protocol (eBioscience, San Diego, CA). Assays with $CD4^+$ cells were performed with 96-well PVDF membrane ELISPot plates (MAIPS4510, EMD Millipore, Billerica, MA). Anti-mouse IFN-γ (AN-18) was used for coating, and biotin-conjugated anti-mouse IFN-γ (R4-6A2) was used as secondary antibody. Spots were detected using Avidin- horseradish peroxidase as a substrate, and quantified using an Advanced Imaging Devices Elispot Reader System ELR06 (Strassberg, Germany) [243].

4.2.6 BoNT/C neutralization assay

Neutralizing antibody titers to BoNT/C were measured by the ability of sera from the immunized mice to neutralize the neurotoxin *in vitro* in combination with the mouse lethality assay [234, 241]. Two hundred microliters of pooled sera from 5-6 mice 4 weeks after the last immunization were initially diluted 1:8 and then diluted in two-fold series (1:8 to 1:1024) in DPBS (Dulbecco's PBS). BoNT/C in 200 µl of DPBS (400 × MLD50) was added into each dilution. After incubation at room temperature for 1 h, the anti-serum and the BoNT/C mixture was injected intraperitoneally into mice, 100 µl (corresponding to 100 × MLD50 of BoNT/C before neutralization) per mouse, 4 mice for each dilution. The mice were monitored for 4 days, and the number of deaths at each sample dilution was recorded. If the toxin was neutralized, the mice were protected from the challenge with toxin. The detection limit for this assay was 0.04 IU/ml due to the limited amount of serum available. Neutralizing antibody titers were defined as the maximum number of IU of antitoxin per ml of serum, resulting in 100% survival after challenge. One IU of BoNT antitoxin neutralized 10,000 × MLD50 neurotoxin [234, 241].

4.2.7 Histological study

To visualize the retention of plasmid DNA in the skin area where the plasmid DNA-coated cationic nanoparticles were applied after the area was treated with microneedles, pVax/Opt-BoNT/C-Hc50 plasmid was labeled with rhodamine using a Label IT® Nucleic Acid Labeling Kit from Mirus Bio LLC (Madison, WI). The hair in

the lower dorsal skin of mice was trimmed using a clipper. Twenty four hour later, the rhodamine-labeled plasmid (5 μg) coated on the cationic PLGA nanoparticles was applied onto the skin area, which was pretreated with microneedles as mentioned above. The area was then covered with Tegaderm® patch. After 4 h, the patch was removed, and the treated area was washed three times with water and paper-dried. The skin was then harvested immediately and cut into two halves. One half was examined horizontally under a fluorescence Olympus BX53 microscope (Olympus, Center Valley, PA); whereas the other half was frozen, sectioned vertically, stained with 4′,6-diamidino-2-phyenylindole (DAPI), and examined under Leica TCS-SP5 confocal microscope with an oil immersion objective (63 × 1.4 NA) (Leica Microsystems GmbH, Mannheim, Germany).

4.2.8 Statistical analysis

Statistical analyses were performed using analysis of variance followed by Fisher's protected least significant difference procedure. A p value of ≤ 0.05 (two-tailed) was considered statistically significant.

4.3 Results and discussion

Previously, by using the β-galactosidase model antigen-encoding plasmid, pCMV-β, we showed that transcutaneous immunization with the pCMV-β coated on cationic PLGA nanoparticles onto a mouse skin area pretreated with microneedles induced significantly strong antigen-specific immune responses than with the 'naked' pCMV-β plasmid alone [85]. The primary aim of the present study is to test the feasibility of using the same microneedle-mediated transcutaneous immunization approach to induce neutralizing antibodies against BoNT. Therefore, we constructed the pVax/opt-BoNT/C-Hc50 plasmid that encodes the codon-optimized BoNT/C-Hc50. The pVax/opt-BoNT/C-Hc50 plasmid was coated on cationic PLGA nanoparticles using the DNA to nanoparticles ratio optimized in our previous study [85]. At the nanoparticles to DNA ratio of 40:1, the particle size and the zeta potential of the resultant DNA-cationic PLGA nanoparticle complex were 120 ± 0.3 nm and +45 ± 2 mV, respectively. Before carrying out immunization studies with the pVax/opt-BoNT/C-Hc50-coated nanoparticles, we confirmed that the plasmid DNA can be delivered through the micropores created on the skin by microneedles into the epidermal layer of the skin. We allowed rhodamine-labeled pVax/opt-BoNT/C-Hc50 coated on cationic nanoparticles to stay on a mouse skin area pretreated with microneedles for 4 h. Shown in Fig. 4.1A are the horizontal views of the skin area under a fluorescence microscope. Clearly, rhodamine-labeled plasmid DNA was only visible in the pores in the skin area pretreated with microneedles, but not detectable in the skin area that was not pretreated with microneedles (Fig. 4.1A). A vertical view of treated skin area under a confocal

microscope showed that rhodamine-labeled plasmid DNA was mostly concentrated in the epidermis layer of the skin (Fig. 4.1B). Therefore, pretreatment of the mouse skin area with microneedles facilitated the pVax/opt-BoNT/C-Hc50 coated on the cationic PLGA nanoparticles to enter the epidermal layer of the skin.

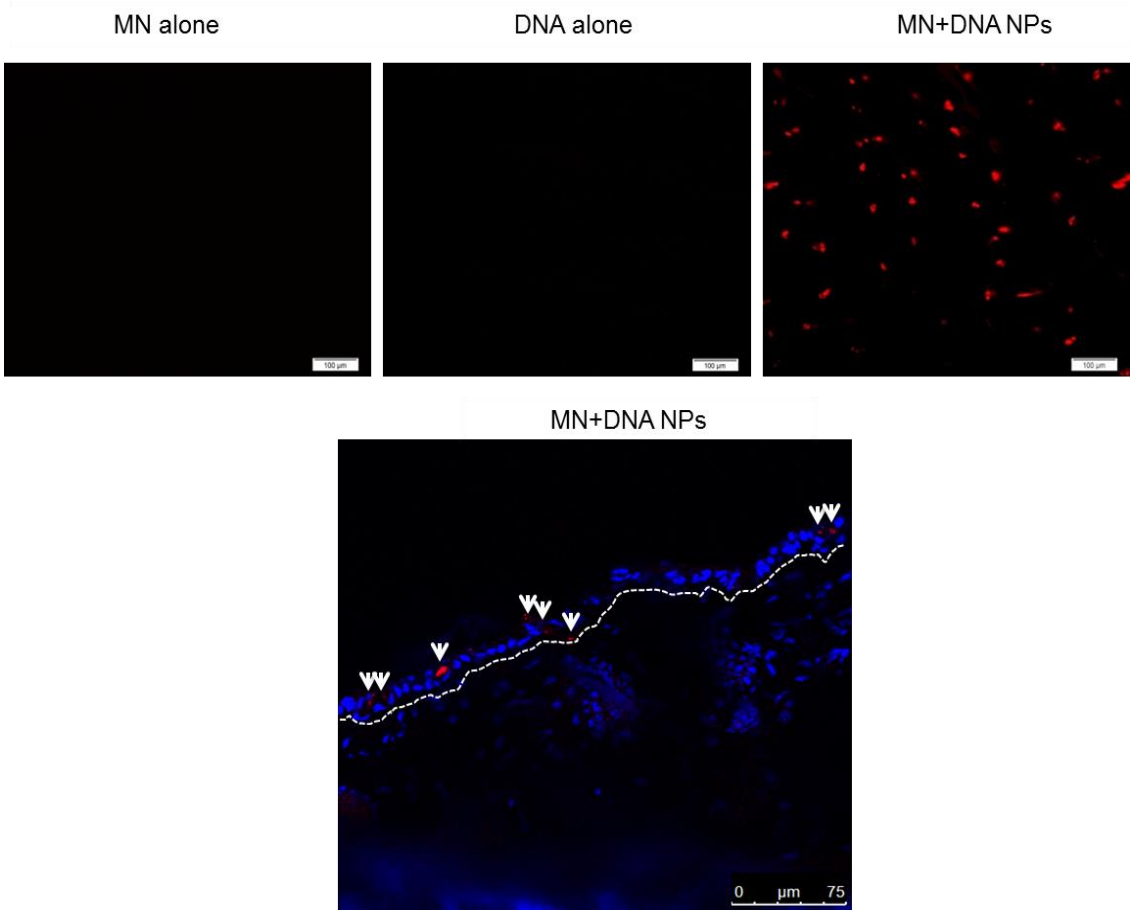

Figure 4.1 Horizontal and vertical microscopic view of microporated mouse skin after treating with rhodamine-labeled pVax/opt-BoNT/C-Hc50 plasmid DNA-coated cationic PLGA nanoparticles.

Typical microscopic graphs, horizontal (A) and vertical (B), of mouse skin area after treated with rhodamine-labeled pVax/opt-BoNT/C-Hc50 plasmid DNA-coated cationic PLGA nanoparticles for 4 h following pretreatment with microneedles. As a control, the mouse skin area was treated with microneedles, but no DNA-coated cationic PLGA

nanoparticles were applied. (MN, microneedles; DNA NPs, pVax/opt-BoNT/C-Hc50-coated cationic PLGA nanoparticles).

4.3.1 Microneedle-mediated transcutaneous immunization with pVax/opt-BoNT/C-Hc50 coated on cationic PLGA nanoparticles induced BoNT/C-neutralizing immune responses

In our first immunization study, pVax/opt-BoNT/C-Hc50 plasmid coated on cationic PLGA nanoparticles was used to immunize immunocompetent hairless SKH-1 Elite mice. Mice were dosed every two weeks for three times with 20 μg of pVax/opt-BoNT/C-Hc50 plasmid per mouse per dose. Four weeks after the last immunization, mice were euthanized to collect blood, fecal samples and BAL samples. Figs. 4.2 A-B show the anti-BoNT/C-Hc50 IgG levels in mouse serum samples. The total anti-BoNT/C-Hc50 IgG concentration in mice that were transcutaneously immunized with the pVax/opt-BoNT/C-Hc50-coated nanoparticles tended to be higher than in mice that were intramuscularly injected with the same pVax/opt-BoNT/C-Hc50-coated nanoparticles, but statistical analysis did not reveal a significant difference between these two groups ($p = 0.146$) (Fig. 4.2A). It happened that one of the five mice in the intramuscularly immunized group was a strong responder (Fig. 4.2B), which was identified as an outlier using the Grubb's extreme studentized deviate (ESD) method. Otherwise, the total anti-BoNT/C-Hc50 IgG levels in the transcutaneously and intramuscularly immunized mice would be different ($p = 0.009$) (Fig. 4.2B).

Shown in Figs. 4.2C-D are the BoNT/C-Hc50-specific IgG1and IgG2a responses in the serum samples of mice four weeks after the last immunization. Transcutaneous immunization induced stronger anti-BoNT/C-Hc50 IgG1 (Fig. 4.2C) and IgG2a (Fig. 4.2D) responses than intramuscular immunization. Moreover, the immune responses

induced by transcutaneous immunization with the pVax/opt-BoNT/C-Hc50-coated nanoparticles were IgG1 and IgG2a balanced. A similar result was reported by others in earlier studies too [85]. For example, Mikszta *et al.* reported that microneedle-based cutaneous delivery of a plasmid DNA induced a balanced IgG1/IgG2a response in mice [151].

Data in Figs. 4.2E-G showed that transcutaneous immunization with the pVax/opt-BoNT/C-Hc50-coated nanoparticles induced BoNT/C-Hc50-specific IgA responses in the serum, fecal, and BAL samples of the immunized mice, whereas BoNT/C-Hc50-specific IgA response was not detected in the samples from the intramuscularly immunized mice, clearly demonstrating that microneedle-mediated transcutaneous immunization with plasmid DNA-coated nanoparticles also induced a specific mucosal response. Mucosal immunity is important in the prevention of infection through the mucosa. BoNTs are the most poisonous substances known in nature. A single gram of crystalline toxins, evenly dispersed and inhaled, would kill more than one million people [233]. Therefore, being able to induce specific mucosal immunity in the mucosa of the respiratory track is expected to be beneficial.

Finally, ELISpot data in Fig. 4.2H showed that significantly more $CD4^+$ cells isolated from the spleens of the transcutaneously immunized mice secreted IFN-γ after exposing to BoNT/C-Hc50, as compared to that from intramuscularly immunized mice, indicating that microneedle-mediated transcutaneous immunization also induced cellular immunity.

Taken together, data in Fig. 4.2 clearly showed that microneedle-mediated transcutaneous immunization with the pVax/opt-BoNT/C-Hc50 plasmid coated on the cationic PLGA nanoparticles induced stronger BoNT/C-Hc50-specific immune responses than intramuscular immunization with the same plasmid coated on the nanoparticles. Importantly, transcutaneous immunization with the pVax/opt-BoNT/C-Hc50-coated nanoparticles also induced BoNT/C-Hc50-specific serum and mucosal IgA responses.

The bioactive capability of the sera of mice immunized with the pVax/opt-BoNT/C-Hc50 plasmid coated on the cationic PLGA nanoparticles was also evaluated. Pooled sera from immunized mice in the same group were used for *in vitro* toxin neutralization. As shown in Fig. 4.3A, up to 64-fold diluted sera from the immunized mice were sufficient to completely neutralize 100 × MLD50 of active BoNT/C and resulted in a 100% survival rate after the BoNT/C toxin was injected into naive mice (Fig. 4.3A). Sera obtained from unimmunized mice were not able to neutralize active BoNT/C and thus resulted in 0% survival even at 8-fold dilution. This translated to a neutralization titer of 6.4 U/ml, and the neutralization titers in transcutaneously immunized mice and intramuscularly immunized mice were not different (Fig. 4.3B). Thus, microneedle-mediated transcutaneous immunization with a BoNT/C-Hc50-plasmid coated on cationic PLGA nanoparticles is capable of inducing BoNT/C-neutralizing antibody responses. A multivalent DNA vaccine that encodes the Hc50 of all the BoNT serotypes is expected to protect against all BoNTs.

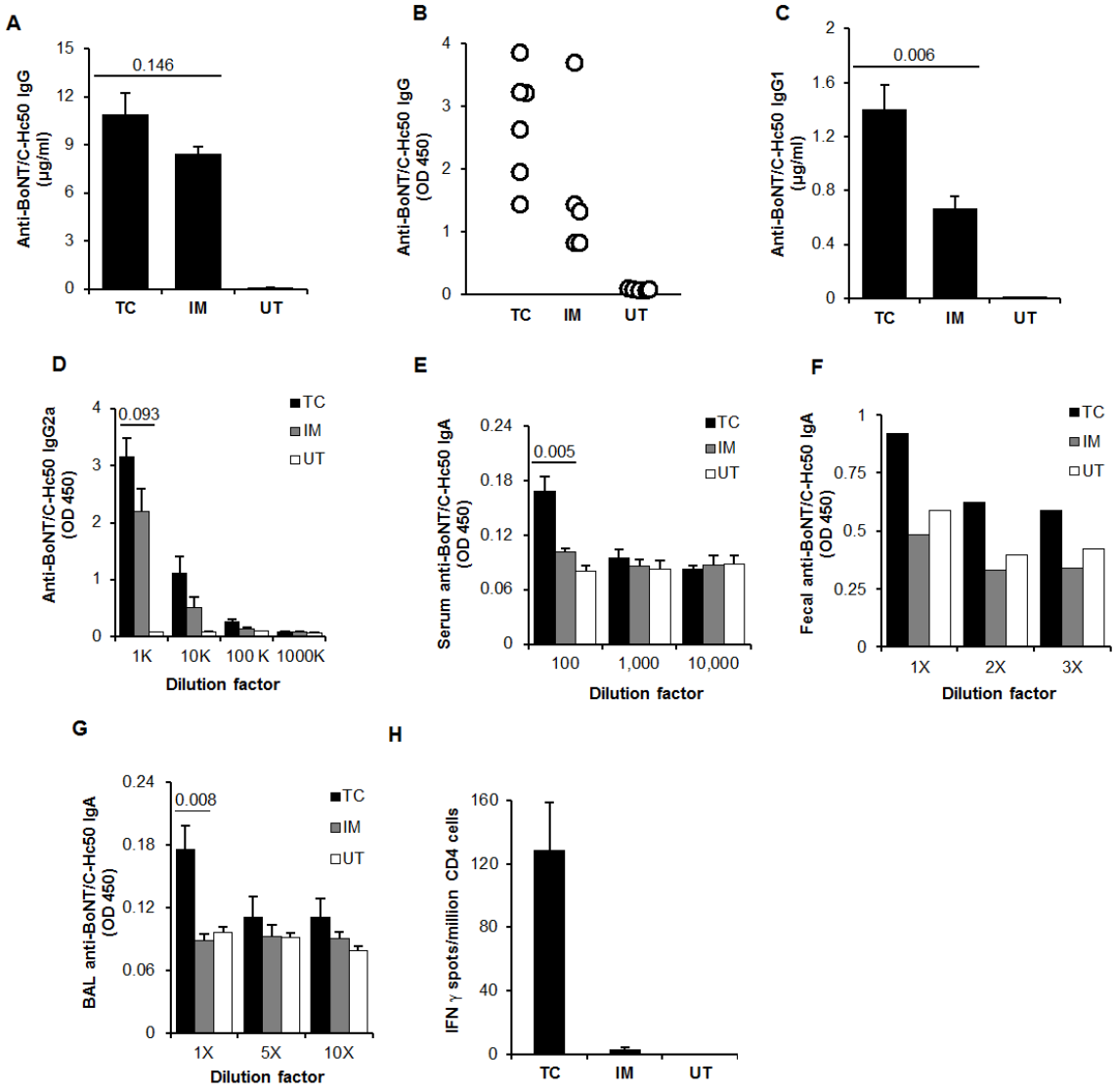

Figure 4.2 Immunization with pVax/opt-BoNT/C-Hc50 coated on cationic PLGA nanoparticles.

Antibody and cellular immune responses induced by transcutaneous immunization of mice with pVax/opt-BoNT/C-Hc50-coated cationic PLGA nanoparticles on a skin area pretreated with microneedles. (A) Serum anti-BoNT/C-Hc50 IgG concentration. (B)

Serum anti-BoNT/C-Hc50 IgG levels (OD values from individual mouse serum samples after 10,000-fold dilution). (C-D) Serum anti-BoNT/C-Hc50 IgG1 (C) and anti-BoNT/C-Hc50 IgG2a (D). (E-G) Anti-BoNT/C-Hc50 IgA in serum (E), fecal (F), and BAL samples (G). (H) IFN γ spot-forming splenocytes after re-stimulation with BoNT/C-Hc50 for 48 h. SKH1 Elite mice were dosed on day 0, 14, and 28 with 20 µg pVax/opt-BoNT/C-Hc50 plasmid per mouse. Data reported, mean ± S.E.M (n = 5-6), are 4 weeks after the last immunization. (TC, transcutaneous; IM, intramuscular; UT, untreated).

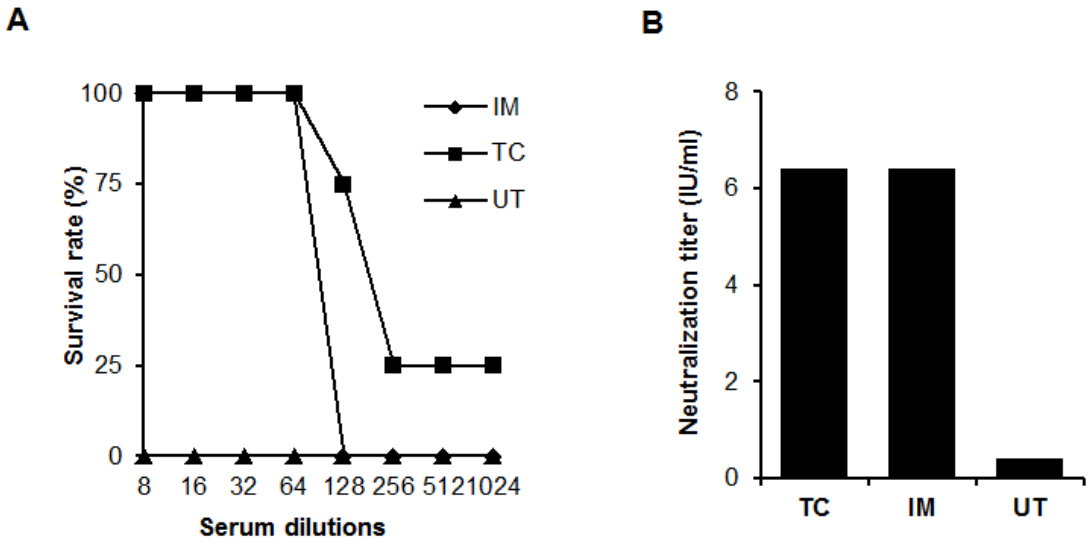

Figure 4.3 Botulinum neurotoxin neutralization assay.

(A) Survival rates of naïve mice after challenge with BoNT/C (n = 4 for each dilution). (B) Serum anti-BoNT/C-Hc50 neutralization titers (IU/ml), 1 IU = 10,000 × MLD50. SKH1 Elite mice (n = 5-6) were dosed on day 0, 14, and 28 with pVax/opt-BoNT/C-Hc50 plasmid coated on cationic PLGA nanoparticles. A volume of 25 µl of serum from each mouse in the same group collected four weeks after last immunization was pooled. The pooled sera were diluted 1:8 initially with Dulbecco's PBS and then, in two-fold, serially to determine anti-BoNT/C-Hc50 neutralizing antibody titers in naïve C57BL/6 mice. (TC, transcutaneous; IM, intramuscular; UT, untreated).

4.3.2 Transcutaneous immunization with OVA-encoding plasmid coated on cationic PLGA nanoparticles

In the above study, we used hairless SKH-1 Elite mice. Although immunocompetent, the SKH-1 Elite mice were hairless at the time of the DNA immunization. In order to understand whether microneedle-mediated transcutaneous immunization with plasmid DNA coated on cationic PLGA nanoparticles is also feasible to induce systemic and mucosal immunities in normal hairy mice, we carried out another immunization study with C57BL/6 mice. We also used another plasmid, the OVA-encoding pCI-neo-sOVA plasmid, and at a lower dose, 4 μg per mouse per dose, instead of the 20 μg dose of pVax/opt-BoNT/C-Hc50 used in the above experiment. Mice were transcutaneously immunized with the pCI-neo-sOVA-coated PLGA nanoparticles every two weeks for three times. As a control, another group of mice were intramuscularly injected with the same pCI-neo-sOVA-coated nanoparticles. The pCI-neo-sOVA-coated nanoparticles (particle size, 120 nm; zeta potential, 45 mV) were prepared by complexing pCI-neo-sOVA plasmid with cationic PLGA nanoparticles at a 40:1 particle to DNA ratio. Six weeks after the last immunization, mice were euthanized to collect blood, fecal samples and BAL samples to determine OVA-specific antibody responses. As shown in Fig. 4.4A, the serum anti-OVA IgG level in the transcutaneously immunized mice was significantly higher than in the intramuscularly immunized mice ($p = 0.04$). In addition, anti-OVA IgA was detected in the fecal samples (Fig. 4.4B) and BAL samples (Fig. 4.4C) of the transcutaneously immunized mice, but not the intramuscularly immunized mice. This result is also significant in a way as it demonstrates that irrespective of

antigens encoded by the plasmid DNA, the dose of the DNA used or mouse strain used, plasmid DNA coated on the surface of cationic PLGA nanoparticles is able to induce strong systemic and mucosal immune responses when administered topically on a skin area pretreated with microneedles. At a lower dose of plasmid DNA (i.e., 4 µg per mouse per dose in this study), microneedle-mediated transcutaneous immunization induced a stronger immune response than intramuscular immunization, likely because of the 'dose sparing' effect [132]. 'Dose sparing' effect in microneedle-mediated transcutaneous immunization had already been reported by others before. For example, Alarcon *et al.* reported that microneedle-mediated transcutaneous immunization with 'naked' plasmid DNA (i.e., pCMV-HA) at lower dose (i.e., 1 µg) induced a stronger antibody response than intramuscular injection of the same plasmid DNA at the same dose. However, at higher doses (i.e., 5 and 50 µg), there was not any significant difference in the immune responses in the transcutaneously and intramuscularly immunized mice [137].

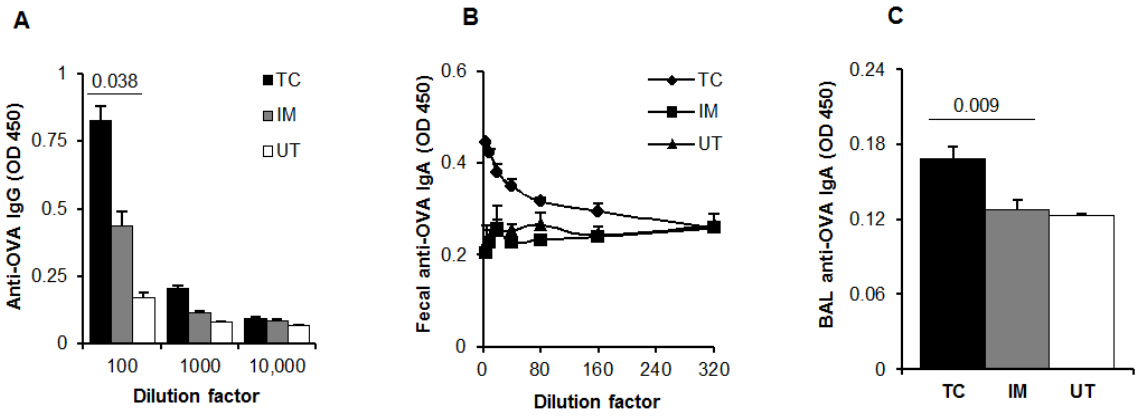

Figure 4.4 Immunization with OVA-encoding plasmid coated on cationic PLGA nanoparticles.

Antibody response induced by transcutaneous immunization of mice with pCI-neo-sOVA-coated cationic PLGA nanoparticles after administering on a skin area pretreated with microneedles. Shown are serum anti-OVA IgG (A), fecal anti-OVA IgA (B), and BAL anti-OVA IgA (C). C57BL/6 mice were dosed on day 0, 14, and 28 with 4 µg pCI-neo-sOVA plasmid per mouse. Data in A and C are 6 weeks after the last immunization, whereas data in B are 4 weeks after the last immunization. All data reported are mean ± S.E.M. from 5 mice per group. (TC, transcutaneous; IM, intramuscular; UT, untreated).

4.4 Conclusion

In the present study, we showed that it is feasible to induce BoNT-neutralizing antisera by transcutaneously immunizing mice on a skin area pretreated with microneedles with a plasmid DNA that encodes the Hc50 fragment of BoNT serotype C and is coated on cationic PLGA nanoparticle. Moreover, at a proper plasmid DNA dose, transcutaneous immunization with plasmid DNA coated on the cationic PLGA nanoparticles not only induced a stronger immune response than intramuscular immunization with the same plasmid-coated nanoparticles, but also induced antigen-specific mucosal immunity. Microneedle-mediated transcutaneous immunization using plasmid DNA that encodes the Hc50 fragment of various BoNT serotypes and is coated on our cationic PLGA nanoparticles may be developed into a platform technology to prevent against botulinum intoxication.

Chapter Five

General Conclusions

For a successful transcutaneous immunization, the transportation of antigen inside the skin and recognition of antigen by antigen presenting cells are important. We discovered that both can be achieved by using microneedles in combination with nanoparticles. Microneedles can enhance the permeation of antigen inside the skin whereas the nanoparticles can act as an immune adjuvant. We have shown that the immunogenicity of protein-based vaccine or plasmid DNA vaccine topically applied onto a skin area pretreated with microneedles can be enhanced by formulating the protein or plasmid DNA into nanoparticles.

In chapter 2, we have shown that transcutaneous immunization with protein antigen conjugated on nanoparticles on a skin area pretreated with microneedles induced a stronger immune response than with the antigens alone. The dose of the antigen determined whether microneedle-mediated transcutaneous immunization can induce a stronger immune response than subcutaneous immunization with the same antigen conjugated on nanoparticles. Finally, using an *ex vivo* model in mice, we showed that the risk of bacterial infection associated with microneedle treatment is not higher than that risk associated with injection with a hypodermic needle.

In chapter 3 and chapter 4, we formulated plasmid DNA-coated cationic PLGA nanoparticles and administered them through microneedle pretreated skin. We found that transcutaneously administered plasmid DNA coated on the surface of cationic nanoparticles induced a stronger immune response than with the plasmid DNA antigen

alone. Moreover, we found that the surface charge of the DNA-coated nanoparticles had an effect on *in vitro* skin permeation and *in vivo* immune responses. At a proper plasmid DNA dose, transcutaneous immunization with plasmid DNA coated on PLGA nanoparticles was able to induce a stronger immune response than intramuscular immunization with the same plasmid DNA coated on PLGA nanoparticles. Importantly, microneedle-mediated transcutaneous immunization was also able to generate mucosal immunity, but intramuscular immunization cannot. Finally, we showed that microneedle-mediated transcutaneous immunization using the pVax/opt-BoNT/C-Hc50 plasmid coated on cationic PLGA nanoparticles induced BoNT/C-neutralizing antibody responses in a mouse model, indicating the feasibility of developing a novel transcutaneous DNA vaccine to prevent against botulinum intoxication.

References

[1] M.M. Levine, M.B. Sztein, Vaccine development strategies for improving immunization: the role of modern immunology, Nat Immunol, 5 (2004) 460-464.
[2] G.M. Glenn, M. Rao, G.R. Matyas, C.R. Alving, Skin immunization made possible by cholera toxin, Nature, 391 (1998) 851.
[3] A.S. Beignon, J.P. Briand, S. Muller, C.D. Partidos, Immunization onto bare skin with heat-labile enterotoxin of Escherichia coli enhances immune responses to coadministered protein and peptide antigens and protects mice against lethal toxin challenge, Immunology, 102 (2001) 344-351.
[4] A.S. Beignon, J.P. Briand, R. Rappuoli, S. Muller, C.D. Partidos, The LTR72 mutant of heat-labile enterotoxin of Escherichia coli enhances the ability of peptide antigens to elicit CD4(+) T cells and secrete gamma interferon after coapplication onto bare skin, Infect Immun, 70 (2002) 3012-3019.
[5] G.M. Glenn, D.N. Taylor, X. Li, S. Frankel, A. Montemarano, C.R. Alving, Transcutaneous immunization: a human vaccine delivery strategy using a patch, Nat Med, 6 (2000) 1403-1406.
[6] P. Karande, S. Mitragotri, Transcutaneous immunization: an overview of advantages, disease targets, vaccines, and delivery technologies, Annu Rev Chem Biomol Eng, 1 (2010) 175-201.
[7] J.D. Bos, M.M. Meinardi, The 500 Dalton rule for the skin penetration of chemical compounds and drugs, Exp Dermatol, 9 (2000) 165-169.
[8] H. Schaefer, T.E. Redelmeier, Skin Barrier, Principles of Percutaneous Absorption, Karger, Basel, (1996).
[9] G.M. Glenn, R.T. Kenney, Mass vaccination: solutions in the skin, Curr Top Microbiol Immunol, 304 (2006) 247-268.
[10] J. Banchereau, R.M. Steinman, Dendritic cells and the control of immunity, Nature, 392 (1998) 245-252.
[11] J.R. La Montagne, A.S. Fauci, Intradermal influenza vaccination--can less be more?, N Engl J Med, 351 (2004) 2330-2332.
[12] R.T. Kenney, S.A. Frech, L.R. Muenz, C.P. Villar, G.M. Glenn, Dose sparing with intradermal injection of influenza vaccine, N Engl J Med, 351 (2004) 2295-2301.
[13] R.B. Belshe, F.K. Newman, J. Cannon, C. Duane, J. Treanor, C. Van Hoecke, B.J. Howe, G. Dubin, Serum antibody responses after intradermal vaccination against influenza, N Engl J Med, 351 (2004) 2286-2294.
[14] C. Ponvert, P. Scheinmann, Vaccine allergy and pseudo-allergy, Eur J Dermatol, 13 (2003) 10-15.
[15] D.J. Shedlock, D.B. Weiner, DNA vaccination: antigen presentation and the induction of immunity, J Leukoc Biol, 68 (2000) 793-806.
[16] R.M. Ruprecht, Live attenuated AIDS viruses as vaccines: promise or peril?, Immunol Rev, 170 (1999) 135-149.
[17] S.D. Patil, D.G. Rhodes, D.J. Burgess, DNA-based therapeutics and DNA delivery systems: a comprehensive review, AAPS J, 7 (2005) E61-77.

[18] A.J. Phillips, The challenge of gene therapy and DNA delivery, J Pharm Pharmacol, 53 (2001) 1169-1174.
[19] S. Cornelie, O. Poulain-Godefroy, C. Lund, C. Vendeville, E. Ban, M. Capron, G. Riveau, Methylated CpG-containing plasmid activates the immune system, Scand J Immunol, 59 (2004) 143-151.
[20] E. Ban, L. Dupre, E. Hermann, W. Rohn, C. Vendeville, B. Quatannens, P. Ricciardi-Castagnoli, A. Capron, G. Riveau, CpG motifs induce Langerhans cell migration in vivo, Int Immunol, 12 (2000) 737-745.
[21] G.M. Glenn, T. Scharton-Kersten, R. Vassell, C.P. Mallett, T.L. Hale, C.R. Alving, Transcutaneous immunization with cholera toxin protects mice against lethal mucosal toxin challenge, J Immunol, 161 (1998) 3211-3214.
[22] S.A. Hammond, C. Tsonis, K. Sellins, K. Rushlow, T. Scharton-Kersten, I. Colditz, G.M. Glenn, Transcutaneous immunization of domestic animals: opportunities and challenges, Adv Drug Deliv Rev, 43 (2000) 45-55.
[23] T. Scharton-Kersten, J. Yu, R. Vassell, D. O'Hagan, C.R. Alving, G.M. Glenn, Transcutaneous immunization with bacterial ADP-ribosylating exotoxins, subunits, and unrelated adjuvants, Infect Immun, 68 (2000) 5306-5313.
[24] S.A. Frech, R.T. Kenney, C.A. Spyr, H. Lazar, J.F. Viret, C. Herzog, R. Gluck, G.M. Glenn, Improved immune responses to influenza vaccination in the elderly using an immunostimulant patch, Vaccine, 23 (2005) 946-950.
[25] D.C. Tang, M. DeVit, S.A. Johnston, Genetic immunization is a simple method for eliciting an immune response, Nature, 356 (1992) 152-154.
[26] J.B. Ulmer, J.J. Donnelly, S.E. Parker, G.H. Rhodes, P.L. Felgner, V.J. Dwarki, S.H. Gromkowski, R.R. Deck, C.M. DeWitt, A. Friedman, et al., Heterologous protection against influenza by injection of DNA encoding a viral protein, Science, 259 (1993) 1745-1749.
[27] E.F. Fynan, R.G. Webster, D.H. Fuller, J.R. Haynes, J.C. Santoro, H.L. Robinson, DNA vaccines: protective immunizations by parenteral, mucosal, and gene-gun inoculations, Proc Natl Acad Sci U S A, 90 (1993) 11478-11482.
[28] Z. Shi, D.T. Curiel, D.C. Tang, DNA-based non-invasive vaccination onto the skin, Vaccine, 17 (1999) 2136-2141.
[29] S. Watabe, K.Q. Xin, A. Ihata, L.J. Liu, A. Honsho, I. Aoki, K. Hamajima, B. Wahren, K. Okuda, Protection against influenza virus challenge by topical application of influenza DNA vaccine, Vaccine, 19 (2001) 4434-4444.
[30] P.M. Elias, Epidermal lipids, barrier function, and desquamation, J Invest Dermatol, 80 Suppl (1983) 44s-49s.
[31] M.R. Prausnitz, S. Mitragotri, R. Langer, Current status and future potential of transdermal drug delivery, Nat Rev Drug Discov, 3 (2004) 115-124.
[32] M.R. Prausnitz, J.A. Mikszta, M. Cormier, A.K. Andrianov, Microneedle-based vaccines, Curr Top Microbiol Immunol, 333 (2009) 369-393.
[33] A. Ahad, M. Aqil, K. Kohli, Y. Sultana, M. Mujeeb, A. Ali, Transdermal drug delivery: the inherent challenges and technological advancements, Transdermal drug delivery/Asian Journal of Pharmaceutical Sciences, 5 (2010) 276-288.

[34] M.K. Kim, N.M. Kini, T.J. Troshynski, H.M. Hennes, A randomized clinical trial of dermal anesthesia by iontophoresis for peripheral intravenous catheter placement in children, Ann Emerg Med, 33 (1999) 395-399.
[35] E. Holzle, N. Alberti, Long-term efficacy and side effects of tap water iontophoresis of palmoplantar hyperhidrosis--the usefulness of home therapy, Dermatologica, 175 (1987) 126-135.
[36] B. Berner, S.M. Dinh, Electronically assisted drug delivery: an overview, in: B. Berner, S.M. Dinh (Eds.), Electronically Controlled Drug Delivery, CRC Press, Boca Raton, FL, (1998) 3-7.
[37] G. Vandermeulen, E. Staes, M.L. Vanderhaeghen, M.F. Bureau, D. Scherman, V. Preat, Optimisation of intradermal DNA electrotransfer for immunisation, J Control Release, 124 (2007) 81-87.
[38] M.R. Prausnitz, Do high-voltage pulses cause changes in skin structure?, Journal of Controlled Release, 40 (1996) 321-326.
[39] R.K. Subedi, S.Y. Oh, M.K. Chun, H.K. Choi, Recent advances in transdermal drug delivery, Arch Pharm Res, 33 (2010) 339-351.
[40] A.R. Denet, R. Vanbever, V. Preat, Skin electroporation for transdermal and topical delivery, Adv Drug Deliv Rev, 56 (2004) 659-674.
[41] A.R. Denet, V. Preat, Transdermal delivery of timolol by electroporation through human skin, J Control Release, 88 (2003) 253-262.
[42] M.R. Prausnitz, E.R. Edelman, J.A. Gimm, R. Langer, J.C. Weaver, Transdermal delivery of heparin by skin electroporation, Biotechnology (N Y), 13 (1995) 1205-1209.
[43] R. Vanbever, G. Langers, S. Montmayeur, V. Preat, Transdermal delivery of fentanyl: rapid onset of analgesia using skin electroporation, J Control Release, 50 (1998) 225-235.
[44] M.R. Prausnitz, V.G. Bose, R. Langer, J.C. Weaver, Electroporation of mammalian skin: a mechanism to enhance transdermal drug delivery, Proc Natl Acad Sci U S A, 90 (1993) 10504-10508.
[45] J.J. Drabick, J. Glasspool-Malone, A. King, R.W. Malone, Cutaneous transfection and immune responses to intradermal nucleic acid vaccination are significantly enhanced by in vivo electropermeabilization, Mol Ther, 3 (2001) 249-255.
[46] R. Heller, J. Schultz, M.L. Lucas, M.J. Jaroszeski, L.C. Heller, R.A. Gilbert, K. Moelling, C. Nicolau, Intradermal delivery of interleukin-12 plasmid DNA by in vivo electroporation, DNA Cell Biol, 20 (2001) 21-26.
[47] S. Mitragotri, J. Kost, Low-frequency sonophoresis: a noninvasive method of drug delivery and diagnostics, Biotechnol Prog, 16 (2000) 488-492.
[48] A. Boucaud, M.A. Garrigue, L. Machet, L. Vaillant, F. Patat, Effect of sonication parameters on transdermal delivery of insulin to hairless rats, J Control Release, 81 (2002) 113-119.
[49] S. Mitragotri, Healing sound: the use of ultrasound in drug delivery and other therapeutic applications, Nat Rev Drug Discov, 4 (2005) 255-260.
[50] T. Tanner, R. Marks, Delivering drugs by the transdermal route: review and comment, Skin Res Technol, 14 (2008) 249-260.

[51] M. Ogura, S. Paliwal, S. Mitragotri, Low-frequency sonophoresis: current status and future prospects, Adv Drug Deliv Rev, 60 (2008) 1218-1223.
[52] P. Schratzberger, J.G. Krainin, G. Schratzberger, M. Silver, H. Ma, M. Kearney, R.F. Zuk, A.F. Brisken, D.W. Losordo, J.M. Isner, Transcutaneous ultrasound augments naked DNA transfection of skeletal muscle, Mol Ther, 6 (2002) 576-583.
[53] M. Endoh, N. Koibuchi, M. Sato, R. Morishita, T. Kanzaki, Y. Murata, Y. Kaneda, Fetal gene transfer by intrauterine injection with microbubble-enhanced ultrasound, Mol Ther, 5 (2002) 501-508.
[54] R. Rao, S. Nanda, Sonophoresis: recent advancements and future trends, J Pharm Pharmacol, 61 (2009) 689-705.
[55] A.C. Sintov, I. Krymberk, D. Daniel, T. Hannan, Z. Sohn, G. Levin, Radiofrequency-driven skin microchanneling as a new way for electrically assisted transdermal delivery of hydrophilic drugs, J Control Release, 89 (2003) 311-320.
[56] J. Bramson, K. Dayball, C. Evelegh, Y.H. Wan, D. Page, A. Smith, Enabling topical immunization via microporation: a novel method for pain-free and needle-free delivery of adenovirus-based vaccines, Gene Ther, 10 (2003) 251-260.
[57] W. Hull, Heat-Enhanced Transdermal Drug Delivery: A Survey Paper, The Journal of Applied Research, 2 (2002) 1-9.
[58] Available at: www.synera.com. Accesses 11 April 2013.
[59] R. Kumar, A. Philip, Modified Transdermal Technologies: Breaking the Barriers of Drug Permeation via the Skin Tropical Journal of Pharmaceutical Research, 6 (2007) 633-644.
[60] M.S. Roberts, Targeted drug delivery to the skin and deeper tissues: role of physiology, solute structure and disease, Clin Exp Pharmacol Physiol, 24 (1997) 874-879.
[61] S.N. Murthy, A. Sen, Y.L. Zhao, S.W. Hui, pH influences the postpulse permeability state of skin after electroporation, J Control Release, 93 (2003) 49-57.
[62] J. Lisziewicz, J. Trocio, L. Whitman, G. Varga, J. Xu, N. Bakare, P. Erbacher, C. Fox, R. Woodward, P. Markham, S. Arya, J.P. Behr, F. Lori, DermaVir: a novel topical vaccine for HIV/AIDS, J Invest Dermatol, 124 (2005) 160-169.
[63] B.R. Sloat, H.K. Tran, Z. Cui, Vaccinology: Principles and Practice, Chapter 21. Needle-Free Jet Injection for Vaccine Administration, Blackwell Publishing Ltd, (2012) 324-335.
[64] J. Haensler, C. Verdelet, V. Sanchez, Y. Girerd-Chambaz, A. Bonnin, E. Trannoy, S. Krishnan, P. Meulien, Intradermal DNA immunization by using jet-injectors in mice and monkeys, Vaccine, 17 (1999) 628-638.
[65] S. Manam, B.J. Ledwith, A.B. Barnum, P.J. Troilo, C.J. Pauley, L.B. Harper, T.G. Griffiths, 2nd, Z. Niu, L. Denisova, T.T. Follmer, S.J. Pacchione, Z. Wang, C.M. Beare, W.J. Bagdon, W.W. Nichols, Plasmid DNA vaccines: tissue distribution and effects of DNA sequence, adjuvants and delivery method on integration into host DNA, Intervirology, 43 (2000) 273-281.
[66] R.J. Mumper, Z. Cui, Genetic immunization by jet injection of targeted pDNA-coated nanoparticles, Methods, 31 (2003) 255-262.

[67] J.C. Aguiar, R.C. Hedstrom, W.O. Rogers, Y. Charoenvit, J.B. Sacci, Jr., D.E. Lanar, V.F. Majam, R.R. Stout, S.L. Hoffman, Enhancement of the immune response in rabbits to a malaria DNA vaccine by immunization with a needle-free jet device, Vaccine, 20 (2001) 275-280.
[68] D. Chen, M. Burger, Q. Chu, R. Endres, C. Zuleger, H. Dean, L.G. Payne, Epidermal powder immunization: cellular and molecular mechanisms for enhancing vaccine immunogenicity, Virus Res, 103 (2004) 147-153.
[69] D. Chen, R. Endres, Y.F. Maa, C.R. Kensil, P. Whitaker-Dowling, A. Trichel, J.S. Youngner, L.G. Payne, Epidermal powder immunization of mice and monkeys with an influenza vaccine, Vaccine, 21 (2003) 2830-2836.
[70] D. Chen, R.L. Endres, C.A. Erickson, Y.F. Maa, L.G. Payne, Epidermal powder immunization using non-toxic bacterial enterotoxin adjuvants with influenza vaccine augments protective immunity, Vaccine, 20 (2002) 2671-2679.
[71] V.P. Shah, C.C. Peck, R.L. Williams, Skin Penetration Enhancement: Clinical Pharmacological and Regulatory Considerations. Pharmaceutical Skin Penetration Enhancement K. A. Walters and J. Hadgraft, Eds. , Marcel Dekker, (1993) 417-427.
[72] A.C. Williams, B.W. Barry, Penetration enhancers, Adv Drug Deliv Rev, 56 (2004) 603-618.
[73] Z. Cui, B.R. Sloat, Topical immunization onto mouse skin using a microemulsion incorporated with an anthrax protective antigen protein-encoding plasmid, Int J Pharm, 317 (2006) 187-191.
[74] G. Xiao, X. Li, A. Kumar, Z. Cui, Transcutaneous DNA immunization following waxing-based hair depilation elicits both humoral and cellular immune responses, Eur J Pharm Biopharm, 82 (2012) 212-217.
[75] Z. Yu, W.G. Chung, B.R. Sloat, C.V. Lohr, R. Weiss, B.L. Rodriguez, X. Li, Z. Cui, The extent of the uptake of plasmid into the skin determines the immune responses induced by a DNA vaccine applied topically onto the skin, J Pharm Pharmacol, 63 (2011) 199-205.
[76] R.A. Heckert, S. Elankumaran, G.L. Oshop, V.N. Vakharia, A novel transcutaneous plasmid-dimethylsulfoxide delivery technique for avian nucleic acid immunization, Vet Immunol Immunopathol, 89 (2002) 67-81.
[77] B. Baroli, Penetration of nanoparticles and nanomaterials in the skin: fiction or reality?, J Pharm Sci, 99 (2010) 21-50.
[78] M. Mezei, V. Gulasekharam, Liposomes--a selective drug delivery system for the topical route of administration. Lotion dosage form, Life Sci, 26 (1980) 1473-1477.
[79] M. Fresta, G. Puglisi, Application of liposomes as potential cutaneous drug delivery systems. In vitro and in vivo investigation with radioactively labelled vesicles, J Drug Target, 4 (1996) 95-101.
[80] L. Li, R.M. Hoffman, Topical liposome delivery of molecules to hair follicles in mice, J Dermatol Sci, 14 (1997) 101-108.
[81] L. Li, V. Lishko, R.M. Hoffman, Liposome targeting of high molecular weight DNA to the hair follicles of histocultured skin: a model for gene therapy of the hair growth processes, In Vitro Cell Dev Biol Anim, 29A (1993) 258-260.

[82] B. Geusens, T. Strobbe, S. Bracke, P. Dynoodt, N. Sanders, M. Van Gele, J. Lambert, Lipid-mediated gene delivery to the skin, Eur J Pharm Sci, 43 (2011) 199-211.
[83] E. Touitou, N. Dayan, L. Bergelson, B. Godin, M. Eliaz, Ethosomes - novel vesicular carriers for enhanced delivery: characterization and skin penetration properties, J Control Release, 65 (2000) 403-418.
[84] Z. Cui, R.J. Mumper, Topical immunization using nanoengineered genetic vaccines, J Control Release, 81 (2002) 173-184.
[85] A. Kumar, P. Wonganan, M.A. Sandoval, X. Li, S. Zhu, Z. Cui, Microneedle-mediated transcutaneous immunization with plasmid DNA coated on cationic PLGA nanoparticles, J Control Release, 163 (2012) 230-239.
[86] M. Kalkanidis, G.A. Pietersz, S.D. Xiang, P.L. Mottram, B. Crimeen-Irwin, K. Ardipradja, M. Plebanski, Methods for nano-particle based vaccine formulation and evaluation of their immunogenicity, Methods, 40 (2006) 20-29.
[87] L.J. Peek, C.R. Middaugh, C. Berkland, Nanotechnology in vaccine delivery, Adv Drug Deliv Rev, 60 (2008) 915-928.
[88] J.P. Scheerlinck, D.L. Greenwood, Virus-sized vaccine delivery systems, Drug Discov Today, 13 (2008) 882-887.
[89] D.T. O'Hagan, M. Singh, Microparticles as vaccine adjuvants and delivery systems, Expert Rev Vaccines, 2 (2003) 269-283.
[90] M.J. Copland, M.A. Baird, T. Rades, J.L. McKenzie, B. Becker, F. Reck, P.C. Tyler, N.M. Davies, Liposomal delivery of antigen to human dendritic cells, Vaccine, 21 (2003) 883-890.
[91] C. Thomas, V. Gupta, F. Ahsan, Influence of surface charge of PLGA particles of recombinant hepatitis B surface antigen in enhancing systemic and mucosal immune responses, Int J Pharm, 379 (2009) 41-50.
[92] B. Slutter, P.C. Soema, Z. Ding, R. Verheul, W. Hennink, W. Jiskoot, Conjugation of ovalbumin to trimethyl chitosan improves immunogenicity of the antigen, J Control Release, 143 (2010) 207-214.
[93] S.T. Reddy, A. Rehor, H.G. Schmoekel, J.A. Hubbell, M.A. Swartz, In vivo targeting of dendritic cells in lymph nodes with poly(propylene sulfide) nanoparticles, J Control Release, 112 (2006) 26-34.
[94] E. Walter, D. Dreher, M. Kok, L. Thiele, S.G. Kiama, P. Gehr, H.P. Merkle, Hydrophilic poly(DL-lactide-co-glycolide) microspheres for the delivery of DNA to human-derived macrophages and dendritic cells, J Control Release, 76 (2001) 149-168.
[95] A.C. Rice-Ficht, A.M. Arenas-Gamboa, M.M. Kahl-McDonagh, T.A. Ficht, Polymeric particles in vaccine delivery, Curr Opin Microbiol, 13 (2010) 106-112.
[96] C. Thomasin, G. Corradin, M. Ying, H.P. Merkle, B. Gander, Tetanus toxoid and synthetic malaria antigen containing poly(lactide)/poly(lactide-co-glycolide) microspheres: importance of polymer degradation and antigen release for immune response, Journal of Controlled Release, 41 (1996) 131-145.
[97] S.K. Mallapragada, B. Narasimhan, Immunomodulatory biomaterials, Int J Pharm, 364 (2008) 265-271.

[98] S. Jain, W.T. Yap, D.J. Irvine, Synthesis of protein-loaded hydrogel particles in an aqueous two-phase system for coincident antigen and CpG oligonucleotide delivery to antigen-presenting cells, Biomacromolecules, 6 (2005) 2590-2600.
[99] Z. Shen, G. Reznikoff, G. Dranoff, K.L. Rock, Cloned dendritic cells can present exogenous antigens on both MHC class I and class II molecules, J Immunol, 158 (1997) 2723-2730.
[100] Z. Cui, R.J. Mumper, Genetic immunization using nanoparticles engineered from microemulsion precursors, Pharm Res, 19 (2002) 939-946.
[101] Z. Cui, R.J. Mumper, Intradermal immunization with novel pDNA coated nanoparticles via a needle-free injection device, AAPS Annual Meeting and Exposition, Toronto, Ontario, Canada, (2002).
[102] Z. Cui, R.J. Mumper, Intranasal administration of plasmid DNA-coated nanoparticles results in enhanced immune responses, J Pharm Pharmacol, 54 (2002) 1195-1203.
[103] Z. Cui, R.J. Mumper, The effect of co-administration of adjuvants with a nanoparticle-based genetic vaccine delivery system on the resulting immune responses, Eur J Pharm Biopharm, 55 (2003) 11-18.
[104] Z. Cui, R.J. Mumper, Coating of cationized protein on engineered nanoparticles results in enhanced immune responses, Int J Pharm, 238 (2002) 229-239.
[105] S. Kaushik, A.H. Hord, D.D. Denson, D.V. McAllister, S. Smitra, M.G. Allen, M.R. Prausnitz, Lack of pain associated with microfabricated microneedles, Anesth Analg, 92 (2001) 502-504.
[106] M.R. Prausnitz, Microneedles for transdermal drug delivery, Adv Drug Deliv Rev, 56 (2004) 581-587.
[107] M.S. Gerstel, V.A. Place, Drug Delivery Device, US Patent No. US3, 964, 482 (1976).
[108] S. Hashmi, P. Ling, G. Hashmi, M. Reed, R. Gaugler, W. Trimmer, Genetic transformation of nematodes using arrays of micromechanical piercing structures, Biotechniques, 19 (1995) 766-770.
[109] S. Henry, D.V. McAllister, M.G. Allen, M.R. Prausnitz, Microfabricated microneedles: a novel approach to transdermal drug delivery, J Pharm Sci, 87 (1998) 922-925.
[110] D.V. McAllister, P.M. Wang, S.P. Davis, J.H. Park, P.J. Canatella, M.G. Allen, M.R. Prausnitz, Microfabricated needles for transdermal delivery of macromolecules and nanoparticles: fabrication methods and transport studies, Proc Natl Acad Sci U S A, 100 (2003) 13755-13760.
[111] F.J. Verbaan, S.M. Bal, D.J. van den Berg, W.H. Groenink, H. Verpoorten, R. Luttge, J.A. Bouwstra, Assembled microneedle arrays enhance the transport of compounds varying over a large range of molecular weight across human dermatomed skin, J Control Release, 117 (2007) 238-245.
[112] Y. Ito, E. Hagiwara, A. Saeki, N. Sugioka, K. Takada, Feasibility of microneedles for percutaneous absorption of insulin, Eur J Pharm Sci, 29 (2006) 82-88.

[113] Y. Ito, J. Yoshimitsu, K. Shiroyama, N. Sugioka, K. Takada, Self-dissolving microneedles for the percutaneous absorption of EPO in mice, J Drug Target, 14 (2006) 255-261.
[114] J. Wang, J. Lu, S.Y. Ly, M. Vuki, B. Tian, W.K. Adeniyi, R.A. Armendariz, Lab-on-a-Cable for electrochemical monitoring of phenolic contaminants, Anal Chem, 72 (2000) 2659-2663.
[115] A. Ovsianikov, B. Chichkov, P. Mente, N.A. Monteiro-Riviere, A. Doraiswamy, R.J. Narayan, Two Photon Polymerization of Polymer–Ceramic Hybrid Materials for Transdermal Drug Delivery, International Journal of Applied Ceramic Technology, 4 (2007) 22-29.
[116] C.S. Kolli, A.K. Banga, Characterization of solid maltose microneedles and their use for transdermal delivery, Pharm Res, 25 (2008) 104-113.
[117] R.F. Donnelly, D.I. Morrow, T.R. Singh, K. Migalska, P.A. McCarron, C. O'Mahony, A.D. Woolfson, Processing difficulties and instability of carbohydrate microneedle arrays, Drug Dev Ind Pharm, 35 (2009) 1242-1254.
[118] J.H. Park, M.G. Allen, M.R. Prausnitz, Biodegradable polymer microneedles: fabrication, mechanics and transdermal drug delivery, J Control Release, 104 (2005) 51-66.
[119] R. Trichur, S. Kim, X. Zhu, J.W. Suk, C.-C. Hong, J.-W. Choi, C.H. Ahn, Development of plastic microneedles for transdermal interfacing using injection molding techniques, Micro Total Analysis System, 1 (2002) 395-397.
[120] M. Yang, J.D. Zahn, Microneedle insertion force reduction using vibratory actuation, Biomed Microdevices, 6 (2004) 177-182.
[121] S.P. Davis, W. Martanto, M.G. Allen, M.R. Prausnitz, Hollow metal microneedles for insulin delivery to diabetic rats, IEEE Trans Biomed Eng, 52 (2005) 909-915.
[122] B. Stoeber, D. Liepmann, Arrays of hollow out-of-plane microneedles for drug delivery, Journal of Microelectromechanical Systems, 14 (2005) 472-479
[123] F. Chabri, K. Bouris, T. Jones, D. Barrow, A. Hann, C. Allender, K. Brain, J. Birchall, Microfabricated silicon microneedles for nonviral cutaneous gene delivery, Br J Dermatol, 150 (2004) 869-877.
[124] S.A. Coulman, D. Barrow, A. Anstey, C. Gateley, A. Morrissey, N. Wilke, C. Allender, K. Brain, J.C. Birchall, Minimally invasive cutaneous delivery of macromolecules and plasmid DNA via microneedles, Curr Drug Deliv, 3 (2006) 65-75.
[125] W. Lin, M. Cormier, A. Samiee, A. Griffin, B. Johnson, C.L. Teng, G.E. Hardee, P.E. Daddona, Transdermal delivery of antisense oligonucleotides with microprojection patch (Macroflux) technology, Pharm Res, 18 (2001) 1789-1793.
[126] W. Martanto, S.P. Davis, N.R. Holiday, J. Wang, H.S. Gill, M.R. Prausnitz, Transdermal delivery of insulin using microneedles in vivo, Pharm Res, 21 (2004) 947-952.
[127] M. Pearton, C. Allender, K. Brain, A. Anstey, C. Gateley, N. Wilke, A. Morrissey, J. Birchall, Gene delivery to the epidermal cells of human skin explants using microfabricated microneedles and hydrogel formulations, Pharm Res, 25 (2008) 407-416.
[128] Z. Ding, F.J. Verbaan, M. Bivas-Benita, L. Bungener, A. Huckriede, D.J. van den Berg, G. Kersten, J.A. Bouwstra, Microneedle arrays for the transcutaneous

immunization of diphtheria and influenza in BALB/c mice, J Control Release, 136 (2009) 71-78.
[129] H.S. Gill, M.R. Prausnitz, Coated microneedles for transdermal delivery, J Control Release, 117 (2007) 227-237.
[130] H.S. Gill, M.R. Prausnitz, Coating formulations for microneedles, Pharm Res, 24 (2007) 1369-1380.
[131] J.W. Hooper, J.W. Golden, A.M. Ferro, A.D. King, Smallpox DNA vaccine delivered by novel skin electroporation device protects mice against intranasal poxvirus challenge, Vaccine, 25 (2007) 1814-1823.
[132] J.A. Matriano, M. Cormier, J. Johnson, W.A. Young, M. Buttery, K. Nyam, P.E. Daddona, Macroflux microprojection array patch technology: a new and efficient approach for intracutaneous immunization, Pharm Res, 19 (2002) 63-70.
[133] G. Widera, J. Johnson, L. Kim, L. Libiran, K. Nyam, P.E. Daddona, M. Cormier, Effect of delivery parameters on immunization to ovalbumin following intracutaneous administration by a coated microneedle array patch system, Vaccine, 24 (2006) 1653-1664.
[134] Y. Xie, B. Xu, Y. Gao, Controlled transdermal delivery of model drug compounds by MEMS microneedle array, Nanomedicine, 1 (2005) 184-190.
[135] Q. Zhu, V.G. Zarnitsyn, L. Ye, Z. Wen, Y. Gao, L. Pan, I. Skountzou, H.S. Gill, M.R. Prausnitz, C. Yang, R.W. Compans, Immunization by vaccine-coated microneedle arrays protects against lethal influenza virus challenge, Proc Natl Acad Sci U S A, 106 (2009) 7968-7973.
[136] H.S. Gill, J. Soderholm, M.R. Prausnitz, M. Sallberg, Cutaneous vaccination using microneedles coated with hepatitis C DNA vaccine, Gene Ther, 17 (2010) 811-814.
[137] J.B. Alarcon, A.W. Hartley, N.G. Harvey, J.A. Mikszta, Preclinical evaluation of microneedle technology for intradermal delivery of influenza vaccines, Clin Vaccine Immunol, 14 (2007) 375-381.
[138] J.A. Mikszta, J.P. Dekker, 3rd, N.G. Harvey, C.H. Dean, J.M. Brittingham, J. Huang, V.J. Sullivan, B. Dyas, C.J. Roy, R.G. Ulrich, Microneedle-based intradermal delivery of the anthrax recombinant protective antigen vaccine, Infect Immun, 74 (2006) 6806-6810.
[139] J.A. Mikszta, V.J. Sullivan, C. Dean, A.M. Waterston, J.B. Alarcon, J.P. Dekker, 3rd, J.M. Brittingham, J. Huang, C.R. Hwang, M. Ferriter, G. Jiang, K. Mar, K.U. Saikh, B.G. Stiles, C.J. Roy, R.G. Ulrich, N.G. Harvey, Protective immunization against inhalational anthrax: a comparison of minimally invasive delivery platforms, J Infect Dis, 191 (2005) 278-288.
[140] P. Van Damme, F. Oosterhuis-Kafeja, M. Van der Wielen, Y. Almagor, O. Sharon, Y. Levin, Safety and efficacy of a novel microneedle device for dose sparing intradermal influenza vaccination in healthy adults, Vaccine, 27 (2009) 454-459.
[141] S.P. Sullivan, D.G. Koutsonanos, M. Del Pilar Martin, J.W. Lee, V. Zarnitsyn, S.O. Choi, N. Murthy, R.W. Compans, I. Skountzou, M.R. Prausnitz, Dissolving polymer microneedle patches for influenza vaccination, Nat Med, 16 (2010) 915-920.

[142] D.G. Koutsonanos, M. del Pilar Martin, V.G. Zarnitsyn, S.P. Sullivan, R.W. Compans, M.R. Prausnitz, I. Skountzou, Transdermal influenza immunization with vaccine-coated microneedle arrays, PLoS One, 4 (2009) e4773.
[143] D.G. Koutsonanos, M. del Pilar Martin, V.G. Zarnitsyn, J. Jacob, M.R. Prausnitz, R.W. Compans, I. Skountzou, Serological memory and long-term protection to novel H1N1 influenza virus after skin vaccination, J Infect Dis, 204 (2011) 582-591.
[144] J.M. Song, Y.C. Kim, P.G. Barlow, M.J. Hossain, K.M. Park, R.O. Donis, M.R. Prausnitz, R.W. Compans, S.M. Kang, Improved protection against avian influenza H5N1 virus by a single vaccination with virus-like particles in skin using microneedles, Antiviral Res, 88 (2010) 244-247.
[145] J.M. Song, Y.C. Kim, A.S. Lipatov, M. Pearton, C.T. Davis, D.G. Yoo, K.M. Park, L.M. Chen, F.S. Quan, J.C. Birchall, R.O. Donis, M.R. Prausnitz, R.W. Compans, S.M. Kang, Microneedle delivery of H5N1 influenza virus-like particles to the skin induces long-lasting B- and T-cell responses in mice, Clin Vaccine Immunol, 17 (2010) 1381-1389.
[146] W.C. Weldon, M.P. Martin, V. Zarnitsyn, B. Wang, D. Koutsonanos, I. Skountzou, M.R. Prausnitz, R.W. Compans, Microneedle vaccination with stabilized recombinant influenza virus hemagglutinin induces improved protective immunity, Clin Vaccine Immunol, 18 (2011) 647-654.
[147] A. Kumar, X. Li, M.A. Sandoval, B.L. Rodriguez, B.R. Sloat, Z. Cui, Permeation of antigen protein-conjugated nanoparticles and live bacteria through microneedle-treated mouse skin, Int J Nanomedicine, 6 (2011) 1253-1264.
[148] J. Donnelly, K. Berry, J.B. Ulmer, Technical and regulatory hurdles for DNA vaccines, Int J Parasitol, 33 (2003) 457-467.
[149] J.F. Nicolas, B. Guy, Intradermal, epidermal and transcutaneous vaccination: from immunology to clinical practice, Expert Rev Vaccines, 7 (2008) 1201-1214.
[150] D.V. McAllister, M.G. Allen, M.R. Prausnitz, Microfabricated microneedles for gene and drug delivery, Annu Rev Biomed Eng, 2 (2000) 289-313.
[151] J.A. Mikszta, J.B. Alarcon, J.M. Brittingham, D.E. Sutter, R.J. Pettis, N.G. Harvey, Improved genetic immunization via micromechanical disruption of skin-barrier function and targeted epidermal delivery, Nat Med, 8 (2002) 415-419.
[152] J. Birchall, S. Coulman, M. Pearton, C. Allender, K. Brain, A. Anstey, C. Gateley, N. Wilke, A. Morrissey, Cutaneous DNA delivery and gene expression in ex vivo human skin explants via wet-etch micro-fabricated micro-needles, J Drug Target, 13 (2005) 415-421.
[153] V. Vemulapalli, Y. Yang, P.M. Friden, A.K. Banga, Synergistic effect of iontophoresis and soluble microneedles for transdermal delivery of methotrexate, J Pharm Pharmacol, 60 (2008) 27-33.
[154] M.R. Prausnitz, R. Langer, Transdermal drug delivery, Nat Biotechnol, 26 (2008) 1261-1268.
[155] J.M. Lane, J. Goldstein, Evaluation of 21st-century risks of smallpox vaccination and policy options, Ann Intern Med, 138 (2003) 488-493.

[156] L. Daugimont, N. Baron, G. Vandermeulen, N. Pavselj, D. Miklavcic, M.C. Jullien, G. Cabodevila, L.M. Mir, V. Preat, Hollow microneedle arrays for intradermal drug delivery and DNA electroporation, J Membr Biol, 236 (2010) 117-125.
[157] Q. Zhou, F. Wang, F. Yang, Y. Wang, X. Zhang, S. Sun, Augmented humoral and cellular immune response of hepatitis B virus DNA vaccine by micro-needle vaccination using Flt3L as an adjuvant, Vaccine, 28 (2010) 1357-1362.
[158] X. Chen, A.S. Kask, M.L. Crichton, C. McNeilly, S. Yukiko, L. Dong, J.O. Marshak, C. Jarrahian, G.J. Fernando, D. Chen, D.M. Koelle, M.A. Kendall, Improved DNA vaccination by skin-targeted delivery using dry-coated densely-packed microprojection arrays, J Control Release, 148 (2010) 327-333.
[159] A. Cattamanchi, C.M. Posavad, A. Wald, Y. Baine, J. Moses, T.J. Higgins, R. Ginsberg, R. Ciccarelli, L. Corey, D.M. Koelle, Phase I study of a herpes simplex virus type 2 (HSV-2) DNA vaccine administered to healthy, HSV-2-seronegative adults by a needle-free injection system, Clin Vaccine Immunol, 15 (2008) 1638-1643.
[160] D.W. Kimberlin, Neonatal herpes simplex infection, Clin Microbiol Rev, 17 (2004) 1-13.
[161] A.S. Kask, X. Chen, J.O. Marshak, L. Dong, M. Saracino, D. Chen, C. Jarrahian, M.A. Kendall, D.M. Koelle, DNA vaccine delivery by densely-packed and short microprojection arrays to skin protects against vaginal HSV-2 challenge, Vaccine, 28 (2010) 7483-7491.
[162] P.C. DeMuth, X. Su, R.E. Samuel, P.T. Hammond, D.J. Irvine, Nano-layered microneedles for transcutaneous delivery of polymer nanoparticles and plasmid DNA, Adv Mater, 22 (2010) 4851-4856.
[163] E.M. Saurer, R.M. Flessner, S.P. Sullivan, M.R. Prausnitz, D.M. Lynn, Layer-by-Layer Assembly of DNA- and Protein-Containing Films on Microneedles for Drug Delivery to the Skin, Biomacromolecules, (2010).
[164] Y.C. Kim, C. Jarrahian, D. Zehrung, S. Mitragotri, M.R. Prausnitz, Delivery systems for intradermal vaccination, Curr Top Microbiol Immunol, 351 (2012) 77-112.
[165] J.S. Robertson, C. Nicolson, R. Harvey, R. Johnson, D. Major, K. Guilfoyle, S. Roseby, R. Newman, R. Collin, C. Wallis, O.G. Engelhardt, J.M. Wood, J. Le, R. Manojkumar, B.A. Pokorny, J. Silverman, R. Devis, D. Bucher, E. Verity, C. Agius, S. Camuglia, C. Ong, S. Rockman, A. Curtis, P. Schoofs, O. Zoueva, H. Xie, X. Li, Z. Lin, Z. Ye, L.M. Chen, E. O'Neill, A. Balish, A.S. Lipatov, Z. Guo, I. Isakova, C.T. Davis, P. Rivailler, K.M. Gustin, J.A. Belser, T.R. Maines, T.M. Tumpey, X. Xu, J.M. Katz, A. Klimov, N.J. Cox, R.O. Donis, The development of vaccine viruses against pandemic A(H1N1) influenza, Vaccine, 29 (2011) 1836-1843.
[166] Y.C. Kim, J.M. Song, A.S. Lipatov, S.O. Choi, J.W. Lee, R.O. Donis, R.W. Compans, S.M. Kang, M.R. Prausnitz, Increased immunogenicity of avian influenza DNA vaccine delivered to the skin using a microneedle patch, Eur J Pharm Biopharm, 81 (2012) 239-247.
[167] J.M. Song, Y.C. Kim, E. O, R.W. Compans, M.R. Prausnitz, S.M. Kang, DNA vaccination in the skin using microneedles improves protection against influenza, Mol Ther, 20 (2012) 1472-1480.

[168] M. Pearton, V. Saller, S.A. Coulman, C. Gateley, A.V. Anstey, V. Zarnitsyn, J.C. Birchall, Microneedle delivery of plasmid DNA to living human skin: Formulation coating, skin insertion and gene expression, J Control Release, 160 (2012) 561-569.
[169] X. Chen, T.W. Prow, M.L. Crichton, D.W. Jenkins, M.S. Roberts, I.H. Frazer, G.J. Fernando, M.A. Kendall, Dry-coated microprojection array patches for targeted delivery of immunotherapeutics to the skin, J Control Release, 139 (2009) 212-220.
[170] Z. Cui, R.J. Mumper, Chitosan-based nanoparticles for topical genetic immunization, J Control Release, 75 (2001) 409-419.
[171] Z. Cui, L. Baizer, R.J. Mumper, Intradermal immunization with novel plasmid DNA-coated nanoparticles via a needle-free injection device, J Biotechnol, 102 (2003) 105-115.
[172] J.M. Barichello, M. Morishita, K. Takayama, T. Nagai, Encapsulation of hydrophilic and lipophilic drugs in PLGA nanoparticles by the nanoprecipitation method, Drug Dev Ind Pharm, 25 (1999) 471-476.
[173] Z. Cui, R.J. Mumper, Microparticles and nanoparticles as delivery systems for DNA vaccines, Crit Rev Ther Drug Carrier Syst, 20 (2003) 103-137.
[174] Z. Ding, E. Van Riet, S. Romeijn, G.F. Kersten, W. Jiskoot, J.A. Bouwstra, Immune modulation by adjuvants combined with diphtheria toxoid administered topically in BALB/c mice after microneedle array pretreatment, Pharm Res, 26 (2009) 1635-1643.
[175] S. Kommareddy, B.C. Baudner, A. Bonificio, S. Gallorini, G. Palladino, A.S. Determan, D.M. Dohmeier, K.D. Kroells, J.R. Sternjohn, M. Singh, P.R. Dormitzer, K.J. Hansen, D.T. O'Hagan, Influenza subunit vaccine coated microneedle patches elicit comparable immune responses to intramuscular injection in guinea pigs, Vaccine, (2013).
[176] S.M. Bal, Z. Ding, G.F. Kersten, W. Jiskoot, J.A. Bouwstra, Microneedle-based transcutaneous immunisation in mice with N-trimethyl chitosan adjuvanted diphtheria toxoid formulations, Pharm Res, 27 (2010) 1837-1847.
[177] B. Slutter, S.M. Bal, Z. Ding, W. Jiskoot, J.A. Bouwstra, Adjuvant effect of cationic liposomes and CpG depends on administration route, J Control Release, 154 (2011) 123-130.
[178] Z. Ding, S.M. Bal, S. Romeijn, G.F. Kersten, W. Jiskoot, J.A. Bouwstra, Transcutaneous immunization studies in mice using diphtheria toxoid-loaded vesicle formulations and a microneedle array, Pharm Res, 28 (2011) 145-158.
[179] H. Hirschberg, S. van Kuijk, J. Loch, W. Jiskoot, J. Bouwstra, G. Kersten, J.P. Amorij, A combined approach of vesicle formulations and microneedle arrays for transcutaneous immunization against hepatitis B virus, Eur J Pharm Sci, 46 (2012) 1-7.
[180] L. Guo, J. Chen, Y. Qiu, S. Zhang, B. Xu, Y. Gao, Enhanced transcutaneous immunization via dissolving microneedle array loaded with liposome encapsulated antigen and adjuvant, Int J Pharm, 447 (2013) 22-30.
[181] R.M. Jacobson, A. Swan, A. Adegbenro, S.L. Ludington, P.C. Wollan, G.A. Poland, Making vaccines more acceptable--methods to prevent and minimize pain and other common adverse events associated with vaccines, Vaccine, 19 (2001) 2418-2427.
[182] M.J. Choi, H.I. Maibach, Topical vaccination of DNA antigens: topical delivery of DNA antigens, Skin Pharmacol Appl Skin Physiol, 16 (2003) 271-282.

[183] K. van der Maaden, W. Jiskoot, J. Bouwstra, Microneedle technologies for (trans)dermal drug and vaccine delivery, J Control Release, 161 (2012) 645-655.
[184] J.H. Park, S.O. Choi, S. Seo, Y.B. Choy, M.R. Prausnitz, A microneedle roller for transdermal drug delivery, Eur J Pharm Biopharm, 76 (2010) 282-289.
[185] K.H. Yoo, J.W. Lee, K. Li, B.J. Kim, M.N. Kim, Photodynamic therapy with methyl 5-aminolevulinate acid might be ineffective in recalcitrant alopecia totalis regardless of using a microneedle roller to increase skin penetration, Dermatol Surg, 36 (2010) 618-622.
[186] S.K. You, Y.W. Noh, H.H. Park, M. Han, S.S. Lee, S.C. Shin, C.W. Cho, Effect of applying modes of the polymer microneedle-roller on the permeation of L-ascorbic acid in rats, J Drug Target, 18 (2010) 15-20.
[187] C.P. Zhou, Y.L. Liu, H.L. Wang, P.X. Zhang, J.L. Zhang, Transdermal delivery of insulin using microneedle rollers in vivo, Int J Pharm, 392 (2010) 127-133.
[188] S.A. Coulman, A. Anstey, C. Gateley, A. Morrissey, P. McLoughlin, C. Allender, J.C. Birchall, Microneedle mediated delivery of nanoparticles into human skin, Int J Pharm, 366 (2009) 190-200.
[189] W. Zhang, J. Gao, Q. Zhu, M. Zhang, X. Ding, X. Wang, X. Hou, W. Fan, B. Ding, X. Wu, S. Gao, Penetration and distribution of PLGA nanoparticles in the human skin treated with microneedles, Int J Pharm, 402 (2010) 205-212.
[190] M.O. Oyewumi, A. Kumar, Z. Cui, Nano-microparticles as immune adjuvants: correlating particle sizes and the resultant immune responses, Expert Rev Vaccines, 9 (2010) 1095-1107.
[191] Y.C. Kim, F.S. Quan, R.W. Compans, S.M. Kang, M.R. Prausnitz, Formulation of microneedles coated with influenza virus-like particle vaccine, AAPS PharmSciTech, 11 (2010) 1193-1201.
[192] Y.C. Kim, F.S. Quan, R.W. Compans, S.M. Kang, M.R. Prausnitz, Formulation and coating of microneedles with inactivated influenza virus to improve vaccine stability and immunogenicity, J Control Release, 142 (2010) 187-195.
[193] Y.C. Kim, F.S. Quan, D.G. Yoo, R.W. Compans, S.M. Kang, M.R. Prausnitz, Improved influenza vaccination in the skin using vaccine coated microneedles, Vaccine, 27 (2009) 6932-6938.
[194] Y.C. Kim, F.S. Quan, D.G. Yoo, R.W. Compans, S.M. Kang, M.R. Prausnitz, Enhanced memory responses to seasonal H1N1 influenza vaccination of the skin with the use of vaccine-coated microneedles, J Infect Dis, 201 (2010) 190-198.
[195] T.W. Prow, X. Chen, N.A. Prow, G.J. Fernando, C.S. Tan, A.P. Raphael, D. Chang, M.P. Ruutu, D.W. Jenkins, A. Pyke, M.L. Crichton, K. Raphaelli, L.Y. Goh, I.H. Frazer, M.S. Roberts, J. Gardner, A.A. Khromykh, A. Suhrbier, R.A. Hall, M.A. Kendall, Nanopatch-Targeted Skin Vaccination against West Nile Virus and Chikungunya Virus in Mice, Small, 6 (2010) 1776-1784.
[196] F.S. Quan, Y.C. Kim, R.W. Compans, M.R. Prausnitz, S.M. Kang, Dose sparing enabled by skin immunization with influenza virus-like particle vaccine using microneedles, J Control Release, 147 (2010) 326-332.
[197] F.S. Quan, Y.C. Kim, A. Vunnava, D.G. Yoo, J.M. Song, M.R. Prausnitz, R.W. Compans, S.M. Kang, Intradermal vaccination with influenza virus-like particles by

using microneedles induces protection superior to that with intramuscular immunization, J Virol, 84 (2010) 7760-7769.
[198] F.S. Quan, Y.C. Kim, D.G. Yoo, R.W. Compans, M.R. Prausnitz, S.M. Kang, Stabilization of influenza vaccine enhances protection by microneedle delivery in the mouse skin, PLoS One, 4 (2009) e7152.
[199] H. Kalluri, A.K. Banga, Transdermal Delivery of Proteins, AAPS PharmSciTech, (2011).
[200] B.R. Sloat, M.A. Sandoval, A.M. Hau, Y. He, Z. Cui, Strong antibody responses induced by protein antigens conjugated onto the surface of lecithin-based nanoparticles, J Control Release, 141 (2010) 93-100.
[201] B.R. Sloat, M.A. Sandoval, Z. Cui, Towards preserving the immunogenicity of protein antigens carried by nanoparticles while avoiding the cold chain, Int J Pharm, 393 (2010) 197-202.
[202] X. Li, B.R. Sloat, N. Yanasarn, Z. Cui, Relationship between the size of nanoparticles and their adjuvant activity: Data from a study with an improved experimental design, Eur J Pharm Biopharm, (2010).
[203] P.E. Laurent, H. Bourhy, M. Fantino, P. Alchas, J.A. Mikszta, Safety and efficacy of novel dermal and epidermal microneedle delivery systems for rabies vaccination in healthy adults, Vaccine, 28 (2010) 5850-5856.
[204] S.M. Bal, J. Caussin, S. Pavel, J.A. Bouwstra, In vivo assessment of safety of microneedle arrays in human skin, Eur J Pharm Sci, 35 (2008) 193-202.
[205] Y.A. Gomaa, D.I. Morrow, M.J. Garland, R.F. Donnelly, L.K. El-Khordagui, V.M. Meidan, Effects of microneedle length, density, insertion time and multiple applications on human skin barrier function: assessments by transepidermal water loss, Toxicol In Vitro, 24 (2010) 1971-1978.
[206] R.F. Donnelly, T.R. Singh, M.M. Tunney, D.I. Morrow, P.A. McCarron, C. O'Mahony, A.D. Woolfson, Microneedle arrays allow lower microbial penetration than hypodermic needles in vitro, Pharm Res, 26 (2009) 2513-2522.
[207] G. Li, A. Badkar, H. Kalluri, A.K. Banga, Microchannels created by sugar and metal microneedles: characterization by microscopy, macromolecular flux and other techniques, J Pharm Sci, 99 (2010) 1931-1941.
[208] Z. Cui, A. Dierling, M. Foldvari, Non-invasive immunization on the skin using DNA vaccine, Curr Drug Deliv, 3 (2006) 29-35.
[209] M.A. Teo, C. Shearwood, K.C. Ng, J. Lu, S. Moochhala, In vitro and in vivo characterization of MEMS microneedles, Biomed Microdevices, 7 (2005) 47-52.
[210] O. Pierucci, Dimensions of Escherichia coli at various growth rates: model for envelope growth, J Bacteriol, 135 (1978) 559-574.
[211] H. Kalluri, A.K. Banga, Formation and closure of microchannels in skin following microporation, Pharm Res, 28 (2011) 82-94.
[212] A.M. Barbero, H.F. Frasch, Pig and guinea pig skin as surrogates for human in vitro penetration studies: a quantitative review, Toxicol In Vitro, 23 (2009) 1-13.
[213] R.F. Donnelly, T.R. Raj Singh, A.D. Woolfson, Microneedle-based drug delivery systems: microfabrication, drug delivery, and safety, Drug Deliv, 17 (2010) 187-207.

[214] M.A. Kutzler, D.B. Weiner, DNA vaccines: ready for prime time?, Nat Rev Genet, 9 (2008) 776-788.
[215] S.M. Bal, B. Slutter, W. Jiskoot, J.A. Bouwstra, Small is beautiful: N-trimethyl chitosan-ovalbumin conjugates for microneedle-based transcutaneous immunisation, Vaccine, 29 (2011) 4025-4032.
[216] G.R. MacGregor, C.T. Caskey, Construction of plasmids that express E. coli beta-galactosidase in mammalian cells, Nucleic Acids Res, 17 (1989) 2365.
[217] M.L. Gu, S.H. Leppla, D.M. Klinman, Protection against anthrax toxin by vaccination with a DNA plasmid encoding anthrax protective antigen, Vaccine, 17 (1999) 340-344.
[218] B.R. Sloat, M.A. Sandoval, D. Li, W.G. Chung, P.D. Lansakara, P.J. Proteau, K. Kiguchi, J. DiGiovanni, Z. Cui, In vitro and in vivo anti-tumor activities of a gemcitabine derivative carried by nanoparticles, Int J Pharm, 409 (2011) 278-288.
[219] L.W. Wang, D.F. Langley, Identification and determination of ionic surface active agents, Arch Environ Contam Toxicol, 5 (1977) 447-456.
[220] M.A. Sandoval, B.R. Sloat, P.D. Lansakara, A. Kumar, B.L. Rodriguez, K. Kiguchi, J. Digiovanni, Z. Cui, EGFR-targeted stearoyl gemcitabine nanoparticles show enhanced anti-tumor activity, J Control Release, 157 (2012) 287-296.
[221] B.R. Sloat, K. Kiguchi, G. Xiao, J. DiGiovanni, W. Maury, Z. Cui, Transcutaneous DNA immunization following waxing-based hair depilation, J Control Release, 157 (2012) 94-102.
[222] B.R. Sloat, Z. Cui, Nasal immunization with anthrax protective antigen protein adjuvanted with polyriboinosinic-polyribocytidylic acid induced strong mucosal and systemic immunities, Pharm Res, 23 (2006) 1217-1226.
[223] M.B. Lutz, N. Kukutsch, A.L. Ogilvie, S. Rossner, F. Koch, N. Romani, G. Schuler, An advanced culture method for generating large quantities of highly pure dendritic cells from mouse bone marrow, J Immunol Methods, 223 (1999) 77-92.
[224] M. Chorny, I. Fishbein, H.D. Danenberg, G. Golomb, Lipophilic drug loaded nanospheres prepared by nanoprecipitation: effect of formulation variables on size, drug recovery and release kinetics, J Control Release, 83 (2002) 389-400.
[225] N. Nafee, S. Taetz, M. Schneider, U.F. Schaefer, C.M. Lehr, Chitosan-coated PLGA nanoparticles for DNA/RNA delivery: effect of the formulation parameters on complexation and transfection of antisense oligonucleotides, Nanomedicine, 3 (2007) 173-183.
[226] S.-W. Pang, H.-Y. Park, Y.-S. Jang, W.-S. Kim, J.-H. Kim, Effects of charge density and particle size of poly(styrene/(dimethylamino)ethyl methacrylate) nanoparticle for gene delivery in 293 cells, Colloids and Surfaces B: Biointerfaces, 26 (2002) 213-222.
[227] S. Mansouri, Y. Cuie, F. Winnik, Q. Shi, P. Lavigne, M. Benderdour, E. Beaumont, J.C. Fernandes, Characterization of folate-chitosan-DNA nanoparticles for gene therapy, Biomaterials, 27 (2006) 2060-2065.
[228] F. Benavides, T.M. Oberyszyn, A.M. VanBuskirk, V.E. Reeve, D.F. Kusewitt, The hairless mouse in skin research, J Dermatol Sci, 53 (2009) 10-18.

[229] A.E. Oran, H.L. Robinson, DNA vaccines, combining form of antigen and method of delivery to raise a spectrum of IFN-gamma and IL-4-producing CD4+ and CD8+ T cells, J Immunol, 171 (2003) 1999-2005.
[230] Z. Cui, DNA vaccine, Adv Genet, 54 (2005) 257-289.
[231] K. Oguma, B. Syuto, H. Iida, S. Kubo, Antigenic similarity of toxins produced by Clostridium botulinum type C and D strains, Infect Immun, 30 (1980) 656-660.
[232] Botulism in the United States, 1899-1998. U.S. Department of Health and Human Services PHS, editor. Handbook for epidemiologists, clinicians and laboratory workers, Atlanta , GA: Centers for Disease Control and Prevention, 1998.
[233] S.S. Arnon, R. Schechter, T.V. Inglesby, D.A. Henderson, J.G. Bartlett, M.S. Ascher, E. Eitzen, A.D. Fine, J. Hauer, M. Layton, S. Lillibridge, M.T. Osterholm, T. O'Toole, G. Parker, T.M. Perl, P.K. Russell, D.L. Swerdlow, K. Tonat, Botulinum toxin as a biological weapon: medical and public health management, JAMA, 285 (2001) 1059-1070.
[234] S. Chen, Q. Xu, M. Zeng, Oral vaccination with an adenovirus-vectored vaccine protects against botulism, Vaccine, 31 (2013) 1009-1011.
[235] CDC, Notice of CDC's discontinuation of investigational pentavalent (ABCDE) botulinum toxoid vaccine for workers at risk for occupational exposure to botulinum toxins, Morb Mortal Wkly Rep (MMWR), 60 (2011) 1454-1455.
[236] A.M. Bennett, S.D. Perkins, J.L. Holley, DNA vaccination protects against botulinum neurotoxin type F, Vaccine, 21 (2003) 3110-3117.
[237] J. Clayton, J.L. Middlebrook, Vaccination of mice with DNA encoding a large fragment of botulinum neurotoxin serotype A, Vaccine, 18 (2000) 1855-1862.
[238] S. Coulman, C. Allender, J. Birchall, Microneedles and other physical methods for overcoming the stratum corneum barrier for cutaneous gene therapy, Crit Rev Ther Drug Carrier Syst, 23 (2006) 205-258.
[239] M.I. Haq, E. Smith, D.N. John, M. Kalavala, C. Edwards, A. Anstey, A. Morrissey, J.C. Birchall, Clinical administration of microneedles: skin puncture, pain and sensation, Biomed Microdevices, 11 (2009) 35-47.
[240] D.M. Hoover, J. Lubkowski, DNAWorks: an automated method for designing oligonucleotides for PCR-based gene synthesis, Nucleic Acids Res, 30 (2002) e43.
[241] M. Zeng, Q. Xu, M. Elias, M.E. Pichichero, L.L. Simpson, L.A. Smith, Protective immunity against botulism provided by a single dose vaccination with an adenovirus-vectored vaccine, Vaccine, 25 (2007) 7540-7548.
[242] I.E. Flesch, A. Wandersee, S.H. Kaufmann, IL-4 secretion by CD4+ NK1+ T cells induces monocyte chemoattractant protein-1 in early listeriosis, J Immunol, 159 (1997) 7-10.
[243] A.S. Irvine, P.K. Trinder, D.L. Laughton, H. Ketteringham, R.H. McDermott, S.C. Reid, A.M. Haines, A. Amir, R. Husain, R. Doshi, L.S. Young, A. Mountain, Efficient nonviral transfection of dendritic cells and their use for in vivo immunization, Nat Biotechnol, 18 (2000) 1273-1278.

Vita

In June of 2001, Amit Kumar entered the Poona College of Pharmacy, Bharati Vidyapeeth University, Pune, India, where he received a Bachelor of Pharmacy degree. In January of 2007, he entered Butler University, Indianapolis and obtained his Master's degree in Pharmaceutics. In September of 2009 he entered the graduate program at Oregon State University. In January of 2010 he transferred to the Ph.D. program in the College of Pharmacy at the University of Texas, at Austin. During this time he worked as a research assistant, and attended various conferences to present his work.

Permanent Address: C/O Dr. Navin Kumar, Rajbagh, Janakpur Road, Pupri, Sitamarhi, Bihar, India 843320

This dissertation was typed by Amit Kumar